nagra National Cooperative for the Disposal of Radioactive Waste

TECHNICAL REPORT 93-23

Kristallin-I

Results in Perspective

December 1994

F.B. Neall (editor)
with contributions from
P. Baertschi, I.G. McKinley, P.A. Smith
T.J. Sumerling, H. Umeki

Hardstrasse 73, CH-5430 Wettingen/Switzerland, Telephone +41-56-37 11 11

nagra National Cooperative for the Disposal of Radioactive Waste

TECHNICAL REPORT 93-23

Kristallin-I

Results in Perspective

December 1994

F.B. Neall [1] (editor)
with contributions from
P. Baertschi [2], I.G. McKinley [2], P.A. Smith [2] [3]
T.J. Sumerling [4], H. Umeki [5]

1) Paul Scherrer Institute, Würenlingen, Switzerland

2) Nagra, Wettingen, Switzerland

3) Currently: Intera Information Technologies, Melton Mowbray, UK

4) Safety Assessment Management, Whitchurch-on-Thames, UK

5) Attached from Power Reactor and Nuclear Fuel Development Corporation, Tokyo, Japan

Hardstrasse 73, CH-5430 Wettingen/Switzerland, Telephone +41-56-37 11 11

This report was prepared on behalf of Nagra. The viewpoints presented and conclusions reached are those of the author(s) and do not necessarily represent those of Nagra.

"Copyright © 1994 by Nagra, Wettingen (Switzerland) / All rights reserved.
All parts of this work are protected by copyright. Any utilisation outwith the remit of the copyright law is unlawful and liable to prosecution. This applies in particular to translations, storage and processing in electronic systems and programs, microfilms, reproductions, etc. "

ZUSAMMENFASSUNG

Bei integrierten Sicherheitsanalysen von geplanten Endlagern für radioaktive Abfälle werden mögliche zukünftige Entwicklungen des Endlagersystems identifiziert. Die Konsequenzen dieser möglichen Entwicklungsszenarien werden mit deterministischen oder probablistischen Modellrechnungen quantifiziert. Die Resultate solcher Studien werden in Form von Konsequenzprofilen (z.B. Dosis an eine ausgewählte Bevölkerungsgruppe) als Funktion der Zeit bis in die ferne Zukunft dargestellt. Die einzelnen Komponenten der Modellketten können zwar getestet werden; es ist aber viel schwieriger die gesamte Analyse zu validieren und die Resultate derart zu präsentieren, dass Vertrauen auf ihre Anwendbarkeit aufgebaut werden kann.

In diesem Bericht wird die Kristallin-I Sicherheitsanalyse eines HAA-Endlagers im kristallinen Grundgebirge der Nordschweiz mit anderen gleichartigen HAA-Studien sowie mit drei Analysen von direkter Endlagerung abgebrannter Brennelemente verglichen, um die "Vernünftigkeit" der Kristallin-I-Resultate nachzuweisen.

Die Ähnlichkeit der betrachteten Endlagerkonzepte ermöglicht es, ein quantitativer Vergleich zwischen dem Kristallin-I-Projekt, seinem Vorgänger Projekt Gewähr und der japanischen Analyse PNC H-3 durchzuführen. Damit kann gezeigt werden, dass Unterschiede im Nahfeld- und Geosphärenverhalten auf drei wichtige Faktoren zurückzuführen sind, die sich ihrerseits aus unterschiedlichen Schwerpunkten in diesen drei Analysen und insbesondere aus dem relativ fortgeschrittenen Zustand des geologischen Untersuchungsprogramms für Kristallin-I ergeben.

Eine angehende Untersuchung der Konsequenzen der verschiedenen Endlagerkonzepte und Modelle, die in Kristallin-I und in den drei Analysen von abgebrannten Brennelementen (SKB 91, TVO 92, AECL 94) benutzt werden, führt zur Identifizierung von einigen wichtigen Faktoren, welche einen Einfluss auf die Resultate der Sicherheitsanalyse ausüben. Die relative Bedeutung dieser Faktoren variiert zwischen den verschiedenen Analysen.

Insgesamt wurden durch die oben erwähnten Vergleiche keine offensichtlichen Fehler oder Mangel in der Kristallin-I-Analyse aufgeworfen. Im Hinblick auf die langfristigen Konsequenzen stimmen die Resultate mit denen anderer Analysen gut überein.

Um Vertrauen auf die Resultate der Kristallin-I-Analyse aufzubauen, wird mit Hilfe von Naturanaloga die Vernünftigkeit der Prognosen für wichtige Prozesse im Endlagersystem aufgezeigt. Die Dosen und assoziierten Risiken, die durch das HAA-Endlager entstehen, werden mit Dosen und Gesundheitsrisiken aus anderen Strahlungsarten (z.B. terrestrische, kosmische, künstliche Strahlung), sowie mit Risiken aus schädlichen Substanzen (z.B. Rauchen), gewöhnlichen Krankheiten und alltäglichen "gefährlichen" Aktivitäten (z.B. Fliegen, Autofahren) verglichen. Mit solchen Vergleichen wird ein breiter Rahmen für die Darstellung der Kristallin-I Resultate geschafft, was für den Nichtfachmann oder sogar technische Gruppen ausserhalb des Gebiets der Abfallentsorgung besser verständlich ist.

RÉSUMÉ

Les analyses de sûreté integrées qui s'appliquent aux dépôts finals de déchets radioactifs compotent l'identification d'évolutions possibles du systeme de dépôt final, ainsi que la quantification de leurs conséquences à l'aide de modèles déterministes ou brobabilistes. Les résultats de ces études sont représentés sous forme de diagrammes représentant les conséquences possibles par rapport ou temps jusqu'à un harzan lointain (par exemple, dose pour une population sélectionnée) où l'axe du temps s'étend jusque loin dans le futur. Même s'il est possible de tester quelques-uns des composants des chaînes de modèles, il est beaucoup plus difficile de valider l'analyse de sûreté globale et de présenter les résultats de manière à ce qu'on puisse avoir confiance dans leur applicabilité.

Dans ce rapport, l'analyse de sûreté "Kristallin-I" d'un dépôt final DHA dans le socle cristallin du nord de la Suisse est comparée avec d'autres études DHA similaires et avec trois analyses du stockage final direct d'éléments combustibles usés afin de prouver le bien fondé les résultats du Kristallin-I.

La similitude entre les concepts de dépôts finals considérés permet une comparaison quantitative entre le projet Kristallin-I, le projet Garantie qui l'a précédé et l'analyse japonaise PNC H-3. Cette comparaison, démontre que les différences de comportement du champ proche et de la géosphère son imputables à trois facteurs principaux qui résultent eux-mêmes de la différence de centres de gravité de ces trois analyses et plus particulièrement du stadede maturite plus élevé du programme de recherches géologiques pour le Kristallin-I.

Un examen détaillé des conséquences des différents concepts de dépôt final et des modèlesx qui sont utiliséss dans le Kristallin-I dans les trois analyses d'éléments combustibles usés (SKB 91, TVO 92, AECL 94) permet d'identifier quelques facteurs de qui exercent une influence sur les résultats des analyses de sûreté. L'importance des ces facteurs varie selon les différentes analyses.

Dans l'ensemble, les comparaisons évoquées n'ont pas mis en évidence des erreurs ou déficiences ou évidentes dans l'analyse de sûreté Kristallin-I. En ce qui concerne les conséquences à long terme, les résultats concordent avec les résultats d'autres analyses.

Afin d'augmenter le degréde confiance dans les résultats Kristallin-I, on recourt à des analogues naturels pour démontrer que les prévisions sur les importants processus dans le système de dépôt final sont raisonnables. Les doses et les risques qui pourraient provenir du dépôt final DHA sont comparésavec les doses et les risques sur la santé engendrés par d'autres sources de rayonnement (radiations terrestres, cosmiques, artificielles par exemple) et avec les risques liés aux matières toxiques (le tabac par exemple), aux maladies courantes, infirmités et activités quotidiennes (avion, voiture). De telles comparaisons présentent les résultats du Kristallin-I dans un contexte plus large, les rendant ainsi compréhensibles aussi bien pour les profanes que pour les spécialistes d'autres domaines scientifiques.

ABSTRACT

Integrated performance assessments of proposed repositories for radioactive waste involve identification of possible paths of future evolution of the repository system and quantification of the consequences of these possibilities using deterministic or probabilistic modelling approaches. The results of such studies are presented as profiles of consequence (e.g. dose to a selected population) as a function of time extending into the distant future. Although individual components of the model chains can be tested, ensuring the validity of the overall assessment is much more difficult, as is presenting the results in a manner which gives confidence in their applicability.

In this report, the Kristallin-I safety assessment of a HLW repository sited in the crystalline basement of Northern Switzerland is compared with assessments of similar HLW disposal concepts, and also with three recent assessments of direct spent fuel disposal, in order to demonstrate the "reasonableness" of the Kristallin-I results.

Similarity of disposal concepts allows a quantitative comparison between Kristallin-I, its predecessor, Project Gewähr, and the Japanese assessment PNC H-3. From this comparison, it is possible to show that differences in near-field and geosphere performances arise from 3 main factors which themselves result from differences in emphasis in the three assessments and, particularly, from the greater maturity of the Swiss geological investigation programme for Kristallin-I.

A detailed examination of the consequences of different disposal concepts and modelling approaches used in Kristallin-I and the three spent-fuel assessments (SKB 91, TVO 92 and AECL 94) leads to the identification of several key factors which influence the results of the performance assessments. The significance of these key factors does, however, vary between these assessments.

Overall, these comparisons gave no indications of obvious errors or deficiencies in the Kristallin-I performance assessment. The results obtained, in terms of long-term consequences, are similar to those reported by the other assessments.

In order to try to build confidence in the results of Kristallin-I, examples from natural analogues are used to illustrate the reasonableness of predictions for key processes in the repository system. The doses and associated risks arising from the HLW repository are compared with doses and health risks from other forms of radiation (e.g. terrestrial, cosmic, man-made), and with risks associated with toxic materials (e.g. from smoking), ordinary illness and disease, and everyday behaviour which has associated hazards (e.g. flying or driving). These comparisons give a wider context for the presentation of the Kristallin-I results, and put them into a form more easily appreciated by the layman (or, indeed, technical audiences outside the waste disposal field).

TABLE OF CONTENTS

LIST OF TABLES

LIST OF FIGURES

1 INTRODUCTION

F.B. Neall and I.G. McKinley

The assessment of concepts for the disposal of radioactive wastes (or any other long-lived toxic materials, for that matter) requires a formal methodology for quantitatively evaluating potential degradation of the barrier system in the far future. Especially for high level radioactive waste (HLW), where very small volumes of waste have high toxicity, engineered barriers may be used to provide isolation for periods far in excess of those considered in normal engineering applications ($>>10^3$ years). Because of this, nuclear waste disposal research has been at the forefront of the development of approaches to both the model evolution of engineered structures over such periods and the evaluation of the consequences of failure of containment in terms of hazard to future populations.

Integrated performance assessments of proposed repositories for HLW generally use a chain of models, which describe processes expected to occur during the lifetime of the repository, to estimate radionuclide releases from the repository, transport through the geosphere and eventual dispersal in the biosphere. The results of these performance assessments are usually presented as profiles of consequence (e.g. dose to a selected population) against time which extends into the distant future. Individual components of the model chains used can be tested to some extent, but how can the results of the integrated assessment be evaluated to ensure confidence in their validity?

This report attempts to address the issue of the applicability of results by examining the Kristallin-I performance assessment from the perspective of other performance assessments carried out over the last decade.

Ensuring confidence in the results of a performance assessment involves a wider examination of the reasonableness and significance of the results. Particularly unhelpful in this respect is the presentation of results in terms of dose, which does not present a clear picture of the hazard involved either to scientists outside the field of radiological protection or to members of the public. Hence, this study also attempts to view the results of the Kristallin-I assessment from perspectives which, by allowing comparisons with more familiar or imaginable processes, indicate how reasonable and how significant in comparison to other sources of radiation are the calculated doses, and how hazardous in comparison with other, more 'everyday', types of risk.

Kristallin-I is an evaluation of the regional studies to characterise the crystalline basement of Northern Switzerland as a potential host rock for HLW and long-lived intermediate-level waste. In addition to a synthesis of the geological findings, a safety assessment is used to put these results into the context of repository performance and to specify further geological characterisation requirements needed to ensure suitability of a particular site. The assessment in Kristallin-I builds on the concepts and methodology of the Project Gewähr 1985 study (NAGRA 1985a) with improved databases (particularly geological) and updated models reflecting developments over the last decade.

Kristallin-I is overviewed in a summary report (NAGRA 1994a) which is supported by a geological synthesis (THURY et al. 1994) and a safety assessment report (NAGRA

1994b). The safety assessment report is, in turn, supported by a range of technical reports and papers documenting the models and databases used.

The key results and conclusions of the Kristallin-I performance assessment are summarised in Chapter 2. A useful way of placing these in context is to compare them with the results of Project Gewähr and a recent Japanese analysis which considers a very similar engineered barrier system. This is done in Chapter 3, with consideration of the approach to performance assessment and the overall aims of the analysis, the model chain and the databases used.

At the time of the earlier Project Gewähr study, very few integrated assessments of such disposal systems had been published (with the notable exception of the Swedish KBS-1, -2, -3 series, KBS 1977; 1978; 1983). Within the last few years, however, many extensive studies have been published for a range of waste types and disposal concepts. Chapter 4 considers Kristallin-I in the perspective of these other assessments, with a general evaluation of the weighting given to particular components of the safety system and more specific comparison of models and databases.

In Chapter 5, the Kristallin-I results are evaluated from a completely different viewpoint: natural analogue studies are used to illustrate that the models used for processes in the repository and the surrounding host rock are adequately realistic and the overall results reasonable when compared with naturally occurring processes. The significance of the calculated doses is illustrated by comparing the predicted radionuclide concentrations and doses due to the repository at long times in the future to naturally occurring concentrations and doses. This chapter also puts into perspective the calculated hazards from such releases by comparing them with other risks which are part of normal life.

Finally, Chapter 6 provides brief concluding remarks which review the extent to which the results from Kristallin-I can be considered to be supported by this study.

The authors of each Chapter are identified and these authors also served as reviewers of the entire report. F.B. Neall was, however, responsible for editing the report and accepts responsibility for its final form.

2 OVERVIEW OF KRISTALLIN-I

F. B. Neall

2.1 Overall aims

The Kristallin-I project completes the regional ("Phase I") geological field investigation of the crystalline basement in Northern Switzerland, which was ongoing at the time of the Project Gewähr in 1985, and presents a synthesis of results. The project also includes a new assessment of the suitability of the crystalline basement as a host rock for a HLW repository. Overall, Kristallin-I fulfils 3 main objectives:

1) To update and complement the earlier Project Gewähr 1985 assessment with extended databases, improved safety assessment tools and models;

2) To serve as a milestone in the Swiss HLW repository development programme, formally completing Phase I of regional investigation with selection of areas for siting demonstration;

3) To provide input to overall waste management planning by forming a benchmark for assessing inventory variants and design alternatives, and for re-assessing research priorities.

The Kristallin-I project has three main components: a geological synthesis (THURY et al. 1994), a safety assessment (NAGRA 1994b) and an exploration study (THURY et al. 1994, chapter 11). The safety assessment considered only the disposal of vitrified HLW and the disposal system analysed is basically the same as that developed in Project Gewähr except for the quantity of waste: a reference 120 GW(e)year power scenario was considered in Kristallin-I, compared to a 240 GW(e)year scenario in Project Gewähr. Individual models and databases were updated to take account of research and developments since 1985. Two reference siting areas were considered with specific discussion of further exploration strategy (for Phases II and III).

2.2 Aims of the Kristallin-I performance assessment

The aims of performance assessment within the Kristallin-I project were (NAGRA 1994b):

- to re-evaluate the crystalline basement of Northern Switzerland as a host rock for a HLW repository using both moderately conservative arguments and Robust[1] arguments and, hence, to quantify the levels of safety that can reasonably be expected;

---

[1] defined as considering all potentially detrimental processes but only those favourable processes which can be confidently relied on (c.f. McCOMBIE et al. 1991 or NAGRA 1984b).

- to improve understanding of the roles of the engineered and geological barriers through quantitative analysis of their performances, including examination of the sensitivity of performance estimates to uncertainties;
- to make a detailed investigation of the potential performance of the geological barriers; to identify key geological characteristics and establish desirable ranges for corresponding parameters as input to the identification of sites for additional field work (Phases II and III);
- to develop and test a more complete safety assessment methodology and tool kit, including an improved and broadened scenario analysis methodology, new models of specific processes identified as important in Project Gewähr (e.g. colloids and non-linear sorption) and new assessment computer codes.

2.3 System concept

2.3.1 Conceptual model for site geology

The main characteristics of the reference geology considered for Kristallin-I are:

- Sedimentary formations, up to several hundreds of metres thick in the potential repository siting areas, overlie the crystalline basement.
- The crystalline basement is cut by major water-conducting faults (Fig. 2.1); the intervening blocks between the faults have lower permeability;
- The upper 350-650 metres of the crystalline basement have higher hydraulic conductivity (higher-permeability domain, HPD) than the deeper basement (low-permeability domain, LPD);
- Advective water flow in the basement is confined to distinct water-conducting features (transmissive elements as shown in Fig. 2.1);
- Reference groundwater in the basement is characterised as low salinity, near-neutral pH and chemically reducing. Regional hydrochemical/isotopic analysis shows a well-defined evolution profile, which is an important constraint on potential hydrology models.

Two regions of potentially suitable crystalline basement at accessible depths have been identified, termed Area West and Area East. Both areas are delimited to the north by the Swiss national borders and to the south by the Permo-Carboniferous trough.

2.3.2 Concept for repository layout

Given the expected geological structures described above, a reference layout has been defined as illustrated in Figure. 2.2. The basic concept of in-tunnel emplacement of HLW packages is as in Project Gewähr. Emplacement panels are located within blocks of low permeability crystalline rock, at a depth of about 1,000 metres. Several different blocks may be used to avoid the major faults, as in Figure 2.2, or a multi-level

repository design may be adopted. Silos for emplacement of long-lived ILW and access shafts are planned to be in separate blocks. Although siting a repository insuch complex geology can be problematic, the major faults could have some positive features offering preferential conduits for water flow (hydraulic cage effect) and acting as mechanically weaker zones which will be the focus of future tectonic movement.

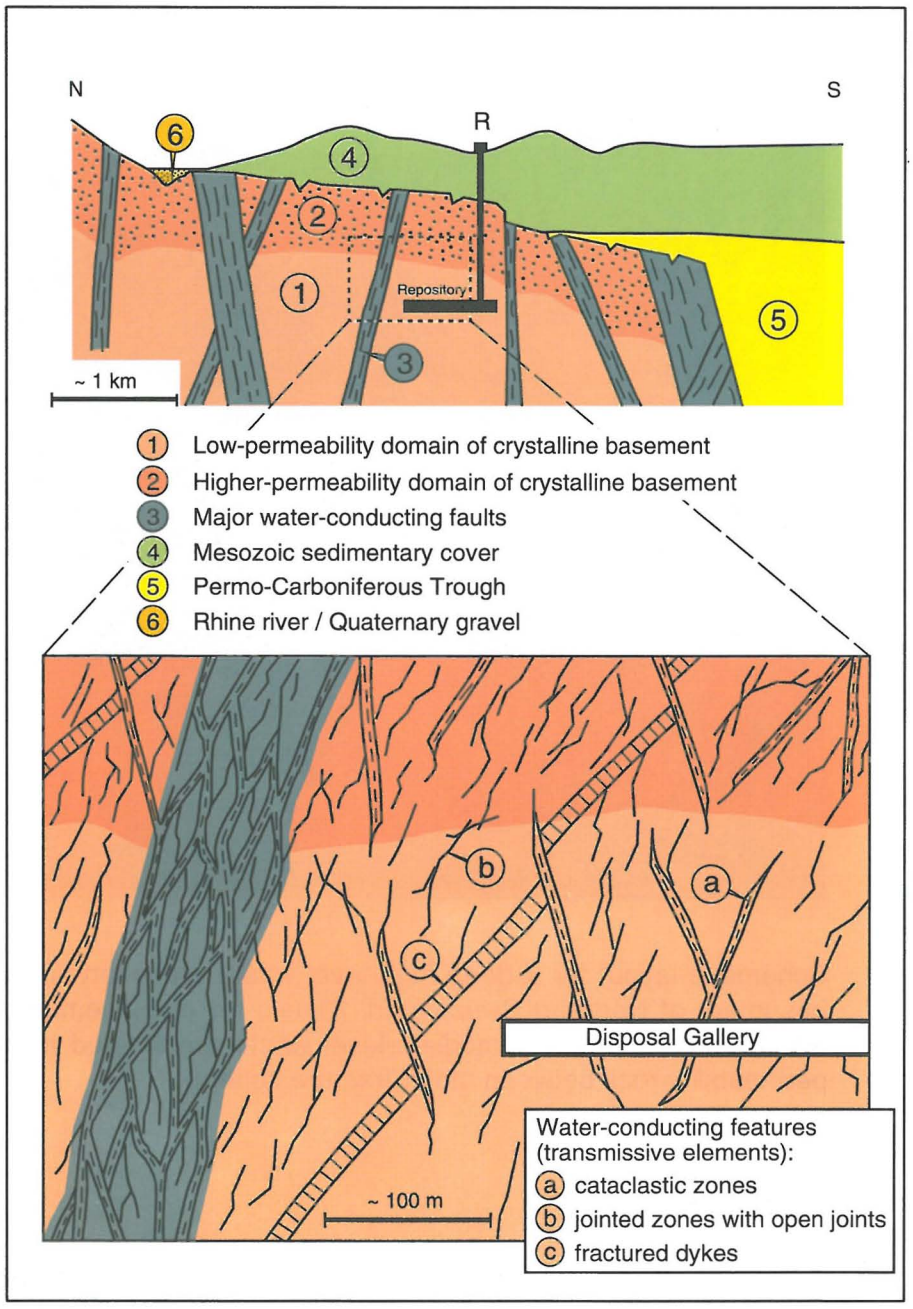

Fig. 2.1: Sketch of the geological structure in a N-S profile through the Northern Swiss crystalline basement illustrating a possible repository (R) location between major faults. The Rhine river forms the Swiss national border with Germany while the basement below or south of the Permo-Carboniferous trough is too deep to be considered for repository siting.

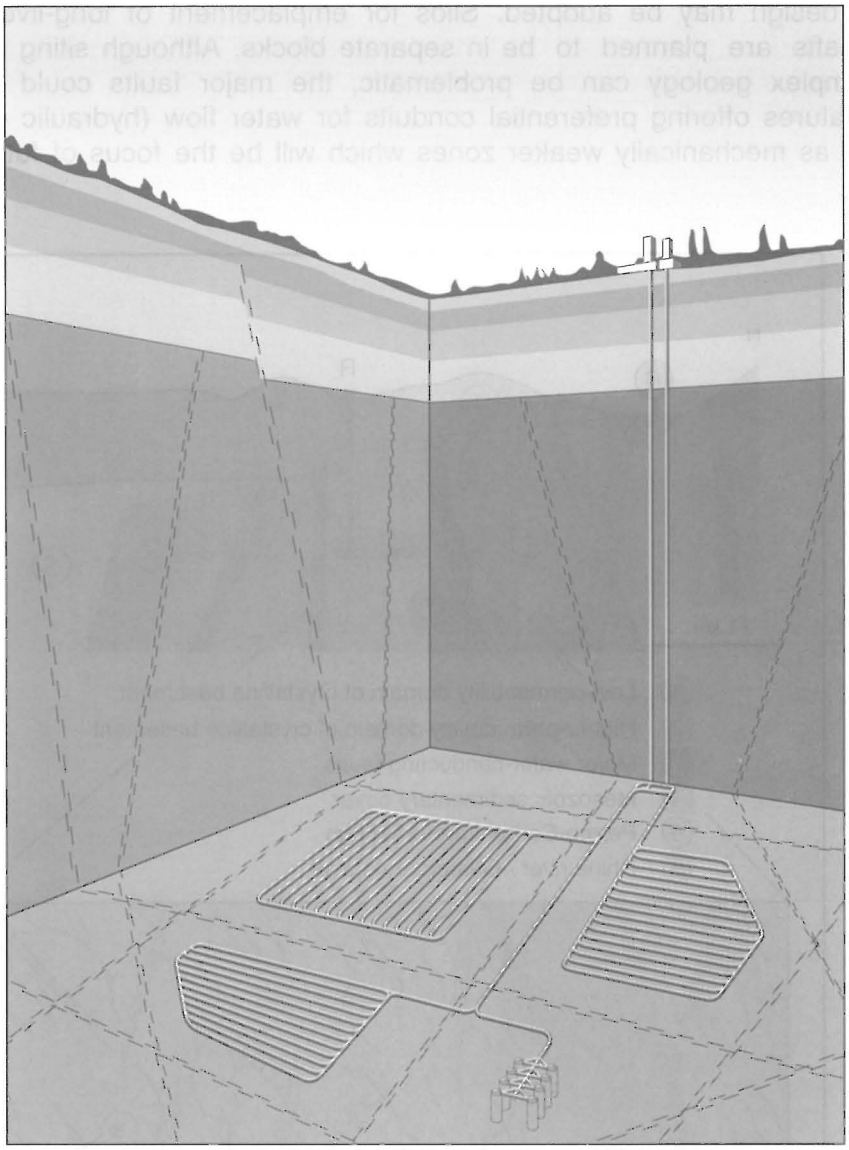

Fig. 2.2: Schematic layout for a deep high-level waste repository in the crystalline basement of Northern Switzerland. Panels for emplacement of high-level waste and silos for intermediate-level waste are located in blocks of low permeability rock between major fracture zones.

2.3.3 Engineered barriers

As in Project Gewähr, the Kristallin-I concept is characterised by massive engineered barriers (Fig. 2.3). Vitrified reprocessing waste contained in stainless steel flasks will be encapsulated in a 25 cm thick cast steel canister. These canisters will then be emplaced horizontally in the repository tunnels at intervals of 5 m, surrounded by blocks of pre-compacted, purified Na bentonite. These massive barriers offer considerable geochemical buffering and, as solute transport is dominated by diffusion, are relative insensitive to groundwater fluxes. Key features of this barrier system are:

- Absolute isolation of the waste for more than 10^3 years (minimum canister failure time); all releases thus occur after the radiogenic thermal transient;
- Low corrosion rate of the glass (dissolution time in the order of 10^5 years)
- Low solubility of many nuclides in the reducing, alkaline environment of the near field
- Retardation of radionuclides during diffusive transport through the compacted bentonite
- Compacted bentonite acts as a colloid filter.

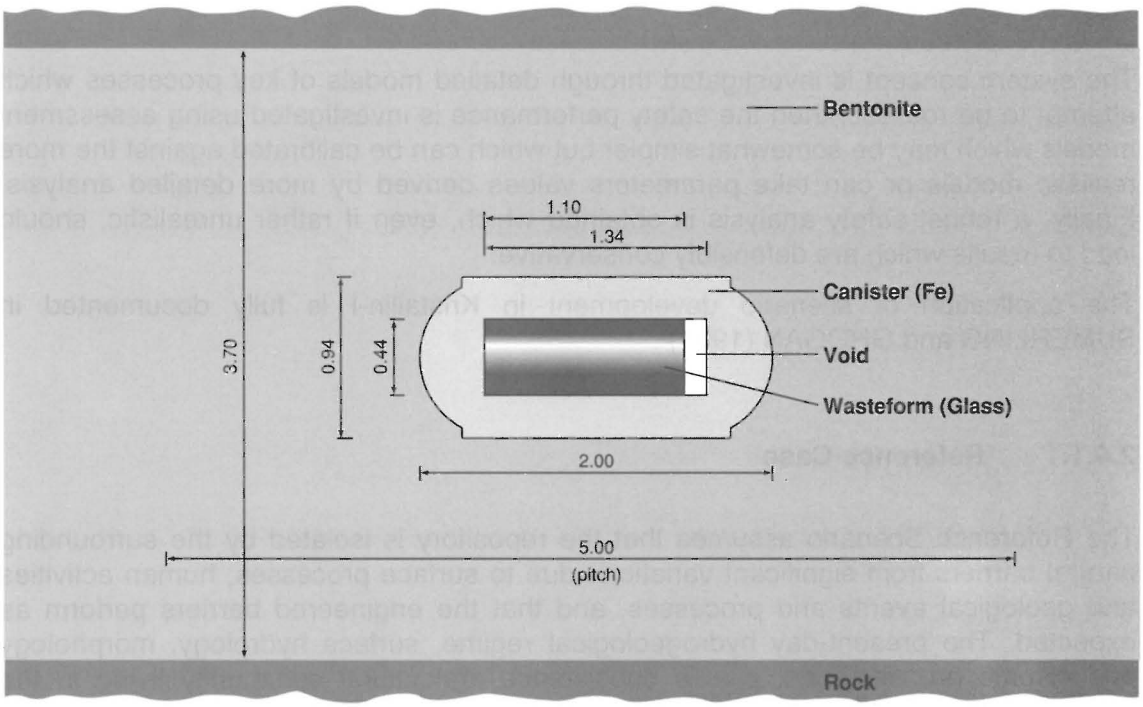

Fig. 2.3: High-level waste emplacement geometry (dimensions given in metres)

2.4 Performance assessment

2.4.1 Scenario development

In the Kristallin-I performance assessment, the basic understanding of the repository system in its geological environment is analysed in a formal manner to identify

possible paths of future evolution. This is the process of scenario development. The procedure includes the following broad stages:

1) Documentation of understanding of the system and processes relevant to its behaviour.
2) Development of a catalogue of all potentially relevant **f**eatures, **e**vents and **p**rocesses (FEPs).
3) Specification of the system concept - a description of the behaviour of the repository system indicating the interactions of all relevant FEPs.
4) Development of the safety assessment concept - a conceptual model of all FEPs to be taken into account in assessment calculations, incorporated into specific Reference and alternative scenarios.
5) Development of the Robust safety assessment concept - incorporating all detrimental FEPs but including only well understood FEPs which contribute to safety., Other FEPs which may contribute to safety but which are not included are Reserve FEPs.

The system concept is investigated through detailed models of key processes which attempt to be realistic; then the safety performance is investigated using assessment models which may be somewhat simpler but which can be calibrated against the more realistic models or can take parameters values derived by more detailed analysis. Finally, a robust safety analysis is obtained which, even if rather unrealistic, should lead to results which are defensibly conservative.

The application of scenario development in Kristallin-I is fully documented in SUMERLING and GROGAN (1994) .

2.4.1.1 Reference Case

The Reference Scenario assumes that the repository is isolated by the surrounding natural barriers from significant variations due to surface processes, human activities and geological events and processes, and that the engineered barriers perform as expected. The present-day hydrogeological regime, surface hydrology, morphology and climate are assumed, plus a subsistence agricultural community living in the exfiltration zone. Within the Reference Scenario, a range of alternative conceptual models for key phenomena is identified. Where there are equally likely alternatives, the model giving the greatest consequences is incorporated in the Reference Model Assumptions.

2.4.2 Hydrogeology

For hydrodynamic modelling, different scales have been considered (Fig. 2.4) with larger scale models providing boundary information for the smaller. The regional-scale model suggests a regional flow pattern for the crystalline basement with recharge in the Southern Black Forest and discharge in the Rhine Valley. This results in flow

generally south-westwards, eastwards through Area East from recharge, then north-westwards through Area West.

From knowledge of the orientation of the main groups of faults, derived by extrapolation from surface mapping and limited subsurface data (boreholes and seismic), idealised fracture zone meshes can be constructed. The combination of these meshes with hydraulic data from boreholes forms the basis of the subregional models of groundwater flow in which the blocks between faults are represented as equivalent porous media but faults are specifically represented as 2D features.

Based on such groundwater-flow modelling, the expected fluxes through a block of low-permeability domain are calculated for a range of hydraulic parameter values. Within the low-permeability domain, advective water flow will occur predominantly in the identified water-conducting features. The calculated water fluxes provide the boundary conditions for the near-field release model, while the hydraulic characteristics of the identified water-conducting features provide input for the geosphere transport model.

2.4.3 Model chain for performance assessment

The model chain for performance assessment is illustrated in Figure 2.5. Transport modelling comprises near field, geosphere and biosphere components; each model contributes input data, in the form of radionuclide fluxes, for the next member of the chain. Further input data for transport modelling is provided by hydrogeological and chemical models. The final result of an assessment calculation is displayed graphically as the annual individual dose arising from all biosphere exposure pathways for time after repository closure.

2.4.4 Inventory of vitrified HLW

The current planning of the Swiss disposal concept for HLW is based on the presently installed nuclear energy production capacity of 3 Gigawatts (electric) with a planned lifetime of 40 years and the reprocessing of all spent fuel. After interim storage for a period of not less than about 40 years, the vitrified waste (contained in 2,693 packages), would be emplaced in the repository. The inventory of safety-relevant nuclides in the Reference Case, at the assumed earliest canister failure time of 1,000 years after emplacement, is given in Table 2.1.

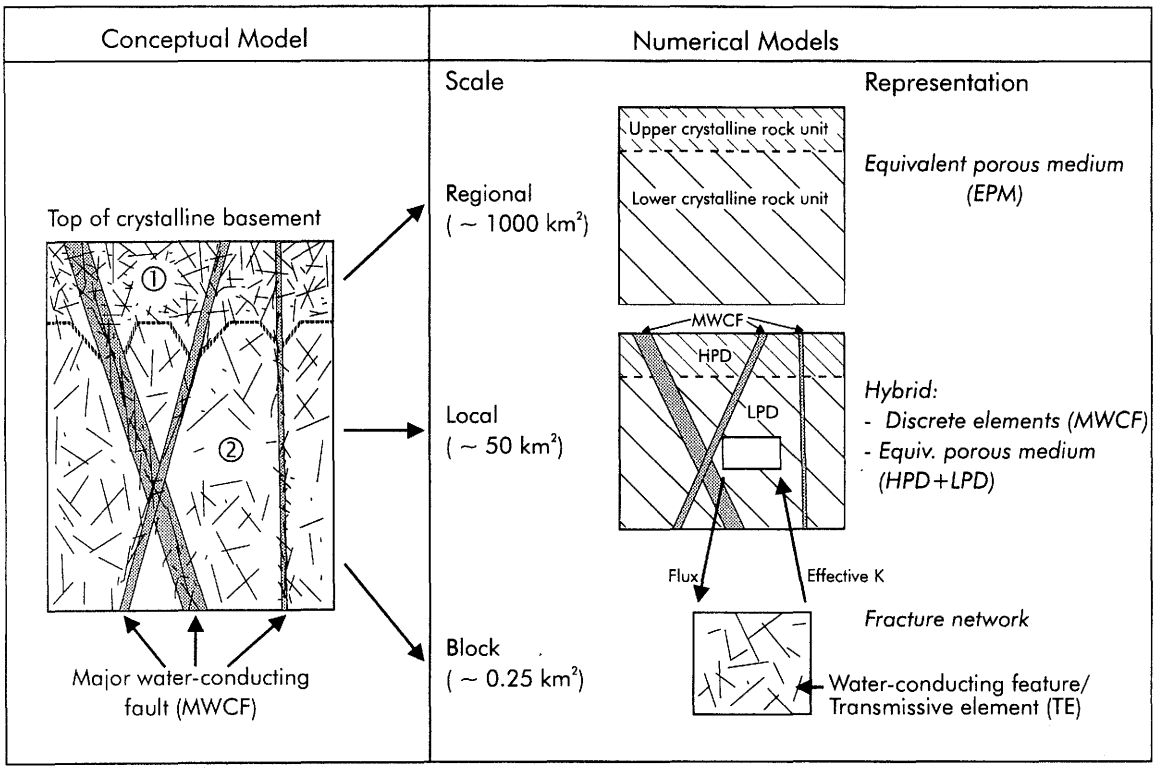

① Upper crystalline rock domain; designated as higher-permeability domain (HPD) in area West
② Lower crystalline rock domain; designated as low-permeability domain (LPD) in area West

Fig. 2.4: Sketch showing the relationship between the hydrogeological conceptual model and the numerical models of groundwater flow at regional, subregional and site scales.

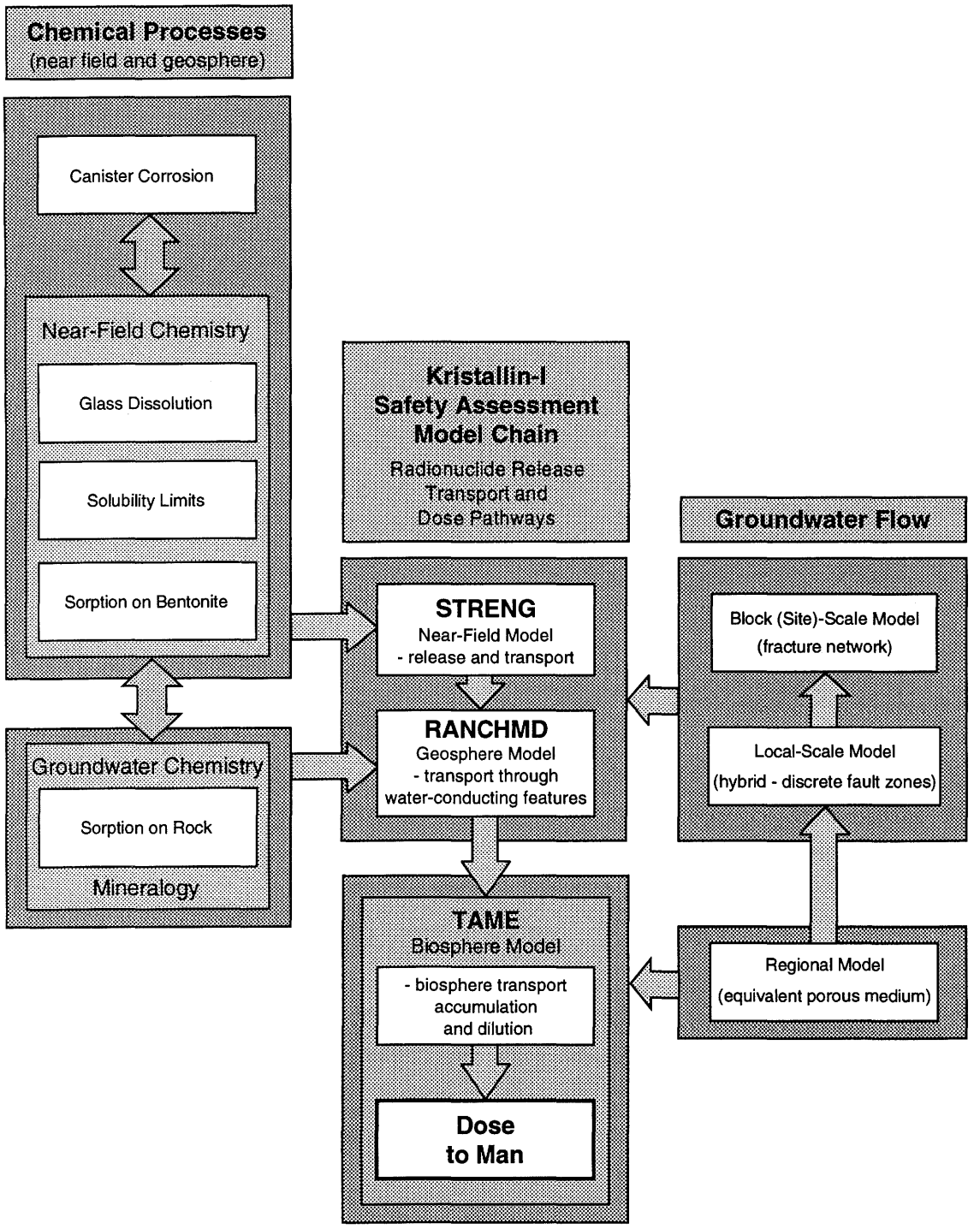

Fig. 2.5: The Nagra assessment model chain (codes STRENG, RANCHMD and TAME) and supporting models

Table 2.1: Inventories of safety-relevant radionuclides and stable isotopes of these elements per waste canister, calculated for the Reference Case canister failure time of 1,000 years after emplacement in the repository (NAGRA 1994b, table 3.7.1)

Inventory			
Nuclides	**Moles**	**Becquerels**	**Half-life** (years)
Single radionuclides and stable isotopes			
Ni-stable	2.32×10^{1}	-	-
^{59}Ni	1.07×10^{-2}	1.88×10^{9}	7.50×10^{4}
Se-stable	8.83×10^{-1}	-	-
^{79}Se	1.07×10^{-1}	2.18×10^{10}	6.5×10^{4}
^{93}Zr	1.06×10^{1}	9.20×10^{10}	1.53×10^{6}
^{99}Tc	1.04×10^{1}	6.48×10^{11}	2.13×10^{5}
Pd-stable	1.40×10^{1}	-	-
^{107}Pd	2.56	5.20×10^{9}	6.50×10^{6}
Sn-stable	9.52×10^{-1}	-	-
^{126}Sn	2.78×10^{-1}	3.67×10^{10}	1.00×10^{5}
^{135}Cs	3.30	1.90×10^{10}	2.30×10^{6}
4N+1 chain (neptunium chain)			
^{245}Cm	3.43×10^{-3}	5.33×10^{9}	8.50×10^{3}
^{241}Am	2.13×10^{-1}	6.51×10^{12}	4.32×10^{2}
^{237}Np	3.49	2.16×10^{10}	2.14×10^{6}
^{233}U	1.06×10^{-3}	8.84×10^{7}	1.59×10^{5}
^{229}Th	2.23×10^{-6}	4.01×10^{6}	7.34×10^{3}
4N+2 chain (uranium chain)			
^{246}Cm	3.38×10^{-4}	9.45×10^{8}	4.73×10^{3}
^{242}Pu	1.72×10^{-2}	6.04×10^{8}	3.76×10^{5}
^{238}U	8.11	2.40×10^{7}	4.47×10^{9}
^{234}U	1.11×10^{-2}	6.01×10^{8}	2.45×10^{5}
^{230}Th	4.58×10^{-5}	7.87×10^{6}	7.54×10^{4}
^{226}Ra	2.38×10^{-7}	1.97×10^{6}	1.60×10^{3}
4N+3 chain (plutonium chain)			
^{243}Am	3.85×10^{-1}	6.90×10^{11}	7.38×10^{3}
^{239}Pu	2.52×10^{-1}	1.39×10^{11}	2.41×10^{4}
^{235}U	9.22×10^{-2}	1.73×10^{6}	7.04×10^{8}
^{231}Pa	2.10×10^{-6}	8.48×10^{5}	3.28×10^{4}
4N chain (thorium chain)			
^{240}Pu	1.68×10^{-1}	3.40×10^{11}	6.54×10^{3}
^{236}U	5.82×10^{-2}	3.29×10^{7}	2.34×10^{7}
^{232}Th	4.89×10^{-6}	4.60	1.41×10^{10}

2.4.5 Near field

The principal components of the engineered barriers of the near field are:

- the vitrified (glass) waste matrix
- the massive steel canister
- the thick, compacted bentonite clay backfill.

The conceptual model for the near field takes into account the following processes which influence the release of radionuclides from the glass into the geosphere:

- decay (and ingrowth) of radionuclides
- canister failure
- glass corrosion
- nuclide dissolution (congruent release from glass)
- nuclide solubility limits
- solute diffusion in bentonite constrained by retardation
- groundwater advection (which affects the outer boundary condition for diffusion through the bentonite buffer).

The model includes several conservative assumptions, particularly:

- the massive steel canisters are all assumed to fail 1,000 years after repository closure (Reference-Case calculations) and thereafter to offer no physical resistance to radionuclide migration;
- no account is taken of sorption and co-precipitation of radionuclides with secondary minerals in the glass and canister corrosion products.

Results of calculations (using STRENG) are nuclide release rates (moles y^{-1}) as a function of time since canister failure, integrated over the whole repository (2,693 canisters).

Some results for the Reference Case are shown in Figure 2.6 in terms of release rates of nuclides to the geosphere over time. Peak release rates of selected nuclides for the Reference Case and several single parameter variations are compared in Figure 2.7. The two histograms show release rates expressed in a) moles per year, and b) according to the dose index, defined as the ratio of annual individual dose (using dose-conversion factors given in NAGRA 1994b) to the regulatory limit of 0.1 mSv y^{-1}. That no case in the latter exceeds unity, suggests that the regulatory guideline can be met without taking into account retardation and decay in the geosphere. Only in the extreme case where all the conservative parameter values are combined, together with effectively unlimited water flow, is the guideline exceeded and then only by ^{239}Pu, ^{240}Pu and ^{243}Am, further illustrating the effectiveness of the engineered barriers.

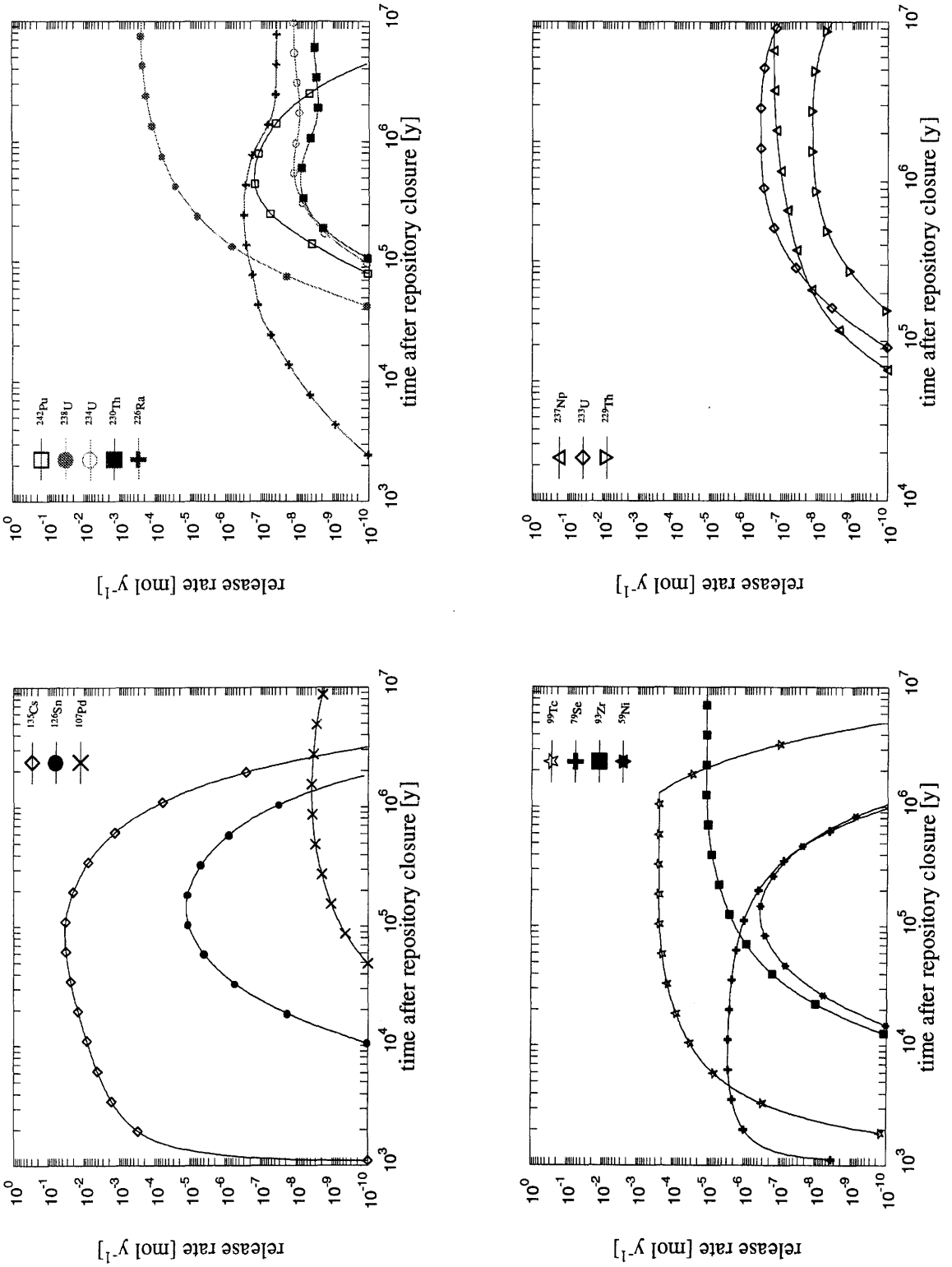

Fig. 2.6: Release rates (for fission products and 2 actinide chains), integrated over the whole repository, as a function of the time elapsed since repository closure for the Reference-Case calculations. A common scale was adopted to facilitate comparison of the results, hence, the curves for some shorter-lived actinide parents do not appear as they have decayed to insignificance.

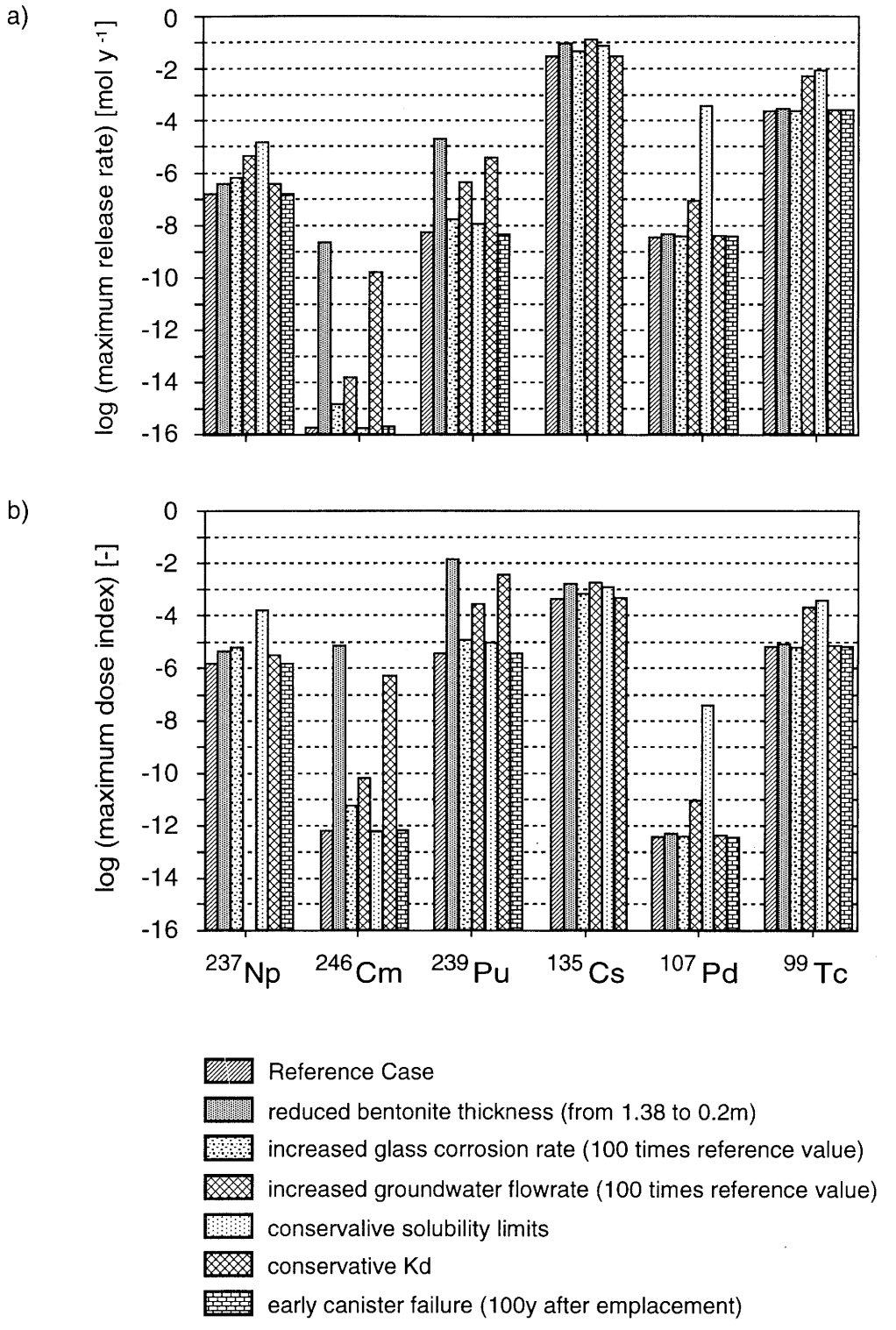

Fig. 2.7: Maximum near-field release rates for selected radionuclides and their sensitivity to parameter variations which increase release rates with respect to the Reference Case. Release rates are expressed as a) moles per year, and b) as a dose index, defined as the ratio of annual individual dose to the regulatory limit of 0.1 mSv y^{-1}.

2.4.6 Geosphere

Nuclides can be transported from the repository into the higher-permeability domain and, thence, to the biosphere, either directly through the low-permeability domain or via both the low-permeability domain and major water-conducting faults. In either case, advection of nuclides in solution through channels in water-conducting features and diffusion into the stagnant pore water of adjacent altered host rock (matrix porosity) are expected to be the dominant transport mechanisms. The geosphere model also takes into account the influence of dispersion of the nuclides, diffusion into and sorption on host rock and transport by groundwater colloids (omitted from the Reference Case, but treated as a model variation to allow scoping calculations to gauge the maximum effect) to calculate the release rates into the biosphere.

Groundwater flow in the low- and higher-permeability domains occurs in a network of smaller water-conducting features of three types with different geological and mineralogical characteristics: cataclastic zones, jointed zones and fractured aplitic/pegmatitic dykes. Each consists of a set of sub-parallel, partially infilled fractures. Water flows through channels in the fracture infill. An example of a cataclastic zone and its conceptualisation for the purpose of transport modelling is shown in Figure 2.8. The complex internal structure of the channels in the water-conducting features is further simplified to a single, representative, parallel-walled or tubular conduit of specified

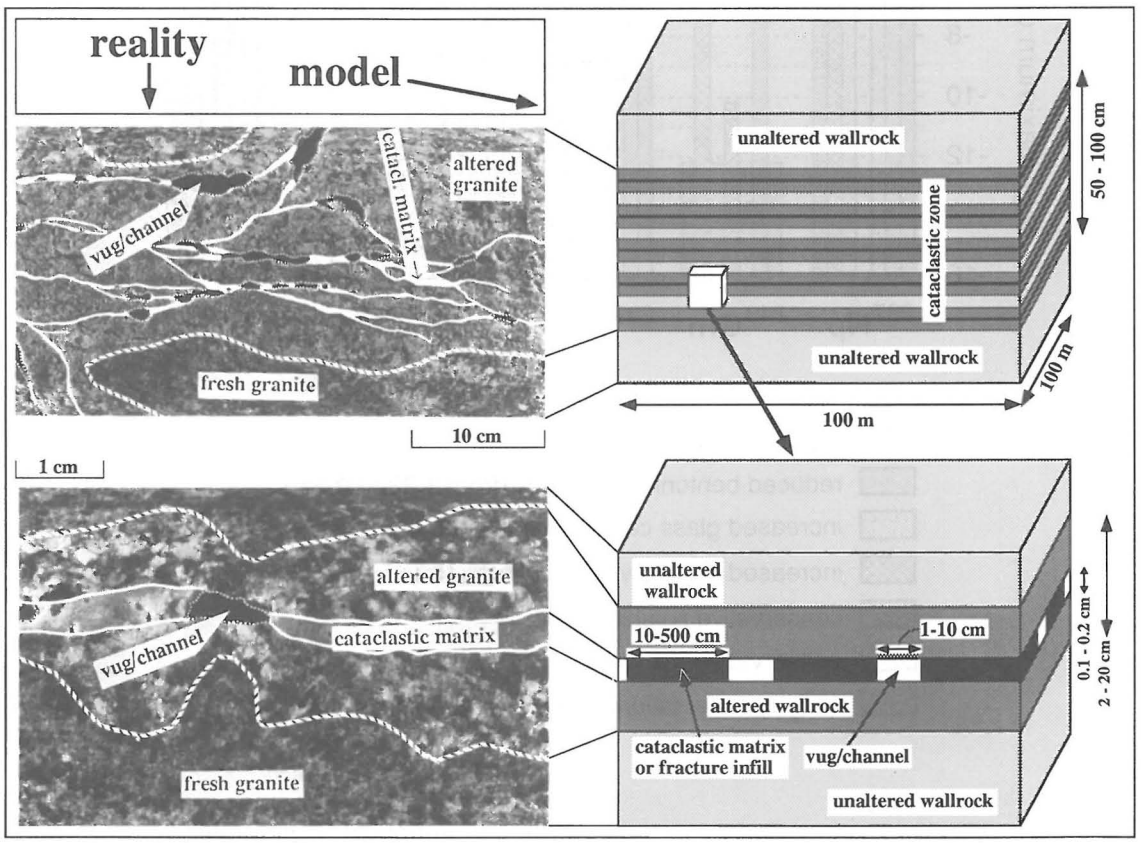

Fig. 2.8: Small-scale conceptual model of cataclastic zones in the crystalline basement compared to "reality" as observed in bore core samples.

width (or radius) and length (migration path length). Variability in the dimensions and frequency of the conduits and the extent of connected matrix porosity is accounted for by defining six model geometries. Cataclastic zones or jointed zones with large, widely spaced conduits and matrix diffusion confined to a spatially-limited altered zone, were found to be the least effective in terms of radionuclide retardation. Consequently, this geometry was used in the Reference Case as, in the absence of further knowledge of the abundance of each type of water-conducting features, it represents a conservative choice.

All calculations have been performed with the codes RANCHMD and RANCHMDNL (for non-linear sorption). Results, given in terms of maximum annual individual doses for specific nuclides for 2 far-field transport scenarios (cataclastic/jointed zones with limited and with unlimited matrix diffusion) are shown in Figure 2.9. For comparison, the results for near-field release (Fig. 2.9) take no account of retardation in the geosphere as radionuclides are released directly from the near field into the geosphere.

Results from the geosphere assessment modelling indicate that:

- the choice of the geometrical representation of the water-conducting features in the low-permeability domain is critical to the calculated performance of the geological barrier;
- the variability in groundwater flow between features can be important - a few water-conducting features carrying high water flow can significantly affect the overall performance of the low-permeability domain as presently calculated;
- the high water fluxes through the major water-conducting faults mean that they provide an insignificant barrier to radionuclide migration compared to the low-permeability domain;
- the use of a non-linear sorption isotherm for caesium does not greatly affect the performance of the low-permeability domain in the Reference Case;
- allowing for transport of radionuclides on colloids naturally present in groundwater has little effect on the Reference-Case results despite the use of conservative parameter values for sorption on colloids and colloid concentration. (But the model used does assume reversible nuclide uptake on such colloids.)

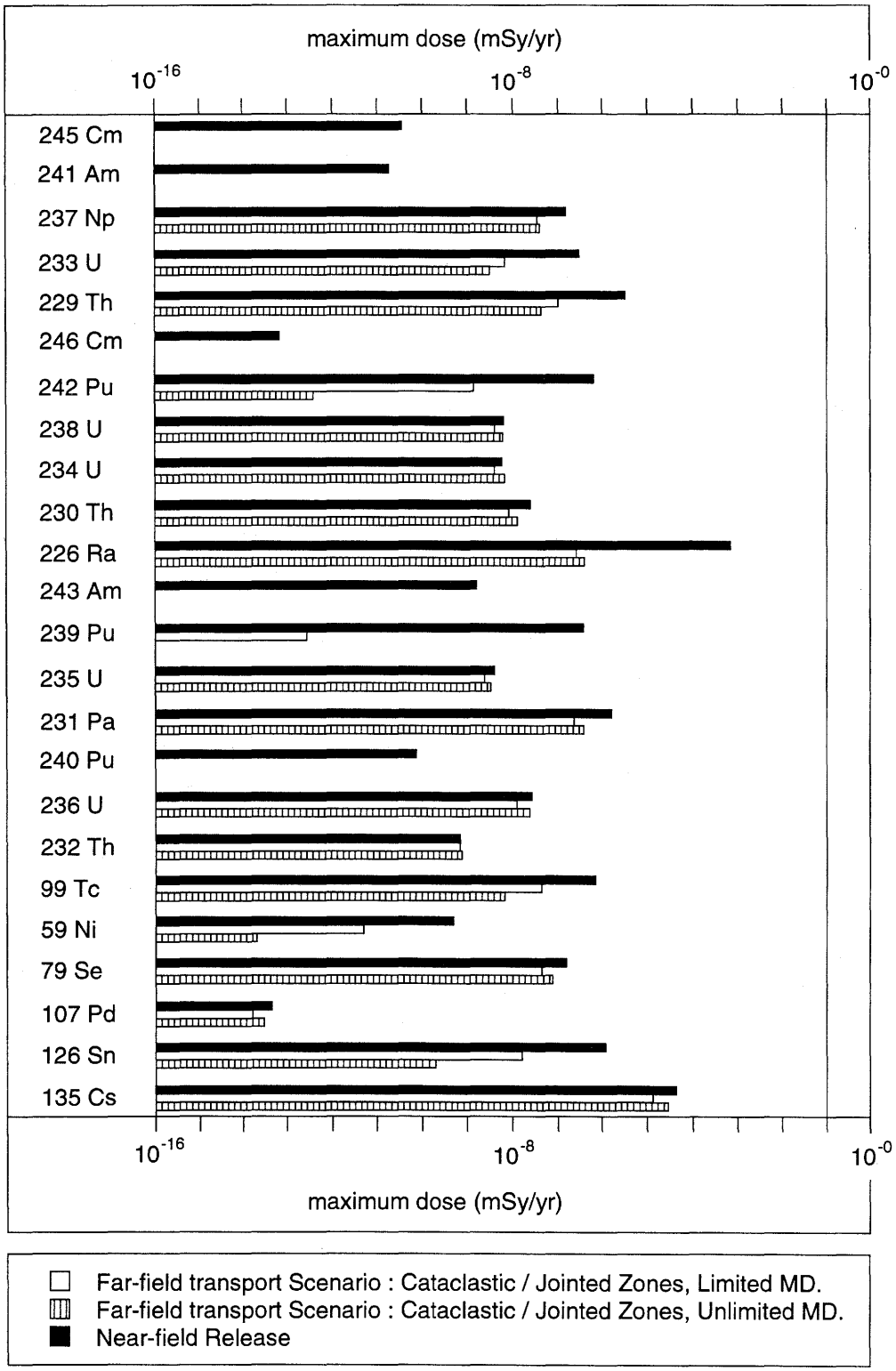

Fig. 2.9: Parameter variations study showing the effect of transport through the cataclastic/jointed zones, with differing extent of accessible matrix for diffusion.

2.4.7 Biosphere

The aim of the biosphere modelling is to convert the estimated releases of radionuclides from the engineered and geological barriers to a scale, in this case dose, which is an acceptable parameter for discussing radiological hazard.

The detailed calculations for the individual dose consider different exposure pathways (external radiation, inhalation, ingestion of water and consumption of various foodstuffs) and are performed with the code TAME. TAME is a linear dynamic compartment model with transfer coefficients which are constant in time (driven by solute and solid material transport). The main physical components of the biosphere reference model are: a local aquifer in the gravel terraces of the Rhine valley, a deep soil layer and a top soil layer, surface water (Rhine river water) and aquatic sediment (Rhine bed sediment).

A number of alternative biosphere scenarios have been identified:

- Rhine valley with gravel terraces containing a local aquifer constitutes the Reference Scenario;
- a tributary valley with terraces and an aquifer is only considered for Area East;
- Rhine river flowing on bedrock, e.g. following erosion of alluvial sediments;
- a deep well with abstraction of water directly from the crystalline basement.

These scenarios (except the deep well scenario for which climate is not relevant) consider a temperate climate, representative of present day, with subsistence arable and livestock farming. Three further alternative scenarios consider climate variations on the case of the Rhine valley with gravel terraces:

- cold climate - tundra climate representative of future periglacial periods;
- humid climate - warm wet conditions representative of possible conditions if glacial cycling ceases;
- arid climate - warm dry conditions representative of possible (less likely) conditions if glacial cycling ceases.

Relevant information for these alternative biosphere scenarios include physical properties in the compartments and water and solid material fluxes determined by topography and climate. The sensitivity of the doses to parameter variations, such as source of irrigation water or local aquifer thickness, are investigated in series of additional calculations.

2.5 Results for the total system

The calculated annual individual dose for the Reference Case is shown in Figur 2.10. The HSK R-21 regulatory limit of 0.1mSv y^{-1} is shown for comparison and also the range of typical natural radiation exposures in Switzerland. It should be noted that:

- The calculated peak annual individual dose is more than two orders of magnitude below the regulatory limit. It occurs at more than 200,000 years after repository closure and is dominated by ^{135}Cs.
- ^{79}Se is also important at earlier times (generally between 10^4 and 10^6 years) and ^{99}Tc makes a significant contribution between about 1 and 3 million years after closure.
- At later times greater than 10^7 years, the long-lived daughters in the 4N+3 (plutonium) chain become important.

The calculated doses are considered to be conservative estimates, partly due to some conservatism in the choice of data but mainly because i) some processes which are expected to have a beneficial effect have been omitted from the Reference Scenario, and ii) the Reference Case includes conservatively selected models of certain key processes.

In addition, the sensitivity of the calculated peak individual dose to parameter variations and alternative model assumptions is quite limited because the behaviour of the dominant nuclide, ^{135}Cs, is relatively insensitive to these changes. Even for the Robust Scenario, in which the most pessimistic representation of the geological barrier is assumed with no retardation of the nuclides between the bentonite-host rock interface and the biosphere, doses occur at earlier times but the peak individual dose calculated is still about two orders of magnitude below the regulatory guideline. If an unlimited groundwater flow rate is used as a parameter variation within the Robust Scenario to give a "zero-concentration" boundary condition at the bentonite-host rock interface (which increases diffusion in the bentonite buffer), the maximum dose is still less than the regulatory guideline by a factor of three (Fig. 2.11).

In summary, the results of the Kristallin-I assessment indicate that:

- Where realistic-conservative parameter values (Reference Case) are used, the calculated annual individual dose is several orders of magnitude below the regulatory guideline of 0.1mSv y^{-1}.
- Parameter variation calculations for the Reference Scenario and alternative scenarios, in which one or more parameters are assigned highly conservative values, also give doses below the regulatory guideline.
- Only in the case of an extremely unlikely combination of many conservative assumptions and models is the regulatory limit approached and even such unlikely scenarios do not give doses above natural background.

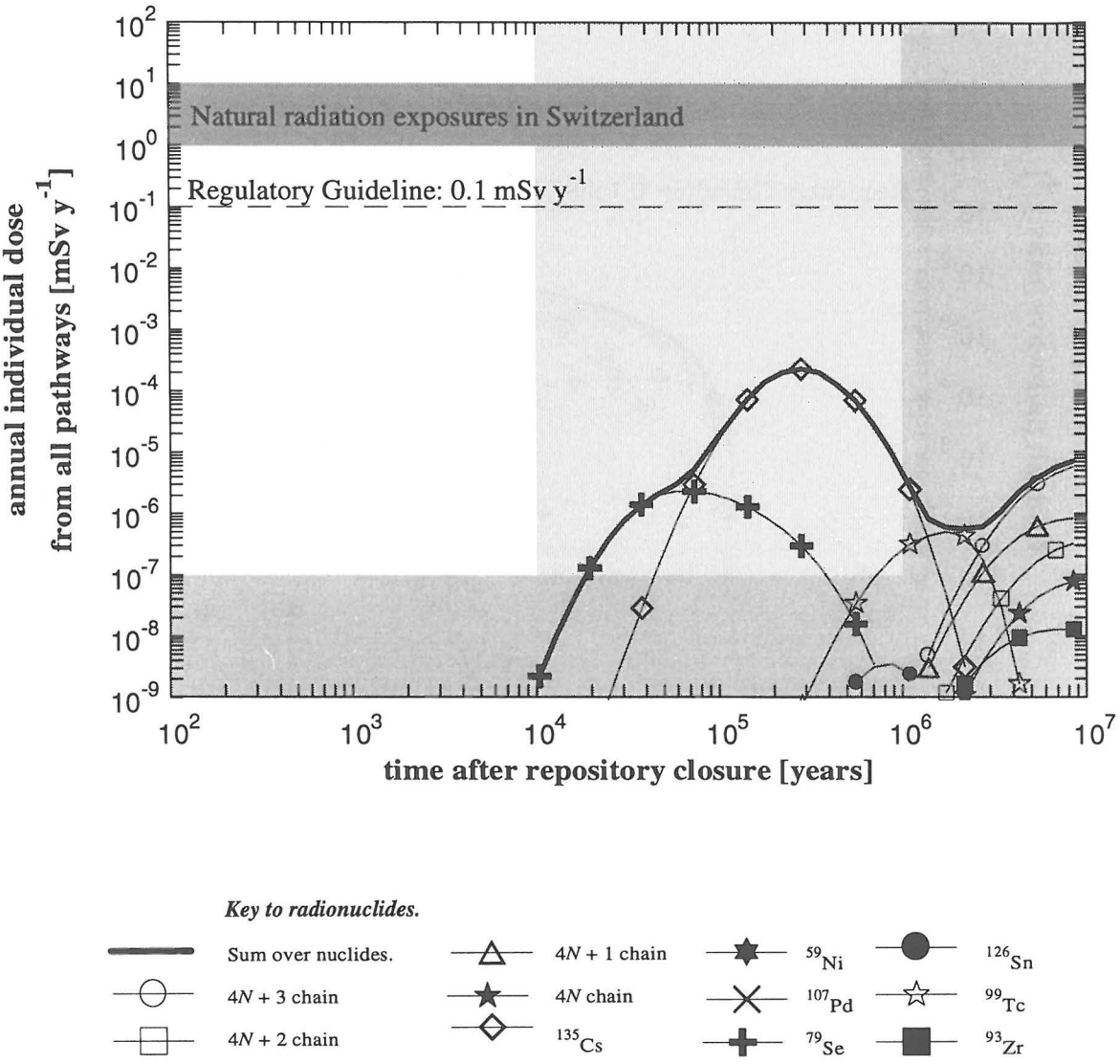

Fig. 2.10: Results of the Kristallin-I Reference-Case calculation - annual individual dose as a function of time after repository closure. The regulatory guideline of 0.1 mSv y^{-1} is shown, together with the range of typical natural background radiation in Switzerland (including radon).

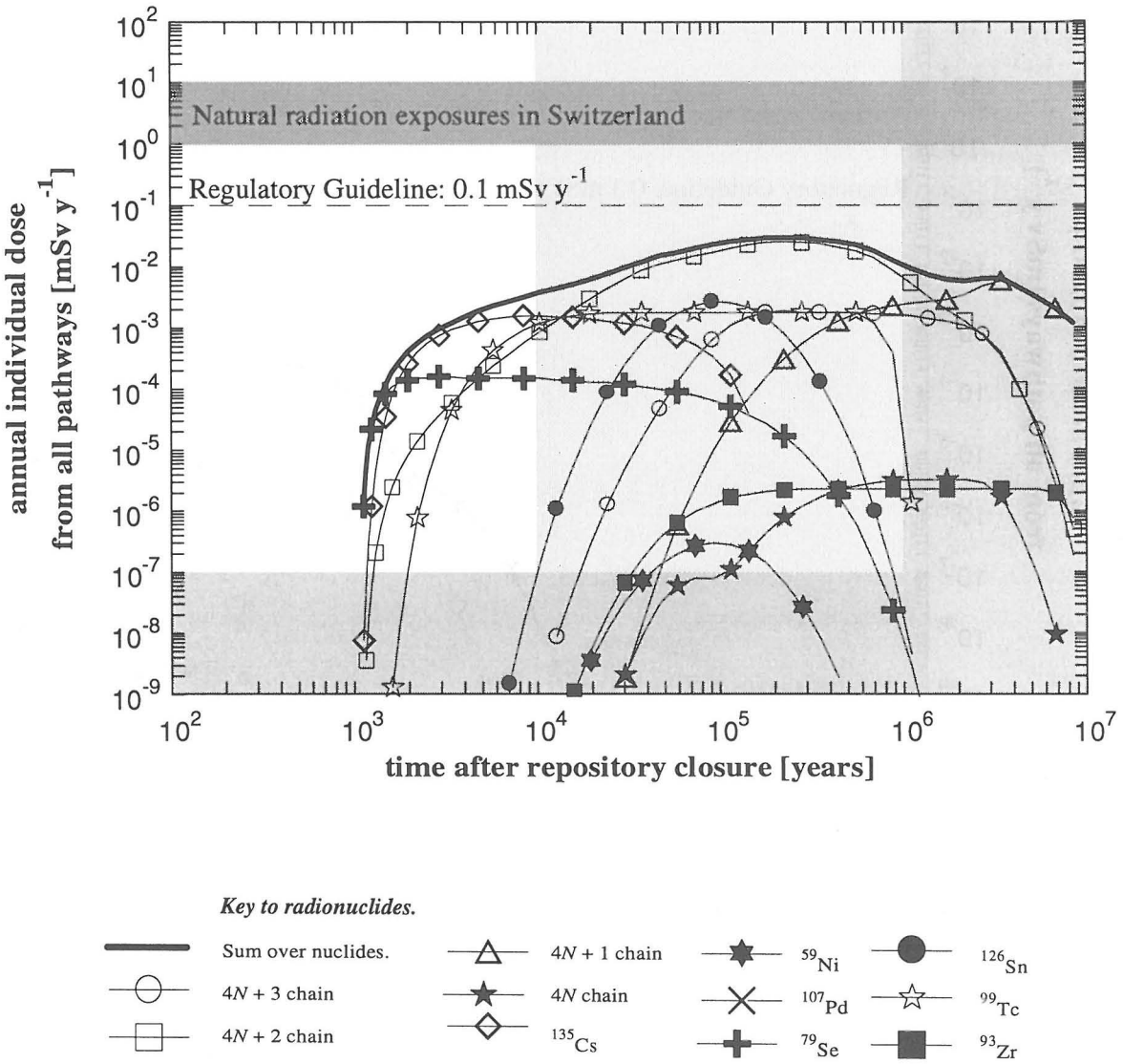

Fig. 2.11: Time history of the annual individual doses in the Robust Scenario assuming a zero-concentration boundary condition at the bentonite-host rock interface. The regulatory guideline of 0.1 mSv y^{-1} is shown, together with the range of typical natural background radiation in Switzerland.

3 COMPARISON OF PROJECT GEWÄHR, H-3 AND KRISTALLIN-I

F.B. Neall, P.A. Smith and H. Umeki

3.1 Introduction

The similarities between the Swiss and Japanese HLW disposal concepts (Table 3.1) make it possible to compare the performance assessments Project Gewähr (NAGRA 1985a) 1985b), Kristallin-I (NAGRA 1994b) and PNC H-3 (PNC 1992) relatively closely. Within this chapter, section 3.2 briefly describes the Project Gewähr and H-3 performance assessments (Kristallin-I has already been described in some detail in Chapter 2), section 3.3 is a comparison of the models used and the implicit assumptions and simplifications in the performance assessments, and section 3.4 compares the results and discusses differences in terms of variations in data and differences in the models.

3.2 Aims and approach of Project Gewähr and H-3

3.2.1 Project Gewähr

Project Gewähr was a legally required demonstration of the feasibility of nuclear waste disposal in Switzerland. The specific aim of performance assessment was to show

" ....quantitatively using safety analysis that the final disposal of all categories of nuclear waste is possible with present-day technology without exposing the population to unacceptable radiation risks (demonstration of long-term safety)" (NAGRA 1985a).

Like Kristallin-I, Project Gewähr was not site-specific and used regional data from the N. Swiss crystalline basement, particularly the Nagra Böttstein borehole. However, the regional geological studies (reported as part of Kristallin-I) were not complete at the time of Project Gewähr and, hence, the geological database was necessarily less extensive than that available for Kristallin-I.

Scenario development was a relatively straightforward procedure in which processes and events (PEs) which could influence radionuclide release from the repository were identified (scenario catalogue). These were then divided according to the analysis needed to treat them so that PEs which are more probable, given the long periods of time involved in the assessment, are differentiated from those which are unlikely. The set of PEs which constitute the base or Reference Scenario represent the likely evolution of the repository system. These PEs were chosen by informal "expert judgement" system. A realistic parameter set for the reference scenario defined the Reference Case.

Steady state groundwater flow was modelled for 3-dimensional volumes with 1- or 2-dimensional discontinuities. The program FEM301 was used to solve the equations to produce maps of hydraulic potential which provided indirect input to the biosphere model by identifying areas of groundwater exfiltration. The potentials were converted into groundwater flow which provided input to the near-field and geosphere models in

the form of specific discharge through the repository and along the transport path, respectively. Local-scale hydrodynamic modelling suggested that flow paths from the repository lead steeply upwards towards the Rhine in the north. The most unfavourable situation occurs when the flow path rises very steeply from the repository location in the middle to the more permeable upper crystalline basement which then provides a rapid transit to the exfiltration zones along the Rhine.

In the near-field hydrology model, the decompressed zone around the tunnel (excavation disturbed zone or EDZ) was considered as a possible route for enhanced radionuclide transport. The mitigating effects of the bentonite swelling pressure are not, however, taken into account.

Table 3.1: Comparison of the Swiss and Japanese HLW disposal concepts which form the basis for the Project Gewähr, Kristallin-I and H-3 performance assessments

	Project Gewähr & Kristallin-I	**PNC H-3**
Repository host rock	Crystalline basement	Not decided
Repository depth	ca. 1,000 m below surface	500-1,000 m below surface
Waste form	Reprocessed waste in borosilicate glass.	Reprocessed waste in borosilicate glass.
Minimum cooling period	40 years ex reactor	34 years ex reactor
Number of canisters	2693 (5895) (1)	~ 40 000
Canister material	Cast steel	Cast steel
Canister size	Ø: 0.94 m; length: 2.0 m	Ø: 1.04 m; length: 1.95 m
Canister thickness	Body: 0.25 m; Lid: 0.15 m	0.3 m
Disposal geometry	Horizontally spaced in tunnels	Horizontally spaced in tunnels. Vertical boreholes along tunnels also considered.
Backfill material	Purified Na-montmorillonite (15 % quartz, <8 % felspars)	Na-montmorillonite 50-55 % with 5+% feldspar, 30+% quartz, ~2 % calcite, pyrite
Backfill thickness	1.38 m	0.98 m
Canister pitch	5 m	7 m
Tunnel pitch	40 m (20 m option also considered)	Not defined
Exclusion zone for faults and shear zones	100 m	Not defined

1) 120 GW(e) Scenario considered in Kristallin-I; Values for the 240 GW(e) Scenario in Project Gewähr given in parentheses.

The base case calculation for the near field took into account only glass corrosion and solubility limits for determining the release rates of the radionuclides to the geosphere. Diffusion and sorption within the bentonite were not considered. One-dimensional radial diffusion with sorption was modelled separately with the program TROUGH, however, to provide an indication of the most important nuclides and to allow an investigation of the consequences of different near-field boundary conditions.

The model for transport in the geosphere took into account advection/dispersion, limited matrix diffusion and sorption through the middle crystalline basement. One-dimensional solutions to the transport equations were provided by the programs RANCH and RANCHMD (including matrix diffusion). These solutions have been checked against 2-dimensional benchmark studies and found to provide a satisfactory approximation. The base case took conservatively low values for transport path lengths, and retardation in the upper crystalline was conservatively ignored on the basis of short transit times, due to higher hydraulic conductivities, relative to the middle crystalline. However, dilution in the upper crystalline provided a significant contribution to the safety case with a dilution factor conservatively estimated as $1.7 \cdot 10^4$, based on the ratio between the specific discharges of the upper and middle crystalline. When exfiltration was assumed to occur into the Rhine gravels (e.g. base case), a further factor of 80 was also included in the model, which is conservative as no benefit was taken for dilution in the Rhine river.

As in Kristallin-I, a biosphere model is used to estimate doses to the population which arise from the presence of the HLW repository. The model similarly considers the distribution of contaminated groundwater between a number of biosphere compartments (e.g. groundwater, soil, soil water and river for the scenario in which exfiltration takes place into the Rhine gravels) and the uptake of radionuclides into foodstuffs and, hence, to man. However, only the ingestion of food and water are considered as exposure pathways but not dust inhalation and external radiation which are taken into account in Kristallin-I. The base scenario for the biosphere is defined by present-day circumstances, allowing, at least in theory, all parameters to be determined.

3.2.2 H-3

PNC H-3 is the first progress report for Japanese research and development on the geological disposal of high-level radioactive waste. Work relating to three areas is described: 1) studies of the geological environment, 2) research and development of disposal technology, and 3) a performance assessment study. The specific aims of the performance assessment were:

- A detailed analysis of the performance of the engineered barrier system (EBS) in combination with the adjacent geological environment
- An analysis of the natural barrier system and evaluation of its compliance with the required overall system performance.

Research on geological disposal of HLW in Japan is at an early stage and no decision has been made about the host-rock type for the repository. The complex geology of Japan with igneous, metamorphic and sedimentary rocks, and its active tectonic environment mean that a wide range of host rocks may be considered. As a result, the H-3 performance assessment was for a generic host rock, and geological parameters

were given modelled or "representative" values which often span a large range from realistic to conservative in order to include values for this range of potential host rocks.

In order to assess barrier performance, a number of groundwater release scenarios were defined in H-3 (groundwater was considered to be the only important means for radionuclide transport). These are descriptions of the processes and mechanisms (FEPs) by which radionuclides are removed from the vitrified waste and transported to the human environment. For the base case scenario, it was assumed that the geological environment was the same as the present-day and conditions (e.g. groundwater flow and chemical properties) remain constant, and that the engineered barriers behaved as designed. Thus, as with Project Gewähr, the base case represented the likely evolution of the repository system. Phenomena which cause sudden changes to the geosphere, such as faulting and igneous activity, or which were judged unlikely, were considered in alternative cases to the base case. Likewise, processes such as diagenesis, weathering and sedimentation, which cause the long-term evolution of the geosphere, were also treated as alternative cases. However, only results from analysis of the base case are presented in H-3.

The program FEMWATER was used to calculate the steady-state flow field in a conceptual 2-dimensional hydrogeological model. The flow field was approximated to a porous medium and various configurations of hydraulic conductivity (e.g. single layer, double layer, additional faults) were considered in order to estimate hydraulic gradients at depth and explore the effect of topographic variations and model boundary conditions. A 3-dimensional analysis of the regional distribution of hydraulic gradients was also carried out for a 600 x 300 km district to a depth of 10 km. Results from this more realistic study suggest that the 2-dimensional model yields very high gradients, however, this was unsurprising considering the conservative assumptions made for topography, distribution of hydraulic conductivity and boundary conditions.

Four different groundwater compositions were defined from geochemical modelling of interaction between water and various mineral assemblages under different conditions, assuming thermodynamic equilibrium. Fresh-reducing-high-pH water is used for the Reference-Case calculations. The other compositions were fresh-reducing-low-pH, saline-reducing-high-pH and saline-reducing-low-pH. The interaction of these water types with both buffer minerals (montmorillonite, calcite etc.) and corrosion products of the steel canister was also modelled in order to determine the composition of the water in contact with the vitrified waste.

As in Kristallin-I and Project Gewähr, the waste canisters were considered to fail simultaneously 1,000 years after repository closure. Release of radionuclides to the geosphere from a single canister was calculated using the program RELEASE in which transport in the backfill is modelled by 1-dimensional radial diffusion.

The retardation available from the geosphere barrier was assessed by considering both fractured and porous media. In both cases, transport was by advection, although diffusion becomes the dominant mechanism for the porous medium with low groundwater flow rates. For the fractured medium, groundwater flow was concentrated in the fractures but the whole extent of the wallrock effective porosity was also available for diffusion.

The geosphere barrier extended from the engineered barrier system to an assessment point at which doses arising from the radionuclide releases were calculated. The geosphere barrier was given an arbitrary thickness which is useful for illustrating its effect and not necessarily corresponding with a realistic situation. A thickness of 10

metres was used for the Reference Case but lengths of 100 and 1,000 metres were also considered. Dilution of the radionuclide-contaminated groundwater by uncontaminated groundwater at the assessment point was taken into account in calculating the doses to the human population.

3.2 Performance assessment

3.2.1 Model chain

A roughly equivalent model chain is used in all three performance assessments (e.g. Fig. 2.5) up to release from the geosphere. At this point the model chains diverge as both Project Gewähr and Kristallin-I use a biosphere model to convert release from the geosphere into a dose to the human population through uptake in the food chain. In H-3, the groundwater release scenarios quantify releases to the biosphere but the biosphere model is replaced by a simple conversion factor. Hence, the comparison of the performance assessments does not include a discussion of the biosphere models.

3.2.2 Near-field model

The processes incorporated in the near-field models and the assumptions made, are summarised in Table 3.2. More specific details are given in numbered comments below.

Apart from details of the composition and thickness of the bentonite backfill, the near-field is almost identical in the three concepts. However, the near-field models used in the performance assessments vary, especially in the complexity of the processes describing the influence of the bentonite buffer. As all models assume simultaneous failure of all steel canisters at 1,000 years, which is the minimum guaranteed time span before corrosion failure of a canister, the inventory of radionuclides in the waste is adjusted to take account of decay and ingrowth to this time. The waste inventory per canister is very similar, with differences in most nuclides of less than 10 % between H-3 and Kristallin-I/Project Gewähr. The exceptions are ^{239}Pu (Kristallin-I: 12 % higher) and ^{230}Th (Kristallin-I: 89 % higher).

Project Gewähr: Project Gewähr uses the simplest model and neglects diffusion and sorption in the bentonite buffer in the Reference Case. Radionuclides in solution are released directly into the geosphere. However, nuclide diffusion through the bentonite is modelled separately to determine the radionuclides which are likely to be important in the geosphere and those which can be neglected because they decay entirely within the near field:

Note: 1) (Table 3.2) The surface area available for dissolution includes the surfaces available from fracturing of the glass block (e.g. due to cooling stresses). To account for this the glass is modelled as small spheres. The total volume of spheres per container is equal to that of the glass cylinder and the total surface area is initially equal to that of the fractured block (approximately 12.5x the surface area of the unfractured block, referred to as the geometric surface area).

Table 3.2: Comparison of assumptions for the near-field radionuclide release models of Project Gewähr, Kristallin-I and H-3 (see text for notes)

Model process and assumptions	**Project Gewähr**
Rock ambient temperature	55 °C
Bentonite re-saturation	Instantaneous on repository closure
Canister failure	Fail simultaneously at 1,000 yrs. No transport resistance after failure
Canister corrosion products	Buffer Eh. Co-precipitation and sorption properties ignored.
Glass corrosion rate	Dependent on Surface Area which is *f*(t)
Surface area for glass dissolution	Glass modelled as spheres of equivalent volume to account for increased sur face area due to fracturing. Initial SA 12.5x geometric, decreases with volume (1)
Radionuclide dissolution	Congruent with glass dissolution
Elemental solubility limits	Shared amongst all radio-isotopes not including stable nuclides
Natural U abundance in groundwater	Ignored
Transport in backfill	Considered only to eliminate short-lived nuclides from consideration
Colloids	Filtered by bentonite
Bentonite alteration	No changes over timescale of interest (10^7 years)
Bentonite inner boundary condition	Not applicable
Bentonite outer boundary condition	Not applicable
Heterogeneity in groundwater flow over repository	Ignored in base case (scoping calculations)

Table 3.2 (cont.): Comparison of assumptions for the near-field radionuclide release models of Project Gewähr, Kristallin-I and H-3 (see text for notes)

Kristallin-I	**H-3**
55 °C	Not known; 25 °C used for modelling
Instantaneous on repository closure	Water diffuses in over 100 yrs
Fail simultanously at 1,000yrs. No transport restance after failure.	Fail simultaneously at 1,000 yrs. No transport resistance after failure.
Buffer Eh. Co-precipitation and sorption properties ignored.	Buffer Eh. Co-precipitation and sorption properties ignored.
Dependent on Surface Area which is *f*(t)	Time independent
Glass modelled as spheres of equivalent volume to account for increased surface area due to fracturing. Initial SA 12.5x geometric, decreases with volume (1)	Glass geometric surface area increased by 10x to account for fracturing (4)
Congruent with glass dissolution	Congruent with glass dissolution
Shared amongst all isotopes including stable nuclides in glass.	Not shared: elemental solubility assigned to each radio-isotope (5)
Ignored	Synthetic groundwater containing no U.
Diffusion in porewater only, advection unimportant due to low permeability.	Diffusion in porewater only, advection shown to be unimportant
Filtered by bentonite	Filtered by bentonite
No changes over timescale of interest (10^7 years)	Montmorillonite not altered (6) but calcite removed by reaction with groundwater
Solubility limited concentration in reservoir volume (except Cs, Ni) (2) otherwise limited by supply rate from glass	Solubility limit for low solubility nuclides; glass dissolution controlled concentration for highly soluble nuclides (7)
Mixing tank with diffusive flux in equal to advective flux to geosphere. Concentration depends on groundwater flow	Zero concentration of nuclides (equivalent to infinite groundwater flow).
Ignored in base case (scoping calculations)	Ignored

Kristallin-I: The near-field model used in Kristallin-I is essentially the same as Project Gewähr except that the barrier effect of the bentonite buffer is included in the Reference Case:

Note: 2) As radionuclides are released by dissolution of the glass, they are dissolved in a reservoir of water which represents the volume of water in the contact with fractured glass. The reservoir is modelled as an annulus outside the glass and thus, there is no retardation due to diffusion of the solute out of the glass fractures. If the solubility limit of an element is exceeded, further release from the glass results in precipitation of a secondary mineral which is stored in the reservoir. The dissolved nuclides, up to their solubility limited concentration, are available for diffusion. Some elements are not solubility limited (e.g. Cs and Ni), thus their concentration in the reservoir is determined by glass dissolution and diffusion.

H-3: Although the near-field model used in H-3 is a little more sophisticated in the range of processes considered than Project Gewähr and Kristallin-I, in practice, lack of essential data means that assumptions and estimates must be made which result in little improvement on the simpler Kristallin-I case. The concept used differs from that of the Swiss because the bentonite buffer is thinner (< 1 m) and contains only 50-55 % Na-montmorillonite. The remainder is quartz sand (30-35 %) and other mineral impurities which are expected to favourably influence the chemical environment (e.g. calcite and pyrite):

Note: 3) Consideration of the resaturation of bentonite by diffusion of groundwater has no practical effect on the near-field model as resaturation time is within the 1,000 year assumed minimum life of the canisters, after which they are assumed to fail leading to glass dissolution.

Note: 4) The available surface area of the glass used was ten times the initial geometric surface area to account for fractures. This value remains constant and the dissolution rate does not change with time

Note: 5) Shared solubility limits for isotopes of an element, as used in Project Gewähr and Kristallin-I, affect the releases of isotopes of solubility-limited elements with two or more isotopes and are particularly important for U isotopes. In Kristallin-I, the nuclide inventory per canister includes stable isotopes of Pd, Se and Sn which also have the effect of diluting the radioisotopes of these elements under the shared solubility limit condition. However, not sharing an elemental solubility limit between its isotopes is conservative, even if very unrealistic, as it results in higher isotope release rates. In Kristallin-I and Project Gewähr, no account is taken of precipitation of radionuclides due to ingrowth in the bentonite or geosphere. In H-3 however, such precipitation is taken into account.

Note 6) The duration of chemical buffering provided by the components of the bentonite material was found by chemical modelling to be dependent on the amount of calcite rather than ion exchange capacity of the montmorillonite clay. However, calculation of the duration required knowledge of groundwater flow and the amount of calcite in the bentonite material. Hence the buffering may last 10^3 - 10^7 years for fresh reducing high pH groundwater (Reference Case), depending on the values chosen for these parameters. Calculations of radionuclide solubility were made for both calcite-buffered conditions and calcite depleted, unbuffered conditions.

Note: 7) In practice this is very similar to Kristallin-I as the only nuclide modelled with a sufficiently high solubility limit to be actually limited in solution by the glass dissolution rate is Cs.

3.2.3 Geosphere models

The geosphere model used in Project Gewähr forms a prototype for that used in the other two performance assessments, hence this model is described in some detail and only variations from it are described for Kristallin-I and H-3.

3.2.3.1 Project Gewähr

The Swiss crystalline basement in the area of interest comprises a 300-500 m thick zone of relatively higher permeability rock (upper crystalline) overlying a low permeability zone (middle crystalline). The planned repository will be located in the middle crystalline, some 200 m below the middle/upper boundary. The middle crystalline was modelled as an inhomogeneous porous medium with "permeable" zones (hydrau lic conductivity $>10^{-12}$ ms^{-1}) containing fractures and veins in which most of the water flow was expected to occur. Three types of flow system were identified in the permeable zones:

- Kakirite zones[1], with vuggy to porous quartz veins surrounded by impermeable kakirite;
- Kakirite zones intersecting or displacing dykes;
- Strongly fissured aplite and pegmatite dykes.

For the impermeable zones with hydraulic conductivity $<10^{-12}$ ms^{-1}, it was conservatively assumed that water flow was concentrated in microfractures rather than throughout the pore space.

The veins within the kakirite zones were modelled as a network of tubes of constant radius surrounded by altered wallrock. The aplite and pegmatite dykes were described as planar fractures. Water velocity in the fractures and veins was determined from the groundwater flow rate, number of tubes or fractures per unit area perpendicular to flow, and the cross-sectional area of the tubes or fractures.

Advective groundwater flow was assumed to be the dominant mechanism for radionuclide transport. The radionuclides are carried in solution and solubility limits are not exceeded within the geosphere. Hydrodynamic dispersion was modelled to account for molecular diffusion and mechanical dispersion due to variability in flow path length.

---

[1] Kakirite zones: Megascopically sheared and brecciated rock in which fragments of the original material are surrounded by gliding surfaces along which intensive granulation and some recrystallisation has occurred. American Geological Institute, Glossary of Geology, 2nd Edition, 1980.

Matrix diffusion of the radionuclides in stagnant porewater adjacent to flowing fractures/pores was restricted to the altered wallrock in the kakirite zones with the possibility of diffusion from the kakirite into the undisturbed crystalline host rock neglected. For the aplite/pegmatite dykes, diffusion was restricted to a thin (1 mm) altered layer around the water-carrying fractures. In this latter case, the diffusion is considered sufficiently fast that it can be approximated by use of an effective retention factor in the transport equations. Interaction between nuclides and the wallrock pore surfaces is assumed to be instantaneous, reversible equilibrium sorption. Linear (i.e. concentration independent) isotherms are used for all radionuclides.

Dilution occurs in aquifers along the flow path, e.g. from the middle to the upper crystalline basement, a dilution factor of $2x10^4$ was used.

For the Reference Case, the geosphere transport is within the vein system of the kakirite zones of the middle crystalline basement.

3.2.3.2 Kristallin-I

For Kristallin-I, the model for the geosphere transport changed less than the language used to describe it: the "permeable zones" become "transmissive elements" which consist of sets of sub-parallel, partially infilled fractures in which water flows through openings within the fracture infill. The three types of flow system are then:

- cataclastic zones;
- jointed zones;
- fractured aplite/pegmatite dykes and aplitic gneisses.

Due to their similar behaviour, no distinction is made between cataclastic and jointed zones in the modelling. They are both described using two different geometries: small, closely-spaced openings modelled as veins, and broad, widely-spaced openings modelled as fractures, to encompass the range of opening width and separation observed. The fractured dykes and gneisses are described with a fracture model.

All three geometries are considered with both limited (only altered wallrock immediately adjacent to, or surrounding, an opening) and unlimited matrix diffusion. However, it is important to note that unlimited matrix diffusion still involves only a fraction of the volume of wallrock in a transmissive element as altered wallrock between openings is not accessed.

Radionuclide sorption occurs on the surfaces of pores within the porous region accessed by diffusion. Sorption on fracture surfaces is neglected. Linear isotherms are used for all nuclides except ^{135}Cs for which a Freundlich isotherm was also used (in RANCHMDNL).

Although transport of radionuclides in solution by groundwater flow was assumed to be the main mechanism for their movement, transport by colloids was also considered. Sorption of radionuclides onto colloids reduces the "free" nuclide concentration and, thus, may reduce retardation of nuclides by diffusion and sorption.

For the Reference-Case geosphere, the transmissive element geometry used was cataclastic/jointed zones with broad, widely spaced openings. Limited matrix diffusion

was assumed. The effect of groundwater colloids was neglected and conservative linear isotherms were used for wallrock sorption of all nuclides.

3.2.3.3 H-3

As H-3 is not site- or host rock-specific, the models and parameters used to describe the geosphere must encompass a wide range of possibilities. Consequently, although a dual porosity flow model of the host rock was used, the fracture elements are much simpler than in Project Gewähr or Kristallin-I: the fractures are described as simple parallel-sided structures with 1-D advection/dispersion plus 1-D matrix diffusion perpendicular to the fracture planes. An alternative model of the geosphere as an equivalent porous medium is also considered in H-3 but the discussion here focuses on the fractured medium geosphere model because of its greater similarity to Kristallin-I and Project Gewähr.

Water velocity in the fractures is obtained from the groundwater flow rate and by using the cubic law[2] to compute the fracture apertures. In the absence of geological information, it may be necessary to use this method despite its inaccuracy for natural fractured media.

Radionuclide diffusion into the fracture wallrock and sorption on fracture and pore surfaces is modelled in a similar manner to the other assessments except that **all** host rock is available for diffusion. This is a major difference from both Project Gewähr and Kristallin-I in which only part of the wallrock of a permeable zone or transmissive element is available for diffusion and the zones or transmissive elements, themselves, only constitute about 10 percent of the whole host rock volume. Hence, for radionuclides for which sorption is important, there is around 3 orders of magnitude greater volume of host rock available for diffusion/and sorption in the H-3 geosphere, which results in greater retardation.

However, it must also be noted that in the H-3 Reference Case, the radionuclide releases are assessed in terms of doses arising at an arbitrary point 10 metres from the engineered barriers system, thus the geosphere consists of only 10 metres thickness of host rock. Such a conservative limit to the extent of the geosphere offsets some of the less conservative assumptions used in the model.

---

[2] The cubic law relates fracture aperture to hydraulic conductivity by the relationship $K = \frac{x^3}{12\,d}$

where K is the fracture permeability, × the fracture aperture and d the fracture spacing. However, it is known to be inaccurate for natural systems as it uses average fracture aperture and ignores the influence of narrow sections in determining overall conductivity.

3.3 Results of the performance assessments

3.3.1 Results of the near-field models

The results of the near-field models are shown in Figures 3.1 (Project Gewähr), 3.2 (H-3) and 2.7 (Kristallin-I). However, the results are not directly comparable in graphical form as the units for presentation of release rate are different (Project Gewähr and Kristallin-I: mol. y^{-1}; H-3: GBq y^{-1}) and release rates are integrated over the whole repository for Project Gewähr and Kristallin-I but given for a single canister in H-3. Values for maximum radionuclide release rates for H-3 have been taken from Figure 4.4.1 in the H-3 Report (PNC 1992) and converted from GBq y^{-1} to mol.y^{-1} to facilitate comparison. Maximum nuclide release rates per canister for the Kristallin-I Reference Case were obtained in the form of tabulated STRENG output (Dr. E. Curti (PSI), pers. comm. c.f. NAGRA 1994b).

The results of the near-field Reference-Case models for Project Gewähr, Kristallin-I and H-3 are shown in Table 3.3. The maximum release rate of a nuclide is given, in moles per year (mol.y^{-1}), and also the time in years after canister failure (Kristallin-I and H-3, only) at which this maximum occurs (t_{max}).

Notable differences include:

- The maximum near-field release rates for Kristallin-I are generally lower than for H-3. For several nuclides: ^{243}Am, ^{107}Pd, ^{79}Se, ^{126}Sn, ^{239}Pu, ^{230}Th and ^{234}U, the Kristallin-I release is several orders of magnitude lower. The notable exception is ^{99}Tc.
- Although ^{135}Cs dominates the near-field nuclide release in both assessments, ^{99}Tc, ^{238}U and ^{235}U are then the most abundant nuclides released for Kristallin-I in contrast to the larger releases of ^{79}Se, ^{126}Sn and ^{107}Pd in H-3.
- The times after canister failure of the maximum radionuclide release rates are much earlier in H-3 than in Kristallin-I, except for short-lived ^{243}Am and ^{240}Pu. For the long-lived isotopes of U, Th and Np, t_{max} differs by at least three orders of magnitude between the two assessments.

The release rates for Project Gewähr (Table 3.3) are not directly comparable with those from the other two assessments as they are controlled only by dissolution of the glass and solubility limits; there is no retardation due to the bentonite and, therefore, no decay or ingrowth is included except within the glass itself. Release rates from Project Gewähr near field are given for interest only and the following discussion focuses on the results of H-3 and Kristallin-I.

Table 3.3: Release of safety-relevant nuclides from the near field (per canister) for Project Gewähr, Kristallin-I and H-3 (see associated text in section 3.3.1)

	Maximum release (mol.y^{-1})			t_{max} (y)	
Nuclide	**PG 85**	**K-I**	**H-3**	**K-I**	**H-3**
^{79}Se	1.3×10^{-8}	1.0×10^{-9}	1.2×10^{-4}	8.0×10^{3}	7.0×10^{1}
^{99}Tc	1.0×10^{-6}	9.4×10^{-8}	1.2×10^{-10}	1.3×10^{6}	8.0×10^{1}
^{107}Pd	1.0×10^{-8}	1.4×10^{-12}	1.5×10^{-7}	1.0×10^{6}	5.0×10^{1}
^{126}Sn	7.6×10^{-9}	4.8×10^{-9}	3.2×10^{-6}	1.3×10^{5}	7.0×10^{3}
^{135}Cs	1.0×10^{-4}	1.3×10^{-5}	4.4×10^{-3}	8.0×10^{4}	4.0×10^{2}
^{245}Cm	1.0×10^{-7}	6.3×10^{-17}		8.0×10^{4}	
^{241}Am	7.6×10^{-6}	1.8×10^{-18}		8.8×10^{4}	
^{237}Np	2.0×10^{-9}	6.0×10^{-11}	3.2×10^{-10}	1.3×10^{7}	5.0×10^{3}
^{233}U	6.4×10^{-11}	1.4×10^{-10}	4.8×10^{-8}	2.5×10^{6}	5.0×10^{3}
^{229}Th	1.3×10^{-8}	4.8×10^{-12}		2.5×10^{6}	
^{246}Cm	1.0×10^{-8}	6.2×10^{-20}		6.4×10^{4}	
^{242}Pu	1.0×10^{-7}	5.8×10^{-11}		5.0×10^{5}	
^{238}U	2.5×10^{-9}	9.3×10^{-8}	5.1×10^{-8}	1.0×10^{7}	7.0×10^{3}
^{234}U	4.6×10^{-12}	4.6×10^{-12}	5.5×10^{-8}	1.0×10^{7}	5.0×10^{3}
^{230}Th	1.0×10^{-8}	1.3×10^{-12}	1.8×10^{-8}	1.0×10^{7}	5.0×10^{3}
^{226}Ra	2.8×10^{-8}	1.1×10^{-10}		2.5×10^{5}	
^{243}Am	1.0×10^{-5}	2.6×10^{-15}	4.5×10^{-11}	8.0×10^{4}	6.0×10^{4}
^{239}Pu	1.0×10^{-7}	2.0×10^{-12}	1.5×10^{-9}	1.6×10^{5}	8.0×10^{4}
^{235}U	2.3×10^{-10}	8.2×10^{-9}	1.1×10^{-7}	1.0×10^{7}	3.0×10^{4}
^{231}Pa	1.1×10^{-9}	1.7×10^{-12}		8.0×10^{6}	
^{240}Pu	4.3×10^{-8}	1.0×10^{-16}	7.4×10^{-14}	8.0×10^{4}	1.0×10^{5}
^{236}U	7.6×10^{-11}	2.1×10^{-9}	3.5×10^{-8}	6.4×10^{6}	8.0×10^{3}
^{232}Th	1.3×10^{-8}	1.2×10^{-9}	5.3×10^{-9}	4.0×10^{7}	4.0×10^{4}

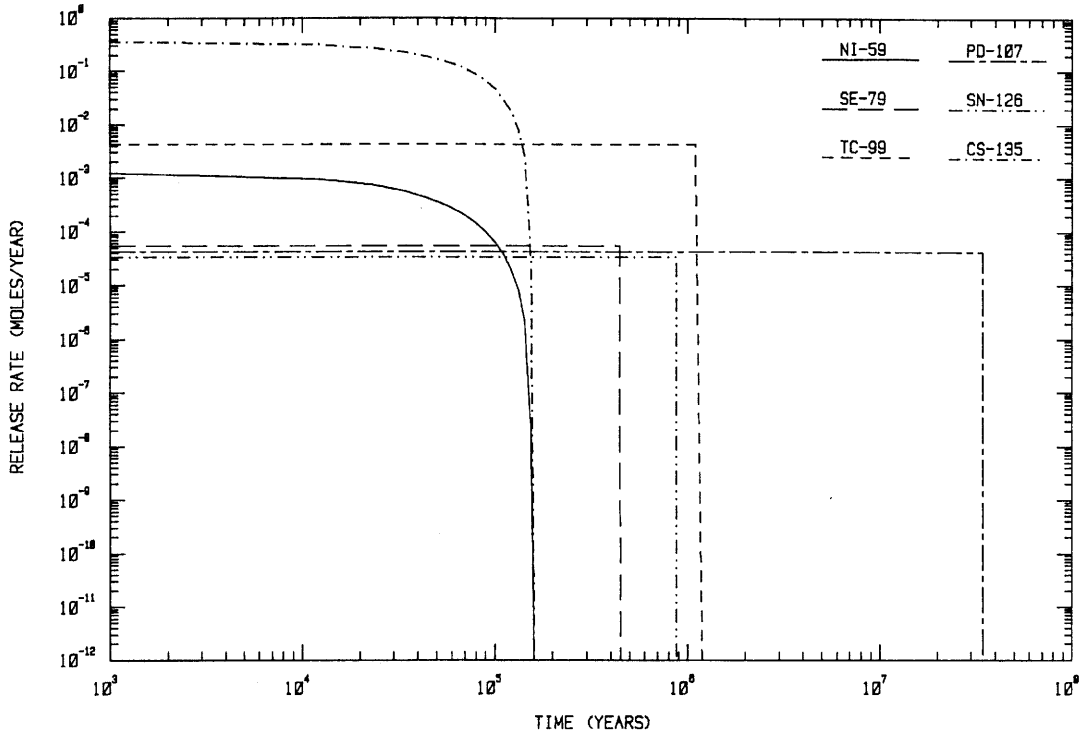

Fig. 3.1a: Project Gewähr calculated release over time from the waste to the geosphere after canister failure; fission and activation products realistic solubility limits.

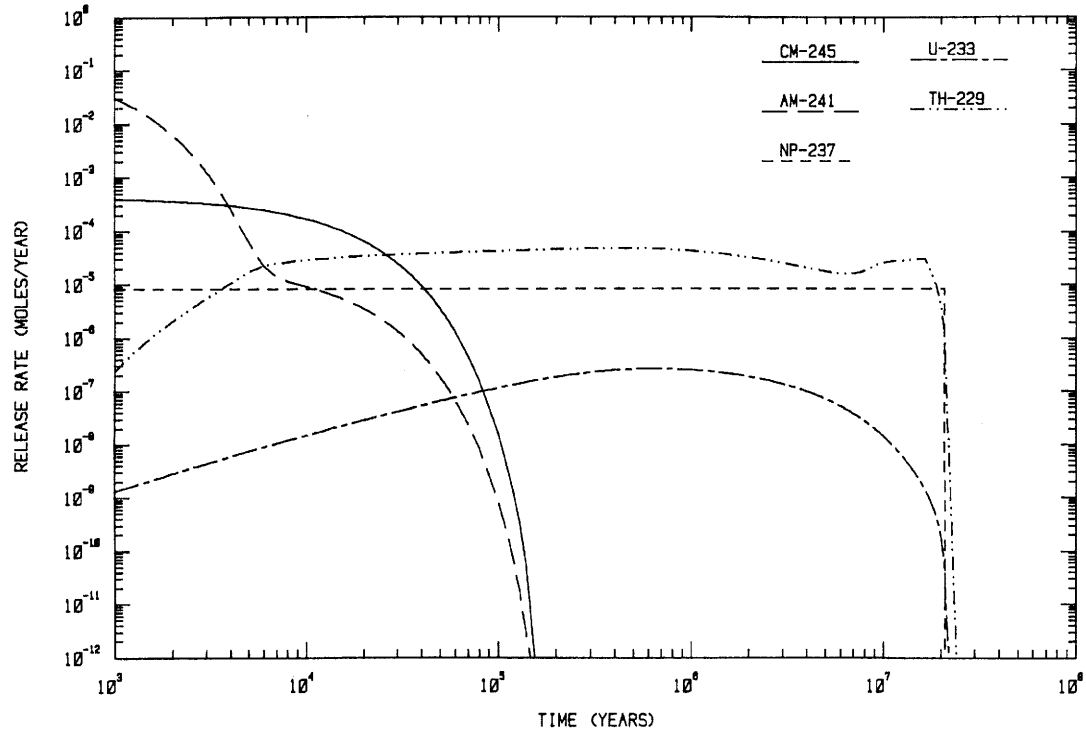

Fig. 3.1b: Project Gewähr calculated release over time from the waste to the geosphere after failure of the canister; ^{245}Cm decay chain realistic solubility limits.

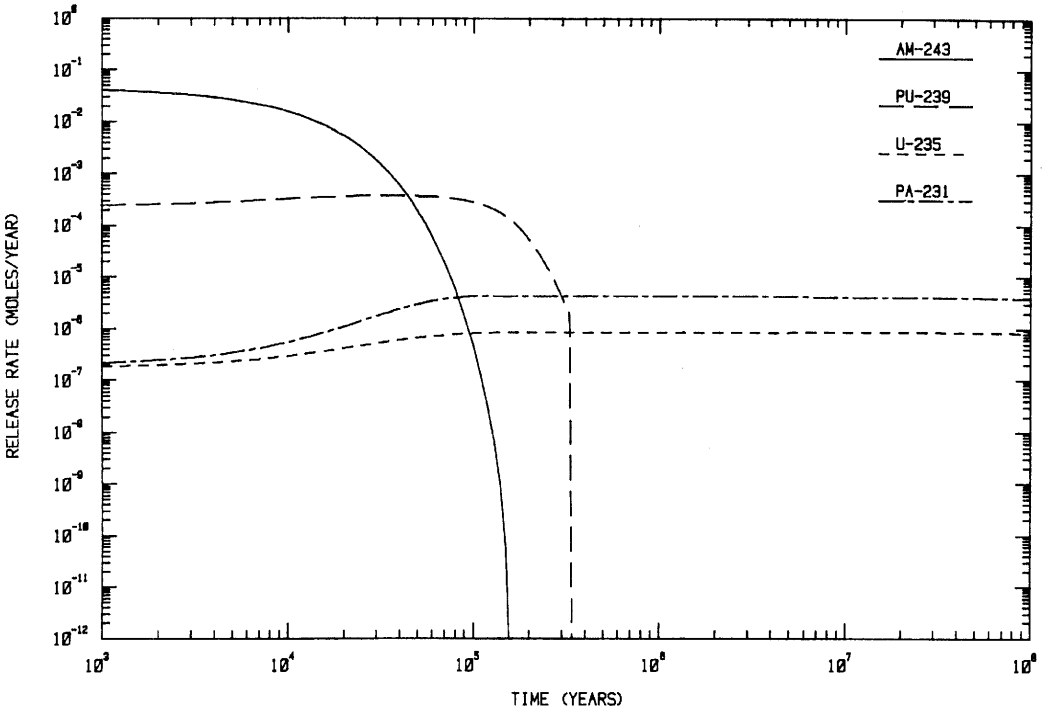

Fig. 3.1c: Project Gewähr calculated release over time after failure of the canisters, from the waste to the geosphere; ^{247}Cm decay chain realistic solubility limits.

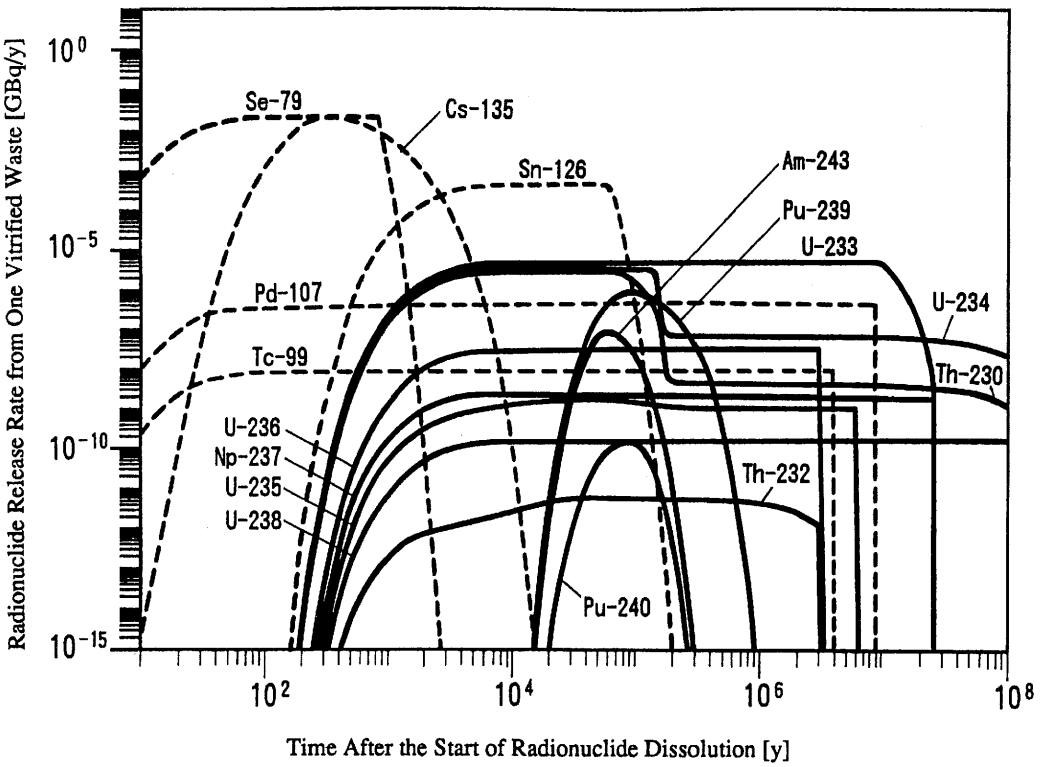

Fig. 3.2: H-3 calculated radionuclide release rate from the engineered barriers for the Reference Case. (Fresh-Reducing-High pH groundwater; realistic solubility limits, single canister). Note that the time scale is given in years after canister failure, i.e. 1,000 years after repository closure.

Table 3.4: Element-specific data used in Kristallin-I and H-3

	Solubility (mol.l^{-1})		**Kd** (m^{3}kg^{-1})	
	Kristallin-I(1)	**H-3**(2)	**Kristallin-I**(1)	**H-3**(2)
Se	1.0×10^{-8}	8.0×10^{-7}	0.05	0.001
Tc	1.0×10^{-7}	1.0×10^{-12} (3)	0.1	0.001
Pd	1.0×10^{-11}	1.3×10^{-9}	1	0.001
Sn	1.0×10^{-5}	2.4×10^{-8}	1	0.1
Cs	high	high	0.01	0.01
Ra	1.0×10^{-10}	-	0.01	-
Th	5.0×10^{-9}	2.5×10^{-10}	5	0.1
Pa	1.0×10^{-10}	-	1	-
U	1.0×10^{-7}	3.9×10^{-10}	5	0.1
Np	1.0×10^{-10}	2.0×10^{-12}	5	0.1
Pu	1.0×10^{-8}	2.5×10^{-11}	5	10
Am	1.0×10^{-5}	6.3×10^{-8}	5	10
Cm	6.0×10^{-8}	-	5	-

Notes: (1) in bentonite pore water at 55 °C; realistic-conservative values
(2) in fresh-reducing-high pH (FRHP) bentonite pore water
(3) analytical detection limit.
A value of 2.0×10^{-10} m^{2}s^{-1} is used for the effective diffusion coefficient, E_pD_p, for all nuclides in Kristallin-I, compared to a value of 3.0×10^{-10} m^{2}s^{-1} used for calculations in H-3.

3.3.1.1 Differences in the maximum release rates

The 1,000 year radionuclide inventories of an individual waste package for Kristallin-I and H-3 are very similar, hence differences in release rates cannot be attributed to dissimilar starting conditions between the two assessments. In any case, most nuclides are solubility limited so that the inventory affects the duration of the release rather than the maximum release rate.

In general terms, the maximum release rate of an element from the near field depends predominantly on its solubility limit (or, for elements which do not reach a solubility limit, on the dissolution rate from the glass) and the delay of the maximum release after the failure of the waste container is due to the elemental diffusion coefficient (Dp) and the retardation in the bentonite which is dependent on sorption[3] (Kd) in the bentonite.

---

[3] Factors such as bentonite porosity and density, which also contribute to the retardation, are very similar in H-3 and Kristallin-I and so do not contribute significantly to differences in the near-field maximum release rates.

This is, of course, a simplification, and radionuclide decay and ingrowth during transport means that the maximum release rates can also be sensitive to retardation. Thus, it is possible that the different Kd values used in Kristallin-I and H-3 result in, or at least contribute to, the differences in near-field release rates between the two assessments. A simple comparison of the data in Table 3.4 shows that the solubility limits used in Kristallin-I are, in general, higher than those used in H-3 and should result in higher maximum release rates for Kristallin-I. Solubility limits cannot, therefore, explain the observed differences in the near-field releases and other factors such as Kd differences and boundary condition assumptions must be investigated.

To test the influence of Kd differences, use can be made of a μ (m), the length scale for diffusion, which may be considered as the distance travelled in one half-life, taking retardation into account.

$$\mu = \sqrt{\frac{t_{1/2}\, D_p}{\ln 2\, R_f}} \qquad (1)$$

where:

R_f is the retardation factor $\frac{1 - E_p\ \rho Kd}{E_p}$ simplified to $\frac{\rho Kd}{E_p}$ when $E_p << 1$

$t_{1/2}$ is the half-life (s)

D_p is the nuclide diffusivity in bentonite ($m^2\ s^{-1}$)

ρ is the density of bentonite (kg m^{-3})

E_p is the effective porosity of the bentonite (-)

Kd is the bentonite sorption coefficient for the nuclide ($m^3\ kg^{-1}$)

The distance travelled in one half-life, μ, can then be compared to the thickness of the bentonite buffer. Values of this ratio (μ/bentonite thickness) less than about one indicate that the nuclide release rate will be sensitive to Kd as there will be significant decay within the bentonite. Conversely, ratios greater than one indicate that travel through the bentonite is quick compared to the half-life and retardation will not significantly affect the maximum release rate.

Values for the ratio are given in Table 3.5 for the most important radionuclides in Kristallin-I and H-3. The ratio is generally higher for nuclides in H-3 so that there are a few nuclides, e.g. ^{126}Sn, ^{233}U and ^{234}U, which are moderately sensitive to Kd in Kristallin-I but not in H-3. For the short-lived nuclides of Am and Pu which are Kd sensitive, there is only a small difference in the calculated value of the ratio due to their effective diffusion coefficients because the difference in Kd values is cancelled by the difference in bentonite thickness. Hence, Kd values cannot account for most of the differences in the maximum release rates between H-3 and Kristallin-I.

A further possibility to account for these differences is the use of different diffusion boundary conditions. In Kristallin-I, the boundary condition at the outside of the bentonite is set by mixing of the diffusive nuclide flux with an amount of groundwater flowing advectively through the repository ('mixing tank' boundary condition). The rate of release of radionuclides by diffusion is equal to their rate of removal by advection, hence, the nuclide concentration at this boundary is dependent on the groundwater flow rate Q. In contrast, the assumption of zero concentration at the boundary in H-3

is equivalent to an infinite flow rate (as the presence of colloids is not considered in H-3). In both assessments, the bentonite inner boundary condition is set by the solubility limits of most elements (except Cs and Ni).

To compare the effect of the different outer boundary conditions, a simple analytical solution for radionuclide release rate (F, moles y^{-1}) in the case of steady state diffusion around a single canister can be used (SMITH 1993):

$$\mathbf{F} = -2\pi r_b' L_c E_p D_p C_s \left[\frac{I_1(r_b') - \kappa K_1(r_b')}{I_0(r_a') + \kappa K_0(r_a')} \right] \qquad (2)$$

and

$$\kappa = -\left(\frac{I_0(r_b') + \xi' I_1(r_b')}{K_0(r_b') - \xi' K_1(r_b')} \right)$$

$$\xi' = 2\pi r_b L_c N_c E_p D_p / Q$$

where:

r_a is the inner radius of the bentonite (m)

r_b is the outer radius of the bentonite (m)

L_c is the length of a waste package (m)

E_pD_p is the effective diffusion coefficient of a nuclide in bentonite ($m^2\ s^{-1}$)

C_s is the elemental solubility limit (M)

Q is the water flow rate through the repository ($m^3\ s^{-1}$)

N_c is the number of waste packages (-)

$I_n(r')$ and $K_n(r')$ are modified Bessel functions of the first and second kinds (-)

$r' = r/\mu$ where μ is as equation (1).

As this approach takes no account of nuclide ingrowth, the calculations were made for the solubility-limited fission products, ^{126}Sn, ^{107}Pd and ^{79}Se but not for members of the actinide chains. The results are presented in Table 3.6. The remaining two order of magnitude differences in the release rates for ^{79}Se and ^{107}Pd between Kristallin-I and H-3 with equivalent water flow, is consistent with the greater solubilities and the influence of longer waste packages, thinner bentonite backfill and lower Kds used in H-3, all of which increase the release rates. The remaining difference for ^{126}Sn release rate can be explained by the contrasting sensitivity to Kd: in H-3 ^{126}Sn is insensitive to Kd (Table 3.5) whereas for Kristallin-I it is moderately sensitive to the higher Kd so that retardation causes a greater decay of the ^{126}Sn within the bentonite.

The large difference in release rate which should arise due to the higher solubility of Sn in Kristallin-I is masked by the influence of the large stable Sn inventory in the Kristallin-I waste where ^{126}Sn is <1 % of total Sn. Elemental solubility is shared between isotopes in Kristallin-I but not in H-3. This causes differences for radio-isotopes of elements which have a large stable inventory in the waste, such as Sn, and for elements with several isotopes such as U. To take U as an example: it is

Table 3.5: The ratio of the diffusion distance travelled in one half-life (μ) to bentonite thickness as an indication of the sensitivity of a nuclide to Kd. Nuclide release is sensitive to Kd when the ratio is less than about 1.0

Nuclide	Kristallin-I	H-3
^{79}Se	4.70	18.5
^{99}Tc	1.90	34.0
^{107}Pd	3.40	190.0
^{126}Sn	0.42	2.30
^{135}Cs	20.0	35.0
^{245}Cm	0.054	-
^{241}Am	0.012	0.015
^{237}Np	0.86	11.0
^{233}U	0.23	2.90
^{229}Th	0.050	0.62
^{246}Cm	0.040	-
^{242}Pu	0.36	0.45
^{238}U	39.0	490.0
^{234}U	0.29	3.6
^{230}Th	0.16	2.0
^{226}Ra	0.53	-
^{243}Am	0.051	0.062
^{239}Pu	0.091	0.11
^{235}U	16.0	193.0
^{231}Pa	0.24	-
^{240}Pu	0.05	0.059
^{236}U	2.80	35.0
^{232}Th	69.0	860.0

noticeable in Table 3.3, that the isotopes of U have similar release rates in H-3 (3.5×10^{-8} - 1.1×10^{-7} moles y^{-1}) whereas for Kristallin-I, there are several orders of magnitude difference (4.6×10^{-12} -9.3×10^{-8} moles y^{-1}) reflecting the proportions of the various U isotopes. However, the total of all maximum release rates for U isotopes for Kristallin-I (Table 3.3) is, at 1.0×10^{-7} mol.y^{-1}, comparable with the highest U release rate for H-3 (^{235}U) under the zero concentration boundary condition.

This is rather coincidental as the higher solubility limit used for U in Kristallin-I should result in higher total U release rates. However, this is offset in H-3 by the 100x higher releases obtained due to the zero concentration boundary condition.

The differences in the relative importance of nuclides contributing to the near-field releases between H-3 and Kristallin-I are clearly a function of the differences in individual nuclide release rates as discussed above. The greater solubility and low sorption of ^{99}Tc in Kristallin-I means that this nuclide is released in greater abundance than any other fission products except ^{135}Cs for this assessment, although it is of less radiological significance to the near-field performance than ^{126}Sn or to the overall performance than ^{79}Se. Likewise, for H-3, the higher solubilities and lower sorption for ^{79}Se and ^{126}Sn compared to U mean that they, with ^{107}Pd, dominate the near-field release.

Table 3.6: Release rates (mol y^{-1}) of selected nuclides from a single canister calculated using a simplified radial diffusion model for the near field to assess the effect of the zero concentration boundary condition on the H-3 results. The releases for the Kristallin-I near field in the case of zero concentration at the bentonite outer boundary are also given

	^{79}Se	^{107}Pd	^{126}Sn
Kristallin-I Reference Case	1.6×10^{-9}	5.6×10^{-12}	3.7×10^{-9}
Kristallin-I Zero concentration boundary	5.1×10^{-8}	1.9×10^{-10}	4.6×10^{-7}
H-3 Reference Case (zero concentration)	6.7×10^{-5}	7.5×10^{-8}	2.0×10^{-6}
H-3 Finite water flow	8.7×10^{-7}	1.0×10^{-9}	2.5×10^{-8}

3.3.1.2 Differences in t_{max}

The bentonite backfill in the H-3 concept is 0.98 m thick in contrast to Kristallin-I where it is 1.38 m thick. The extra diffusion distance results in some delay in t_{max} for Kristallin-I. However, the most important variable determining t_{max} for a radionuclide is the retardation caused by the bentonite which is dependent on the sorption Kd. Kds used in H-3 are lower than for Kristallin-I (see Table 3.4), except for Cs (H-3: 10x higher), Am and Pu (H-3: 2x higher). As noted previously, most other variables are too similar to produce significant differences between Kristallin-I and H-3. For example, in both Kristallin-I and H-3, the effective diffusivities for all nuclides are equal or close to 2×10^{-10} m^2 s^{-1} so that this provides negligible variation in the results.

The differences in t_{max} between Kristallin-I and H-3 are consistent with the combination of diffusion through a thinner bentonite buffer and smaller bentonite Kds for H-3.

3.3.1.3 Summary

- The differences in nuclide near-field release rates between H-3 and Kristallin-I can be explained by differences in the data (elemental solubility and sorption) used when the effect of the different bentonite outer boundary conditions is also taken into account.
- The generally shorter times to the maximum nuclide release rates in H-3 are consistent with the thinner bentonite buffer and lower Kds.

Factors such as bentonite porosity and density and the effective diffusion coefficients, which also contribute to the retardation, are very similar in H-3 and Kristallin-I and so do not contribute significantly to differences in the near-field maximum release rates.

3.3.2 Results of the geosphere models

3.3.2.1 Project Gewähr

Results for the calculated annual dose as a function of time after canister failure for the Project Gewähr base case (but using conservative sorption and diffusion constants for the kakirite zones) are shown in Figure 3.3. The annual dose is given in millirems (100 mrem = 1 mSv).

^{135}Cs clearly dominates the dose from 10^4 years until after 10^7 years when the actinide chains become more important. Also, in comparison with the results from Kristallin-I (Fig. 3.4) the greater contribution from ^{135}Cs, and lesser one from actinide chains, in Project Gewähr is evident.

That the fission products, and ^{135}Cs in particular, are so much more important to the overall dose in Project Gewähr is mainly a result of more conservative data being used in the modelling for these nuclides than for the actinides. The Project Gewähr report (NAGRA 1985a) acknowledges that the behaviour of the actinides was relatively better characterised and thus the results for these nuclides are more realistic. However, the results for the overall dose are well below the statutory limit and, as with Kristallin-I, only unrealistic combinations of conservative data and pessimistic assumptions create a case in which doses exceed this limit.

Direct comparison the overall results from Kristallin-I and Project Gewähr (Fig. 3.6) highlights the much lower doses calculated for the latter assessment. The major contributory factor to these is the greater volume of rock available for diffusion and sorption. There is almost two orders of magnitude difference between the rock diffusion volume for Project Gewähr (1.3 % of host rock, Table 3.7) and Kristallin-I (0.02 %). This difference arises from the greater diffusion depth around veins, and the vein (as opposed to fracture) geometry used in Project Gewähr. The longer flow path length (500 m compared to 200 m) also contributes to lower doses in Project Gewähr. The resultant increased spreading and retardation of the nuclides gives the four orders of magnitude lower doses for this assessment compared to Kristallin-I, despite the higher near-field releases arising from the use of a simple, conservative near-field model.

3.3.2.2 Kristallin-I and H-3

Results for the Kristallin-I Reference-Case calculation are shown in Figure 3.4 and the results for H-3 in Figure 3.5. The dose arising, in both cases, is for total nuclide release from the repository. For clarity of comparison, the total dose from both assessments is plotted in Figure 3.6. It is clear that there are differences in both the magnitude of the doses arising from nuclides and in the relative importance of individual nuclides to the total dose.

In Kristallin-I, the highest dose of about 3×10^{-4} mSv y^{-1} is due to ^{135}Cs at about 2×10^5 years after canister failure. ^{79}Se dominates the dose at earlier times, and the 4N+3 (^{235}U) actinide chain results in a second peak of around 10^{-5} mSv y^{-1} at 10^7 years.

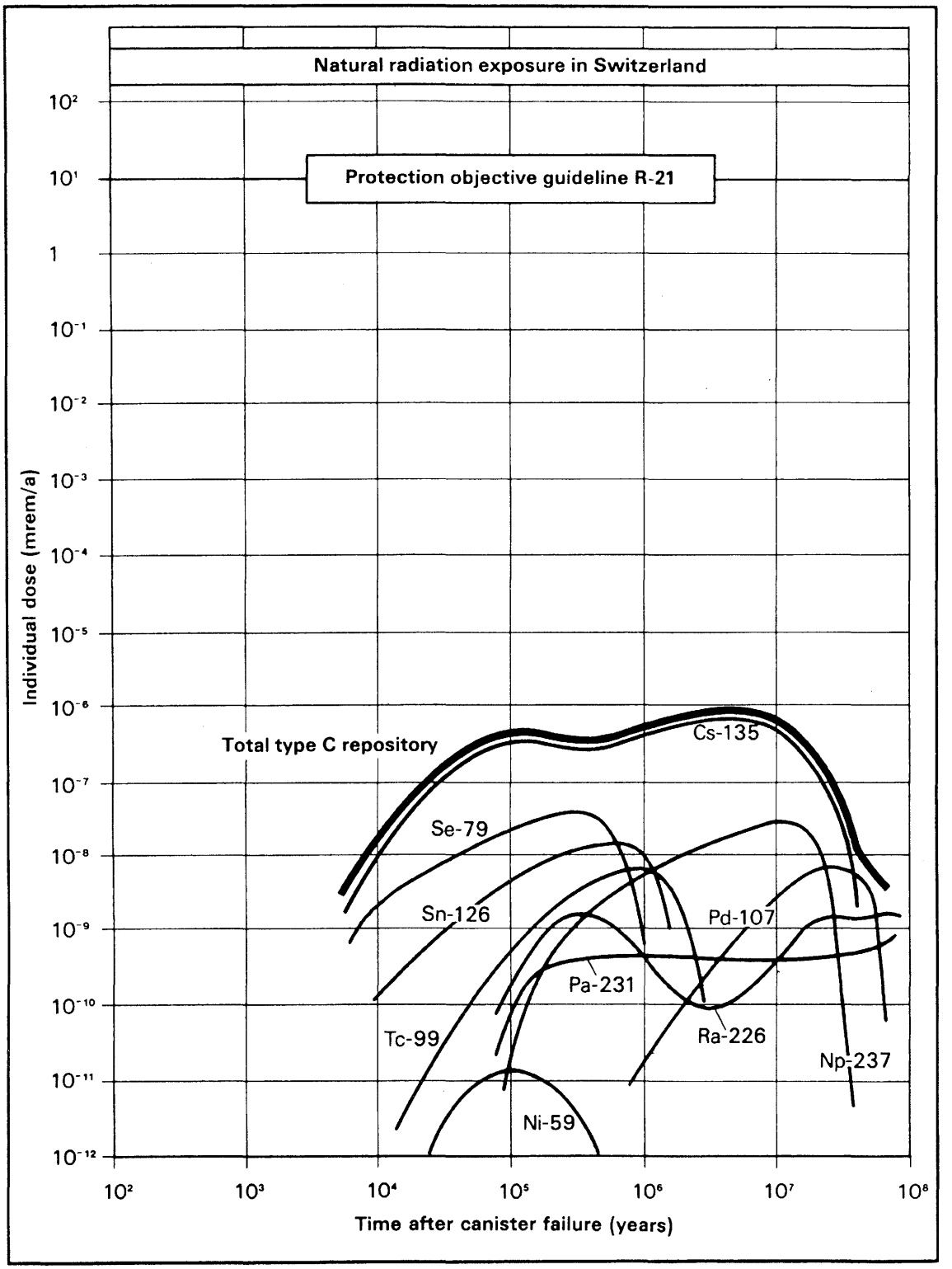

Fig. 3.3: Project Gewähr: Annual individual dose as a function of time with conservative diffusion constants in the kakirite zone and base case parameters for biosphere transport. (100 mrem = 1 msV).

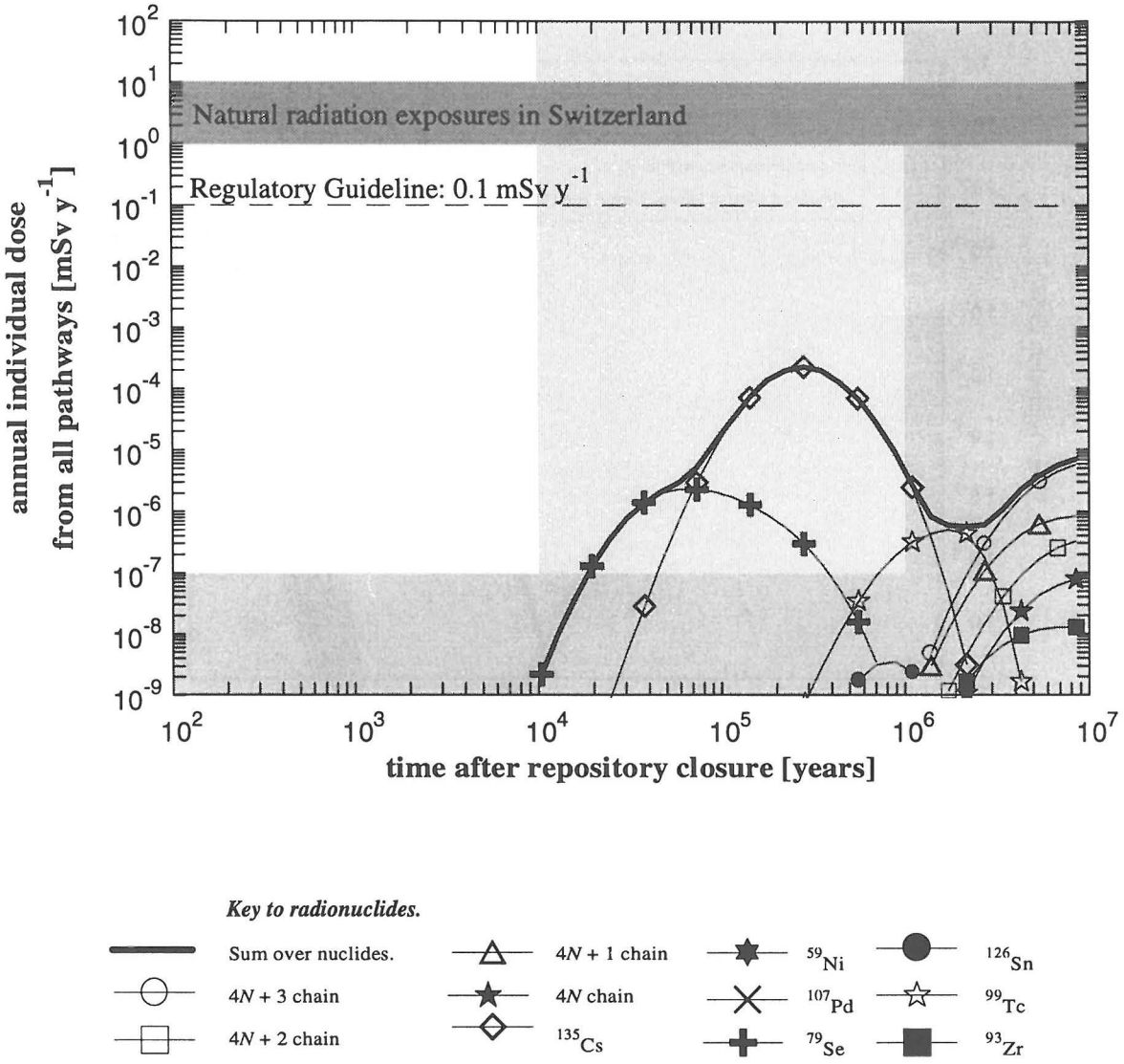

Fig. 3.4: Time development of annual individual dose for the whole repository in the Kristallin-I Reference-Case.

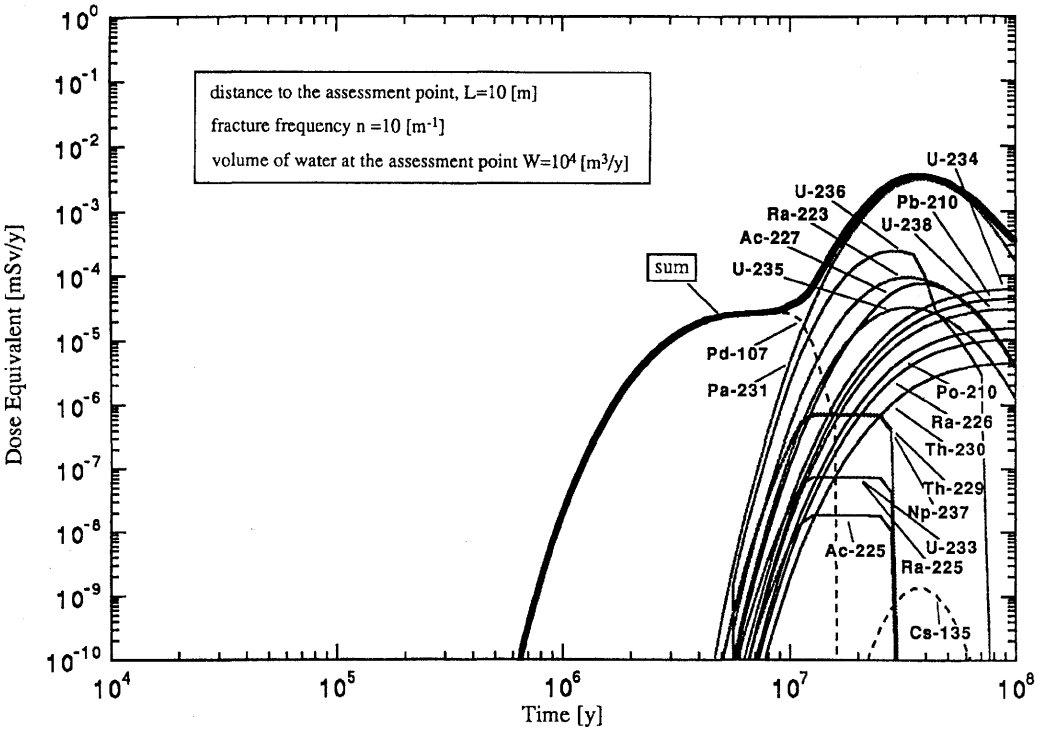

Fig. 3.5: Time development of annual individual dose from the whole repository in the H-3 performance assessment.

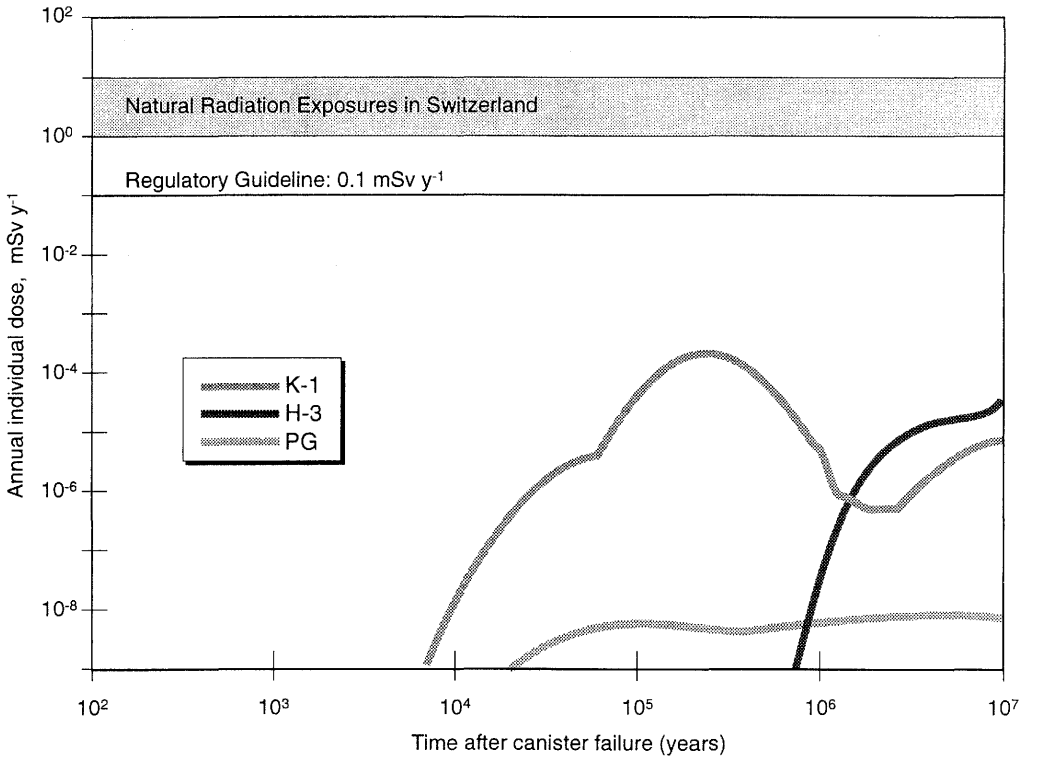

Fig. 3.6 Comparison of total annual individual dose calculated for Kristallin-I, H-3 and Project Gewähr.

In H-3, the only significant fission product is ^{107}Pd, which gives the dominant dose at times less than 10^7 years; all others give negligible contributions to the total dose. Overall, the highest dose is due to ^{231}Pa, which is expected to be in equilibrium with ^{235}U in the 4N+3 actinide chain. The peak dose is slightly greater (5×10^{-3} mSv y^{-1}) than in Kristallin-I and occurs slightly later (3×10^7 years) than the second (4N+3) peak in the latter.

The differences between the results from the two assessments can, therefore, be summarised as:

1) ^{107}Pd the only fission product contributing significantly to the dose in H-3, gives a negligible contribution in Kristallin-I;
2) ^{135}Cs gives the highest dose in Kristallin-I but a negligible dose in H-3;
3) The dose arising from the 4N+3 actinide chain is almost three orders of magnitude greater in H-3 than in Kristallin-I, although the peak occurs at about the same time.

These differences arise from three sources:

- The repository waste inventory for Kristallin-I. This is only some 2,700 canisters compared to ~ 40,000 canisters considered in the H-3 case. Thus, an equal near-field release per canister could result in approximately a 15x greater dose arising for H-3 than Kristallin-I
- Near-field release - as discussed in the previous section, there are significant differences in the release from the near field which can be related to model assumptions and input data, thus input to the geosphere is not the same for the two assessments;
- Geosphere migration barrier effectiveness, which depends on the model used for the geosphere and the input parameters.

3.3.2.3 Geosphere migration barrier effectiveness

The effectiveness of the geosphere as a barrier to migration can be assessed by considering the ratio of transit time to half-life of a nuclide. This ratio can be determined from the steady-state solution to the governing equations for geosphere transport (from SMITH 1993):

$$T / T_{1/2} = LH\left(\lambda E_p R_p\right)^{1/2}\left(E_p D_p\right)^{1/2} \tanh\left((\lambda E_p R_p / E_p D_p)^{1/2} y_p\right) / \left(q \ln 2\right) \qquad (3)$$

where:

λ is the nuclide decay constant (s^{-1})
L is the migration distance through the geosphere (m)
E_p is the matrix porosity (-)
H is the total trace length of open channels in a hypothetical plane of unit area normal to the direction of water flow (m^{-1})
R_p is the retention factor of the matrix (-)

E_pD_p is the effective diffusion coefficient in the matrix (m^2s^{-1})

y_p is the matrix depth available for diffusion (m)

q is the Darcy velocity ($m\ s^{-1}$).

This equation applies to transport in and diffusion from a parallel-sided fracture, in which diffusion takes place normal to the plane of the fracture. It is not applicable, in this form, to vein geometry where diffusion takes place radially from a tube-like conduit. For this reason it is not applicable to the Project Gewähr Reference-Case calculation which considered flow in veins within the kakirite zones, and comparison of results with those from Kristallin-I is limited to qualitative comments in section 3.3.2.1. Values for the non-nuclide-specific parameters in equation (3) used in Kristallin-I, H-3 and Project Gewähr (for interest only) are given in Table 3.7. Also shown is the percentage volume of host rock accessed by diffusion, and thus available for sorption.

Table 3.7: Values of geosphere model parameters for Kristallin-I, H-3 and Project Gewähr

	Kristallin-I	H-3	Project Gewähr
Darcy velocity q ($m\ s^{-1}$)	10^{-13}	5×10^{-12}	10^{-13}
Flow path length L (m)	200	10	500
Length of openings H (m^{-1})	0.04	10	1.4×10^{-2} (2)
Diffusion depth y_p (m)	0.05	0.05	0.5 (2)
Effective porosity E_p (-)	0.05	0.05	0.033
Diffusion volume (1) (%)	0.02	100	1.3

1) The percentage of the host-rock which is available for diffusion and sorption.

2) Vein geometry is used in Project Gewähr base case so H does not apply and the value given is the average number of open channels (i.e. veins) per m^2 over the repository area. The diffusion depth given is the radius of a cylindrical diffusion volume around the vein.

The values of the calculated ratio of transit time to half-life for safety relevant nuclides are given in Table 3.8 for Kristallin-I and H-3. For the fission products, the transit times in H-3 are 1 to 2 orders of magnitude greater than the half lives, so that these nuclides would be expected to decay significantly within the geosphere. The exception to this is ^{107}Pd where the transit time is less than the half-life. This explains the importance of ^{107}Pd relative to other fission products in H-3.

Although the ratio of transit time to half-life is also less than 1.0 for Kristallin-I, the maximum release rate of ^{107}Pd from the near field is some five orders of magnitude less for this assessment than for H-3 (Table 3.3) and around three orders of magnitude less than for other fission products in Kristallin-I, thus ^{107}Pd makes a negligible contribution to the overall dose in Kristallin-I.

This is in contrast to ^{135}Cs which has a very small transit time in Kristallin-I, less than a tenth of the half-life, resulting in minimal decay within the geosphere. This, combined with its high release from the near field (Table 3.3), explains the importance of ^{135}Cs to the overall dose.

Table 3.8 The ratio of transit time to nuclide half-life for Kristallin-I and H-3

Nuclide	Kristallin-I	H-3
^{79}Se	7.07×10^{-1}	1.12×10^{2}
^{99}Tc	1.01×10^{1}	3.93×10^{1}
^{107}Pd	3.53×10^{-1}	6.58×10^{-1}
^{126}Sn	2.01×10^{2}	2.96×10^{2}
^{135}Cs	8.41×10^{-2}	5.32×10^{1}
^{245}Cm	3.74×10^{2}	-
^{241}Am	1.66×10^{3}	3.37×10^{4}
^{237}Np	2.12	1.00×10^{1}
^{233}U	2.45×10^{1}	1.23×10^{2}
^{229}Th	1.80×10^{2}	-
^{246}Cm	5.01×10^{2}	-
^{242}Pu	4.48×10^{1}	-
^{238}U	1.03×10^{-3}	4.57×10^{-3}
^{234}U	1.68×10^{1}	8.27×10^{1}
^{230}Th	4.40×10^{1}	1.77×10^{3}
^{226}Ra	2.73×10^{2}	-
^{243}Am	4.01×10^{2}	8.12×10^{3}
^{239}Pu	2.22×10^{2}	7.26×10^{3}
^{235}U	6.54×10^{-3}	3.06×10^{-2}
^{231}Pa	7.91×10^{1}	-
^{240}Pu	4.26×10^{2}	1.38×10^{4}
^{236}U	1.96×10^{-1}	9.14×10^{-1}
^{232}Th	3.26×10^{-4}	3.06×10^{-2}

The generally better performance of the H-3 geosphere, particularly with respect to the fission products, as indicated by the greater transit time to half-life ratios in Table 3.8, cannot be explained by differences in water flux, although this creates significant differences between the near-field releases: the Darcy flux in H-3 is some fifty times greater than the Kristallin-I flux (Table 3.7). A more significant difference is the amount of wallrock available for diffusion and sorption of the nuclides. The limited matrix diffusion used in Kristallin-I means that only about 0.02 % of the host rock is available for retardation due to sorption of the nuclides, compared to 100 % in H-3 (Table 3.7).

The peak dose in the 4N+3 chain in H-3 which, in contrast to the fission products, is almost three orders of magnitude higher than in Kristallin-I, results from ^{231}Pa which is assumed to be in equilibrium with its parent nuclide ^{235}U. Although the inventories of all its parent nuclides are added to the inventory of ^{235}U, this cannot be directly responsible for the increased dose from this chain. This is because release of ^{235}U from the near field is limited by its solubility during glass dissolution so that a larger inventory only increases the duration of release. Also, the half-life is so long with respect to transit time (Table 3.8) that no significant decay of ^{235}U would be expected for either the H-3 or Kristallin-I geospheres. ^{231}Pa resulting from decay of ^{235}U within the glass will itself decay within the near field (see Table 3.6) and even more substantially within the geosphere (Table 3.8). However, the insignificant decay of ^{235}U within the geosphere means that the large difference in the near-field release of this nuclide (Table 3.3) will be preserved. As discussed in section 3.3.1.1, the differences in near-field release for uranium isotopes between H-3 and Kristallin-I result from the adoption of a zero-concentration boundary condition and, perhaps more importantly for this element, from use of elemental solubilities for individual isotopes in H-3. Hence, the adoption of these assumptions for the near-field model has great implications for the geosphere transport and the overall calculated doses.

3.3.2.4 Relative effectiveness of near-field and geosphere barriers

The effectiveness of the geosphere as a barrier to radionuclide migration can be gauged by comparing the maximum near-field release into the geosphere with the maximum release from the geosphere. In a similar way, the rate of release of a nuclide from the near field can be compared to its release rate from the glass. If in both cases, a ratio is calculated for output to input, then a comparison of these ratios gives an estimate of the relative importance of the near field and geosphere barriers.

Values of these ratios for a selection of important nuclides is given in Table 3.9 for H-3 and Kristallin-I. For all nuclides, the input into the near field is calculated from the dissolution of the glass, taking the maximum values of the dissolution rate and glass surface area to give a maximum nuclide release rate for the first year after canister failure. Values for the geosphere ratio are taken from the H-3 performance assessment report (PNC 1992, Table 4.5-6) and Table 4.14 (this report) for Kristallin-I. Dilution in the high permeability domain is not taken into account for Kristallin-I. This would have contributed a reduction of ~ 2×10^4 in output from the geosphere, hence, total dilution (included within the biosphere model) is a key parameter affecting the dose arising from radionuclide releases.

The near-field ratios are calculated from the estimated nuclide input from the glass, as discussed, and the maximum near-field release rates as given in Table 3.3.

The smaller the value for a ratio, the more effective the barrier has been in reducing radionuclide migration: a value of 1.0 would indicate no reduction between input and release of a nuclide in that barrier.

For Kristallin-I, it is clear that the near field is generally more effective than the conservative geosphere, the exception being for ^{226}Ra. Even nuclides which are not solubility limited (^{135}Cs) or only poorly sorbing (^{79}Se and ^{99}Tc) are better retarded in the near field. The situation is more complicated for relatively short-lived daughter nuclides, such as ^{226}Ra and ^{231}Pa because ingrowth contributes a large proportion of the inventory of these nuclides in the near field and geosphere. Hence, output from the near field of ^{226}Ra is larger than release from the glass, giving a near-field ratio greater than 1.0, because retardation of ^{238}U results in production of ^{226}Ra within the near field which outweighs decay.

For H-3, the geosphere is remarkably more effective in retarding ^{135}Cs and ^{79}Se than the near field. This is due to the high solubility limit and low sorption Kd used for ^{79}Se and the lack of solubility limit for ^{135}Cs which make the near field relatively ineffective. For other nuclides, the effect of the solubility limit on concentration at the bentonite inner boundary is to make the near field more effective than the geosphere, in spite of the conservative outer bentonite boundary condition. It should be noted, also, that the initial (short term) glass dissolution rate used for H-3 (1.6×10^{-9} kg m^{-2} s^{-1}) is much higher than that for Kristallin-I (1.2×10^{-11} kg m^{-2} s^{-1}) resulting in much higher input to the near field. This has very little effect on the actual near-field performance for nuclides (except ^{135}Cs) because of solubility limitation, as mentioned previously, but decreases the near-field ratio by two orders of magnitude compared to that estimated for Kristallin-I.

Table 3.9: Comparison of the effectiveness of the near-field and geosphere barriers for selected radionuclides in Kristallin-I and H-3

Nuclide	Kristallin-I		H-3	
	Near field	Geosphere	Near field	Geosphere
^{135}Cs	1.7×10^{-1}	6.6×10^{-1}	3.7×10^{-1}	8.0×10^{-12}
^{99}Tc	3.8×10^{-4}	8.8×10^{-3}	4.8×10^{-9}	3.3×10^{-6}
^{79}Se	4.1×10^{-4}	4.6×10^{-1}	4.2×10^{-1}	1.9×10^{-14}
^{235}U	3.7×10^{-3}	9.5×10^{-1}	4.3×10^{-4}	8.8×10^{-2}
^{231}Pa	3.4×10^{-2}	2.2×10^{-1}	-	-
^{238}U	4.9×10^{-4}	9.6×10^{-1}	2.5×10^{-6}	9.8×10^{-1}
^{226}Ra	1.9×10^{1}	5.5×10^{-4}	-	-

Near-field ratio: Maximum release rate from near field to maximum dissolution rate from glass.
Geosphere ratio: Maximum geosphere release rate to maximum near-field release rate for a nuclide.

3.4 Conclusions

The differences between the doses arising from the Kristallin-I and H-3 performance assessments can be attributed to a number of differences in the models used and to variations in data, particularly for the near-field calculations. Differences in release from the near-field barrier systems are predominantly due to:

- sharing of elemental solubility between isotopes in Kristallin-I but not in H-3;
- bentonite outer boundary condition for diffusion of zero nuclide concentration in H-3 compared to the 'mixing tank' boundary condition in the Kristallin-I Reference-Case;
- differences in solubility limits (for fission products, except ^{135}Cs) and near-field sorption coefficients (^{107}Pd and ^{99}Tc).

Diffusion and sorption in the bentonite buffer were not considered as part of the Project Gewähr Reference-Case calculation, hence near-field release rates are considerably higher than Kristallin-I due to lack of retardation and decay. However, this was more than compensated for in the geosphere by the effect of a greater volume of the host-rock being available for diffusion, resulting in lower overall doses than for Kristallin-I.

Differences in the geosphere performances between Kristallin-I and H-3 are due to:

1) All host rock being available for diffusion and sorption in H-3 but only around 0.02 % in Kristallin-I;

2) Differences in near-field releases being carried through the geosphere for nuclides with short transit times compared to half-life.

In general, the Kristallin-I near field resulted in lower releases to the geosphere than the H-3 near field. In contrast, the H-3 geosphere performed better than the Kristallin-I geosphere, especially for ^{135}Cs where geosphere effectiveness was also better than that of the H-3 near field.

4 COMPARISON WITH OTHER SAFETY ASSESSMENTS

T. J. Sumerling

4.1 Introduction

The aim of this chapter is to compare selected recent integrated safety assessments with Kristallin-I. The comparison is concerned both with results, in terms of estimated doses and release of radionuclides, and with the identification and comparison of factors underlying these results - the actual characteristics of the disposal systems, the assessment and modelling assumptions and key data choices. As a result, the factors that most affect the estimated performances and doses are identified. Two criteria were used to select assessments for the comparison:

- the assessments compared must consider disposal of HLW or spent fuel in crystalline rock below the water table;
- good quality documentation, published within the last five years, must be available.

Five assessments, apart from Kristallin-I (NAGRA 1994b), were considered to meet these criteria:

- H-3 assessment of HLW in crystalline and sedimentary rocks in Japan (PNC 1992);
- SKI Project 90 assessment of spent fuel in crystalline bedrock in Sweden (SKI 1991);
- SKB 91 assessment of spent fuel in crystalline bedrock in Sweden (SKB 92);
- TVO 92 assessment of spent fuel in crystalline bedrock in Finland (VIENO et al. 1992);
- AECL assessment of spent fuel in a granite pluton in Canada (GOODWIN et al. 1994);

Of these, a detailed comparison of the Kristallin-I and H-3 assessment has already been given in Chapter 3 because of the very great similarities in the waste form and the engineered barrier designs. The SKI Project 90 is unusual because it is a trial of assessment methodology practiced by the regulator; since the assessment covers essentially the same concept as the SKB 91 assessment, it is not included in the following comparison. This chapter, therefore, focuses on a comparison of Kristallin-I with the SKB 91, TVO 92 and AECL 94, three assessments of spent fuel disposal.

The plan of this chapter is as follows. Section 4.2 provides a brief introduction to the objectives, subject and approach of the three assessments. The succeeding sections, 4.3 to 4.5, compare

- the actual disposal systems,
- the model and data choices and
- the calculated performances and doses for a Reference Case.

Section 4.6 concludes by identifying and discussing the factors that most affect the estimated performances and doses in the assessments. All data presented are taken from the primary assessment reports (see references above).

4.2 Objectives, subject and approach of the other assessments

4.2.1 SKB 91

The SKB 91 safety assessment (SKB 91) examines how the long-term safety of a final repository for spent fuel in Sweden is affected by the geological characteristics of the repository site. The following questions are explored:

- What importance do the site-specific characteristics of the bedrock and the hydrological regime around the repository have for overall safety?
- What relative importance do different site-specific characteristics have for safety?
- How can the placement and design of the repository be adapted to conditions on the site in order to take advantage of the safety barrier offered by the bedrock?

The disposal concept for SKB 91 is based on the KBS-3 concept (KBS 1983). This assumes disposal of spent fuel assemblies in lead-filled copper canisters, individually emplaced in vertical deposition holes. The reference repository design has a capacity for disposal of 7,800 tonnes uranium, that is sufficient for the Swedish nuclear programme through to the year 2010.

The topography, geology and other site-specific characteristics considered in the assessment are based on conditions in the Finnsjön area of northern Uppland, 140 km north of Stockholm. Finnsjön was chosen as an example site since an extensive body of data was available from the area. This includes data from the nearby Dannemora mine and SFR low and intermediate waste disposal facility at Forsmark, as well as the results from geological investigations at the site as part of the KBS project, plus subsequent deep borehole investigations.

The hypothetical repository plane is located at about 600 m below ground level, a minimum of 100 m below a major sub-horizontal fracture zone. This is considered to be advantageous from a long-term safety perspective since the sub-horizontal fracture zone appears to effectively isolate deeper (slightly saline) groundwaters from fresh waters above the zone.

The SKB 91 assessment methodology is based on the use of scenarios, and draws on work carried out during the Joint SKI/SKB Scenario Development (ANDERSSON 1989) that was made as part of the SKI Project 90. A Reference Scenario is defined from best understanding of the Finnsjön site with assumptions of present-day climate and hydrological conditions. The Reference Scenario is analysed in detail and alternative assumptions, mainly concerned with geological and hydrogeological uncertainties and repository location/layout at the site, are examined by parameter variations with the same models.

Regional hydrological modelling of the Finnsjön site, in three dimensions, was carried out with the NAMMU code. In NAMMU, the rock is modelled as a homogeneous continuum with discrete water-bearing fracture zones represented explicitly by zones with elevated hydraulic conductivity. NAMMU is used to determine boundary conditions for a more detailed model of the repository area and potential flow pathways from the repository to the surface. This is represented by HYDRASTAR, a stochastic continuum model for conditional simulation developed by SKB. This model takes into account the spatial variability of the bedrock characteristics extrapolated from the variability observed in measurements at the site and related data.

Most of the safety assessment calculations for SKB 91 have been made using the PROPER computer program which links the HYDRASTAR model with models of near-field release, geosphere transport and biosphere.

The near field is represented by the model "Tullgarn" in which release from individual containers is calculated for different failure modes, and compiled to estimate release from the entire repository or segments of the repository. A stand-alone version of Tullgarn, TULL22, is used in stochastic simulations. All calculations of release from a single canister are deterministic but, in the stochastic simulations, each canister has a probability of 1/1,000 of early failure due to an initial defect. Canisters failing due to overpressure and corrosion are also included in the calculations. Hence, the number and location of failed canisters is sampled.

The geosphere is represented by 88 separate dual-porosity stream tubes, each beginning from a segment of the repository and with path length and Darcy flow velocity determined from the HYDRASTAR model. Transport in each stream tube is represented by the FARF31 model which accounts for longitudinal dispersion, matrix diffusion and sorption along the stream tube. The groundwater travel time from the repository to the surface is analysed stochastically based on 500 simulations considering all 88 stream tubes. However, for radionuclide transport calculations, only a small number of the stream tubes will be connected to a repository segment containing a failed canister in each simulation.

In the biosphere, the outflow of each radionuclide from the geosphere (Bq y^{-1}) is multiplied by a conversion factor (Sv Bq^{-1}) to estimate weighted whole body dose commitment to an individual in the critical group in Sv y^{-1}. These conversion factors have been calculated using the BIOPATH compartment model which considers the various dose pathways affecting members of a subsistence farming community taking drinking water from a local well, consuming agricultural products from contaminated soil and fish from a local lake.

4.2.2 TVO 92

The TVO 92 safety analysis (VIENO et al. 1992) examines the long-term safety of a final repository for spent fuel in Finnish bedrock. The aims of the analysis are:

- to establish whether the five areas preliminarily investigated between 1987 and 1992 are suitable as disposal sites,
- to determine whether the planned disposal concept fulfills the safety requirements established by the Finnish regulatory authorities, and

- to provide an up-to-date safety analysis of the disposal concept incorporating data from the site investigations, and new knowledge from research in Finland and abroad, produced since the previous analysis.

The Finnish regulatory requirements specify an individual annual dose limit of 0.1 mSv on radiation doses arising from the repository up to "reasonably predictable times" and also an annual risk limit equivalent to the risk of death corresponding to a dose of 0.1 mSv for "unlikely disruptive events". In addition, they require that radionuclides released from the repository should not lead to significant changes in the (natural) radiation environment.

The disposal concept for TVO 92 is based largely on the KBS-3 concept and is similar to the SKB 91 concept, except that a composite construction disposal canister is proposed. The Advanced Cold Process (ACP) canister consists of a load-bearing inner steel canister encased in a corrosion resistant oxygen-free copper shield. The canister is filled with a granular material, such as quartz sand or lead shot, for internal mechanical support. The repository is designed to accept the spent fuel arising from a projected 40 year operation of the TVO reactors at the Olkiluoto site, expected to amount to 1,840 tons of uranium.

For the safety analysis, it is assumed that the repository is located at the Veitsivaara site. Veitsivaara is one of five representative sites under investigation by TVO and was selected because, at the time that the safety analysis was begun, the site investigation was well advanced and also because the site represented a challenging assessment subject due to its geological complexity.

The hypothetical repository considered in the safety analysis is sited at 500 m below ground level and deliberately placed to intersect significant fracture zones. This is a methodological decision; in practice, it is expected that more favourable repository locations could be found at any of the five sites under investigation.

The basic principle followed in TVO 92 is to employ conservative assumptions, models and data in each stage of the safety analysis such that the results will, with a high degree of confidence, represent upper limits for the actual possible radionuclide releases and radiation doses.

A base case is examined in which it is assumed that the canisters are all initially intact and that engineered barriers behave as expected. This leads to the conclusion that no releases will occur for at least 10 million years. The case of an initially defective ACP canister is analysed in detail. This considers an initial hole in the copper outer shell, leading to corrosion of the inner steel canister. The transport resistance of the bentonite and the limited dimension of possible defects are taken into account when considering water ingress and the flow of oxidant from radiolytic action and hydrogen from corrosion.

The performance of the multi-barrier system is studied for a pessimistic Reference Scenario. This considers a single canister which is assumed to "disappear" at 10,000 years after closure. Other parameters are conservatively selected so that upper limits of consequences are calculated. Sensitivity analysis is then performed based on variations of the Reference Scenario. Features, events and processes not included in the Reference Scenario and sensitivity analysis are treated by mainly qualitative arguments.

Groundwater flow modelling for TVO 92 has been carried out using the FEFLOW model. FEFLOW is a three-dimensional finite-element code based on the continuous

porous medium approach capable of simulating coupled water and heat flows including density effects. Fracture zones are represented as discrete volumes or planes with hydraulic properties set to represent the required transmissivities. A system of four nested hydrological models is used to represent the Veitsivaara site, each of progressively finer resolution and with boundary conditions for each inner model supplied from the next-most outer model.

The near field is represented by a number of analytical models and a numerical code REPCOM which calculates time-dependent release of radionuclides from a single waste container and one-dimensional diffusion through the buffer with linear sorption.

For the geosphere, a very simple model is used considering the total transport resistance of a flow path from the repository to the biosphere through a major fracture zone. Transport in the fracture is modelled by the FTRANS code which considers advection, dispersion, matrix diffusion and sorption along the fracture.

In the biosphere, the outflow of each radionuclide from the far field in Bq y^{-1} is multiplied by a conversion factor (Sv Bq^{-1}). No independent biosphere modelling has been done for the TVO 92 assessment, rather, advantage is taken of the biosphere modelling and dose factors derived in the SKB 91 assessment, since the likely surface environments to which radionuclides might be released from either repository are broadly similar.

4.2.3 AECL 94

The primary objectives of the AECL assessment of a reference disposal system (GOODWIN et al. 1994), here referred to as AECL 94, are to:

1. Develop and document a method for estimating and evaluating the long-term effects and safety of a facility for the disposal of Canada's nuclear fuel waste; and
2. Demonstrate the utility of the method, by applying it to the reference disposal system, a hypothetical implementation of the concept.

Specific objectives of this application include the identification and estimation of possible impacts, comparison of impacts with safety criteria, sensitivity analysis to identify important factors, and examination of derived constraints that could influence the potential impacts.

The method referred to is based on both deterministic and probabilistic risk assessment, where the primary aim is to estimate the *radiological risk to human individuals*. In this context, risk is estimated by the mean of the distribution of radiological dose multiplied by the probability of an adverse effect, where distribution of dose values is obtained by probabilistic simulation.

A particular constraint is that, according to Canadian regulatory criteria, quantitative evaluation of individual risk is only required in the period up to 10,000 years after closure, although, in AECL 94, the simulation is continued to examine results of the modelling up to 100,000 years after closure. While focusing on annual radiation doses and risk to members of the public, the assessment also considers doses to non-human biota and release to the environment of non-radioactive contaminants.

The general AECL disposal concept considers the disposal of spent fuel from Canada's CANDU™ nuclear power generation programme produced up to about the

year 2035. This will result in wastes including 191,000 tonnes of uranium. For the purpose of demonstrating the assessment method, a hypothetical disposal system is defined, referred to as the *reference disposal system*.

The geological and environmental characteristics of the reference disposal system are based on a hypothetical location of the repository at the Whiteshell Research Area (WRA). The WRA is on the edge of the exposed portion of the Canadian shield and has many features in common with sites elsewhere on the shield. The WRA has been extensively studied over a period of 10 years, including the construction of the Underground Research Laboratory (URL), with the result that a consistent set of physical, chemical and geological data is available upon which to base the post-closure assessment.

For the purposes of the assessment, a hypothetical disposal vault is introduced at a depth of 500 m below ground in crystalline basement at a minimum distance of 50 m from a low angle dipping fracture zone that is assumed to continue to below repository depth. In order to "fit" the hypothetical vault into the available rock mass, the reference design concept is modified by truncating disposal rooms which would otherwise contravene the 50 m exclusion zone to the low dipping fault. This results in a reduced capacity of the hypothetical vault of 162,000 tonnes which is considered in the assessment. The spent fuel assemblies are assumed to be loaded into thin-walled titanium containers, which are placed in vertical deposition holes drilled into the floor of the disposal rooms.

Regional hydrological modelling of the WRA site has been carried out with the MOTIF model, considering two nested 2-dimensional sections. The granite layers are modelled as homogeneous units with fracture zones modelled as linear zones with elevated permeability. The simulation of contaminant transport is carried out for the smaller region model only; the effects of the introduction of the repository and of a well drawing different volumes of water are also investigated in this model.

Most of the safety assessment calculations have been made using the SYVAC3-CC3 computer program. This represents the conventional model chain of vault, geosphere and biosphere and is designed for probabilistic risk assessment using Monte Carlo sampling.

The SYVAC3-CC3 near-field model represents releases from the vault considering alternative canister failure modes, prompt releases and congruent release from the waste form, and one-dimensional diffusion through the buffer and backfill, assumed to occur in a direction perpendicular to the vault plane. Redox conditions and nuclide precipitation in the buffer are also considered. Separate sectors (areas) of the vault can be defined so that local differences in temperature, inventory and local hydraulic conditions can be represented. Hence, sources for alternative geosphere flow paths from different sectors of the vault can be simulated; twelve separate sectors are considered in AECL 94.

The SYVAC3-CC3 geosphere model represents the possible alternative transport pathways by a fixed network of one-dimensional flow pathways from the vault sectors to alternative biosphere receptors. The paths are identified from the results of hydrogeological modelling and flow parameters are calibrated against the MOTIF model. The network is divided into segments which have distinct hydraulic and chemical properties. In AECL 94, these connect the 12 vault sectors to the four possible biosphere discharge zones.

SYVAC3-CC3 includes a relatively complex biosphere model which is able to represent simultaneous discharges to the possible natural discharge zones and to a well. The well position and yield can be sampled taking account of demand in the biosphere and geosphere hydrological constraints. Transfers of contaminant between water, sediment and soil bodies are represented, including the implicit use of lake sediment as garden soil. A critical group of variable size is defined and makes use of the various contaminated water and soil bodies.

4.3 Comparison of disposal systems

In order to compare results of the assessments, it is first necessary to compare the disposal systems to identify important differences in the systems themselves. Table 4.1 compares key characteristics of the three disposal systems discussed in the preceding sections and of the Kristallin-I disposal system. These are discussed below, together with some preliminary comments on processes and factors that may be important to the long-term performances of the systems.

4.3.1 Inventory

The total inventories, expressed in terms of tU or total number of canisters, vary by almost two orders of magnitude between the lowest, TVO 92, and highest, AECL. However, this is misleading as the uranium fuel is of different initial composition and has undergone different irradiation history. The natural uranium CANDU^{TM} fuel is associated with, in general, a factor of four to five lesser activities of longer-lived fission and activation products due to its lower initial ^{235}U content and lower burnup.

Table 4.2 shows the origin and half-lives of selected radionuclides which contribute most to long-term radiological impact in the four assessments (see Table 4.5 and section 4.5). Table 4.3 compares waste content and total inventories of radionuclides of these radionuclides considered in each of the assessments. Comparing the waste contents expressed in terms of GBq/tU, the effect of the difference in fuel type between the AECL and the other three systems can be seen. Also very notable is the much reduced inventory of several radionuclides in the Kristallin-I case due to reprocessing. During reprocessing, most of the uranium (and plutonium) is separated for possible re-use with only a fraction of about 0.15 % being left in the wastes (ALDER & McGINNES 1994). The fuel cladding will be stripped from the fuel before reprocessing and radionuclides associated with activation of the cladding, such as ^{94}Nb and some ^{14}C, will be included in intermediate level waste streams. Volatile fission products, notably the ^{14}C and ^{129}I, will be lost from the high-level waste during reprocessing and either discharged or retained in sludges and filters which will also be disposed as intermediate-level wastes. Hence, the effective absence of ^{14}C, ^{94}Nb and ^{129}I in Kristallin-I waste and the much reduced uranium isotope inventories.

Table 4.1: Key characteristics of the disposal systems considered in the performance assessments

	SKB 91	**TVO 92**	**AECL 94**	**Kristallin-1**
Typical waste characteristics	Spent BWR & PWR fuel ~3 % enriched U 38 GWd/tU	Spent BWR fuel ~3 % enriched U 36 GWd/tU	Spent CANDU natural U fuel 8 GWd/tU	Vitrified waste from PWR & BWR fuel ~3 % enriched U 33 GWd/tU
Total inventory considered in assessment[1]	8750 tU contained in 5,830 canisters	1840 tU contained in 1,150 canisters	162,000 tU contained in 119,000 canisters	Wastes from 3730 tU contained in 2,700 canisters
Canister type Typical content [2]	Copper with cast lead fill 1.5 tU	Composite Cu-steel with granular fill 1.6 tU	Thin-walled titanium with glass bead fill 1.4 tU	Massive cast steel canister 1.4 tU [2]
Emplacement Buffer material and thickness	In individual deposition holes from drifts Bentonite clay - 35 cm radially - 150 cm above	In individual deposition holes from drifts Bentonite clay - 35 cm radially - 150 cm above	In individual deposition holes from drifts Bentonite clay - 25 cm radially - ~150 cm above	Centrally in disposal tunnel Bentonite clay - 138 cm radially - 3 m between canisters
Repository - depth bgl. - disposal area - exclusion zone[3]	 600 m 0.9 km^2 100 m	 500 m 0.2 km^2 none	 500 m 3.2 km^2 50 m	 1,000 m 0.5 km^2 100 m
Host-rock Typical hydraulic conductivities[4]	Granodiorite < 100 m bgl. 10^{-8} -10^{-7} ms^{-1} > 100 m bgl. 10^{-10} -10^{-8} ms^{-1} Fract. zones[5] 10^{-7} -10^{-5} ms^{-1}	Migmatic gneiss or granite < 200 m bgl. 10^{-11} -10^{-7} ms^{-1} > 200 m bgl. 10^{-11} -10^{-9} ms^{-1} Fract. zones 10^{-9} -10^{-4} ms^{-1}	Granite < 150 m bgl. 10^{-8} ms^{-1} > 300 m bgl. 10^{-12} ms^{-1} Fract. zones 10^{-6} ms^{-1}	Gneiss or granite < 500 m btb. 10^{-10} -10^{-7} ms^{-1} > 500 m btb. 10^{-12} -10^{-10} ms^{-1} Fract. zones 10^{-7} -10^{-6} ms^{-1}
Overlying geo-units or discharge zone	Discontinuous moraine, peat and lakes	Discontinuous moraine, peat and lakes	Discontinuous moraine, peat and lakes	Thick Mesozoic sediments over site, gravels in Rhine valley discharge zone

Notes:

1) Inventories considered in assessment, which may differ from quantities considered in respective general concepts.
2) Wastes corresponding to given amounts of uranium, see Table 4.3.
3) Distance to nearest major fracture zone assumed in design and assessment.
4) Typical values for the upper weathered zones, at depth including the repository level, and for major fracture zones. bgl = below ground level; btb = below top of basement.
5) Excludes the major subhorizontal zone (Zone 2) overlying the repository, which has markedly higher conductivity: 10^{-5} -10^{-4} ms^{-1}.

The lower part of Table 4.3 compares total inventories. Considering the fission products, there is a factor of not more than 20 between the TVO 92 and AECL 94 inventories, with SKB 91 and Kristallin-I inventories being mainly intermediate. The very large differences in the uranium inventories are striking. However, as uranium tends to be solubility limited in the near field of all the disposal systems, the U inventory does not determine U release from the near field. Indeed, in the case of spent fuel disposal, if uranium dissolution is assumed to control the release of radionuclides from the waste matrix, then the higher ratio of ^{238}U to other nuclides in the AECL waste is a positive advantage, although the prompt release fraction will remain significant.

4.3.2 Waste form and canister type

The Kristallin-I waste is a borosilicate glass incorporating wastes from reprocessing, whereas the other assessments all consider spent fuel. The implications of this for radionuclide inventory have been noted above. Both the glass and the UO_2 fuel matrix are very insoluble. However, in the case of the spent fuel, significant fractions of many radionuclides are not incorporated in the fuel matrix and will potentially be available for release relatively quickly following canister failure.

Table 4.2: Origin and half-lives of selected radionuclides

Nuclide	Origin and comments	Half-life (years)
^{14}C	FP in fuel and AP in cladding	5,730
^{79}Se	Fission product (FP) in fuel	65,000
^{94}Nb	Activation product (AP) in cladding	20,000
^{99}Tc	Fission product in fuel	210,000
^{129}I	Fission product in fuel	16,000,000
^{135}Cs	Fission product in fuel	2,300,000
^{235}U	Primary fissile isotope in fuel	700,000,000
^{231}Pa	Daughter product of ^{235}U	33,000
^{238}U	Most abundant isotope in fuel	4,500,000,000
^{226}Ra	Daughter (^{238}U-^{234}U-^{230}Th-^{226}Ra)	1,600

Table 4.3: Content of wastes and total inventories of key radionuclides considered in the assessments

Radionuclide content (GBq/tU)	**SKB 91**	**TVO 92**	**AECL 94**	**Kristallin-I**
^{14}C	39.	23.	50.	< 0.03 (1)
^{79}Se	17.	16.	3.3	16.
^{94}Nb	4.7	4.9	0.4	~ 0.
^{99}Tc	540.	520.	130.	460.
^{129}I	1.3	1.3	0.3	< 0.001 (1)
^{135}Cs	18.	24.	1.0	24.
^{235}U	0.53	0.67	0.16	0.001
^{238}U	12.	12.	12.	0.017
Total inventory (TBq)	**SKB 91**	**TVO 92**	**AECL 94**	**Kristallin-I**
^{14}C	340	42	8100	~ 0
^{79}Se	150	29	540	60
^{94}Nb	41	9	59	~ 0
^{99}Tc	4700	960	21000	1800
^{129}I	11	2	47	~ 0
^{135}Cs	160	44	160	51
^{235}U	4.6	1.2	26	0.005
^{238}U	110	22	2000	0.065

Notes:

1) Upper limits for possible content based on COGEMA specification, actual activities are probably much less.

All four disposal systems include a high integrity canister although materials, and consequently expected failure modes, are different. The copper and copper-shielded canisters of SKB 91 and TVO 92 are expected to be effectively corrosion proof and initial defects are postulated in order to obtain a radionuclide release within a reasonable timescale. The AECL thin-walled titanium canister and the thick steel Kristallin-I canisters are both expected to fail, but only after the period of significant heat generation from the wastes. The former relies on a small thickness of a high cost material, very resistant to corrosion, and the dominant failure mode is expected to be crevice corrosion. With titanium, significant gas production from the corrosion of the canister is also avoided. The Kristallin-I steel canister is expected to fail due to mechanical stresses but only after significant corrosion has occurred; it is sufficiently thick to act as sacrificial corrosion barrier. The Kristallin-I canister has another important role of ensuring reducing conditions locally, due to iron corrosion products and un-corroded steel.

4.3.3 Emplacement and buffer

All four disposal systems include a bentonite clay buffer to protect the canister from mechanical stresses and also to provide a low-permeability hydraulic barrier to reduce solute transport. Bentonites considered for use in waste disposal environments are sodium-montmorillonites with trace contents of other minerals. For tunnel backfill material above deposition holes (AECL, SKB and TVO concepts), bentonite is mixed with sand.

The geometry of emplacement is identical in the SKB 91 and TVO 92 disposal systems, both considering emplacement in deposition holes drilled in the floor of relatively narrow horizontal drifts. The AECL 94 system is rather similar considering emplacement in deposition holes drilled in the floor of wider horizontal caverns. The Kristallin-I system considers emplacement centrally in roughly circular disposal tunnels. This concept employs a greater volume of bentonite per canister (over 50 m^3 per canister) than any of the other repository designs (e.g. about 9 m^3 for the KBS design adopted in SKB 91 and TVO 92).

4.3.4 Repository plan and location

All four disposal systems consider disposal from, or in, roughly parallel arrays of horizontal drifts, caverns or tunnels on a single level. The quantities of waste to be disposed and thermal considerations determine the areal extent of the repository. The lower radionuclide content and heat output of the AECL waste allows a more compact placement of containers and, hence, a relatively smaller area repository than would be expected based only on comparison of total tU or number of canisters to be disposed.

The significantly greater depth of the Kristallin-I repository is determined by the presence of large thicknesses of overlying weathered basement rock and sediments in the siting region. In all four cases, the repository is actually situated about 300 to 400 m into mainly low-permeability sparsely-fractured crystalline rock, which is only found at greater depth in the Swiss case.

The Kristallin-I and SKB 91 repositories are placed with a 100 m exclusion distance to a nearest major fracture; the exclusion distance is 50 m in the case of the AECL repository. No exclusion zone is assumed for the TVO 92 repository, i.e. the repository tunnels are assumed to be intercepted by fracture zones. This, however, is a methodological decision made for the purposes of the assessment and it is likely that a Finnish repository could be placed to avoid major fracture zones if required. In the case of the Kristallin-I reference disposal concept, for example, fracture zones are avoided by dividing the repository into a small number of panels located in adjacent crystalline blocks.

4.3.5 Site and host geology

All four disposal systems consider disposal in low-permeability crystalline rock which is likely to be intercepted by discontinuities and fractures on a range of scales.

In the SKB 91, TVO 92 and AECL 94 cases, the geometry and properties of the site are based mainly on characteristics at identified sites: Finnsjön, Veitsivaara and the Whiteshell Research Area, respectively. However, in each case the characteristics are believed to be broadly similar to characteristics of a number of potential sites in the respective countries. Some degree of hypothetical modification has been assumed or, in the case of the Whiteshell site, hypothetical information used, which has the effect of making the results of the assessment more generally applicable. In the Kristallin-I assessment, properties generally expected in the crystalline basement rock of Northern Switzerland are assumed; in the comparison here, parameter values quoted are those assumed for Reference Area West (see NAGRA 1994b).

4.3.6 Hydrogeological properties and regime

Comparison of estimated bulk hydraulic conductivities at repository depth, see Table 4.1, indicate possibly slightly lower average values in the AECL 94 and Kristallin-I cases than in the SKB 91 case. However, probably more significant is the contrast between hydraulic conductivities estimated for averagely fractured rock and for major fracture zones in each case; this is markedly less in the case of SKB 91 than in any of the other cases. This is reflected in hydrological modelling of the respective sites. In the TVO 92, AECL 94 and Kristallin-I assessments, detailed hydrogeological modelling shows groundwater flow, and hence possible transport pathways, being strongly conditioned by major subvertical faults (in the case of TVO 92 and Kristallin-I) and low-angle-dipping and subvertical faults (in the case of AECL 94). In hydrogeological modelling of the Finnsjön site, groundwater flow is less affected by subvertical fracture zones, although very strongly affected by a sub-horizontal fracture zone overlying the repository which has significantly higher conductivity than the subvertical zones (see note 5, Table 4.1).

At the Finnsjön, Veitsivaara and the Whiteshell Research Area sites, the basement rock has only thin and discontinuous cover, so that deep groundwaters can emerge directly to the surface environment or shallow wells, often with relatively little near-surface dilution. For a repository in the crystalline basement of Northern Switzerland, the most likely discharge zone is considered to be to gravel aquifers of the Rhine River valley where potentially quite large dilution is possible. However, the possibilities of discharge to the River Rhine running directly over the basement and to a deep groundwater well are also considered in the Kristallin-I assessment.

4.3.7 Groundwater chemistry

The groundwater compositions at the sites reflect the reaction with rocks of granitic composition. The SKB 91, TVO 92 and Kristallin-I reference waters are predominantly sodium-calcium bicarbonate (Na-Ca-HCO_3) in character, with the AECL 94 ground-

water being best described as sodium-calcium chloride-sulphate (Na-Ca-Cl-SO_4). The AECL 94 groundwater would also be described as saline (> 10 $g.l^{-1}$ total dissolved solids). Table 4.4 summarises reference groundwater compositions considered in the assessments. All the waters have HCO_3 concentrations of the order of 10^{-3} M, with variable amounts of Cl and SO_4. Cation concentrations are dominated by Na and Ca with lesser amounts of K and Mg; the fresh Finnsjön water has an unusually high concentration of Fe. The higher temperature, due to the greater depth of the Kristallin-I water is responsible for the greater solubility of quartz, thus higher Si, and lower solubility of calcite (lower Ca). More detailed discussion is given in McKINLEY & SAVAGE (1994).

Table 4.4: Reference groundwater compositions considered in the assessments

	SKB 91 [1]	**TVO 92** [2]	**AECL 94** [3]	**Kristallin-I** [4]
Temperature (°C)	25	25	25	55
pH	6.9	7.8	-	7.7
Eh (mV)	-200	-350	-	-180
	Concentrations in 10^{-3} M			
Na	1.0	0.41	84.	14.
K	0.08	0.06	0.04	0.22
Ca	1.9	0.55	54.	0.35
Mg	0.26	0.22	0.25	0.01
Fe (total)	0.16	0.0014	0.01	0.0001
Si	0.21	0.13	0.18	0.59
HCO_3	3.6	2.0	1.1	4.7
Cl	1.7	0.04	174.	3.6
S (VI)	0.09	0.0005	11.	3.1
S (II)	0.13	0.0022		0.0002

Notes:

1) Fresh Finnsjön water composition used in performance calculations.
2) Kivetty fresh groundwater.
3) WN-M1 groundwater, but note groundwater compositions were sampled in performance calculations.
4) Area West reference groundwater.

4.4 Comparison of model and data choices

4.4.1 Basis for comparison

The methodological approaches differ between the four assessments. Most notably:

- the SKB 91 assessment considers stochastic failure of canisters, and geosphere transport in stochastically generated flow tubes;
- the TVO 92 assessment makes deliberately very conservative assumptions concerning the site properties and connection of the repository to fracture zones;
- the AECL 94 assessment employs a probabilistic methodology in which parameter values are sampled from probability density functions (pdfs) and the performance is assessed according to the arithmetic mean of dose calculated in multiple simulations;
- the Kristallin-I assessment makes conservative assumptions concerning the canister performance, the characteristics of the water-conducting features in the host rock responsible for radionuclide transport, and dilution and retention in the large thicknesses of overlying higher-permeability basement rock.

In order to simplify the comparison, the following discussion focuses on the Reference Case considered in each assessment. The cases considered will be:

- for SKB 91, deterministic near-field performance considering stochastically determined number and position of canister failure due to an initial defect and stochastic simulation of groundwater flow and radionuclide transport;
- for TVO 92, deterministic near-field and geosphere performance considering the complete failure of a single canister at 10,000 years and radionuclide transport through a fracture zone intercepting the repository;
- for AECL 94, the deterministic simulation, in which median values of parameters are selected as input data, here termed the median value input simulation;
- for Kristallin-I, the deterministic "reference" calculation, which adopts "realistic-conservative" values of most parameters and a conservative representation of the geosphere flow system.

Modelling assumptions and data values quoted in the following text and tables all refer to the above cases unless otherwise stated. Concerning radionuclide-specific data, the comparison will focus on those radionuclides that the assessments show are most important to long-term radiological performance.

4.4.2 Timescales of assessments and significant nuclides

Table 4.5 shows the timescales considered in the assessments and radionuclides that contribute most to the estimated doses. Two timescales are distinguished: the time to which the calculational model is believed to have some validity and results can be regarded as quantitatively meaningful; and the time to which results are presented as an extrapolation of a model which is acknowledged to be inappropriate over such timescales.

In the case of the SKB 91 and AECL 94 assessments, the limit of quantitative interpretation is 10,000 years, since neither model includes the effect of groundwater flow changes associated with glacial episodes; these will affect the Scandinavian and Canadian sites very significantly and rather unpredictably. The TVO 92 calculational model for the Reference Case is also only valid up to 10,000 years, but the effects of longer-term processes are considered in sensitivity analysis, see note 1 of Table 4.5. In the Kristallin-I assessment, the limit of quantitative interpretation is 1,000,000 years, limited by uncertain long-term tectonic development and geomorphology. Changes due to glacial episodes can be accommodated in the Swiss model by conservatively determined dilution and transport in the large thickness of overlying higher-permeability domain basement. This layer and overlying sediments are expected to largely buffer conditions in the low-permeability repository host rock against changes due to the expected glacial cycling, tectonic uplift and erosion.

Table 4.5: Timescales for the assessments and radionuclides that contribute most to estimated doses in these periods

Timescales	**SKB 91**	**TVO 92**	**AECL 94**	**Kristallin-I**
Quatitative interpretation	10,000 years	? years [1]	10,000 years [2]	1,000,000 y
Extrapolation /presentation	10^4 to 10^8 y	10^6 y	10^5 y	10^7 y
Key nuclides				
Earlier times	^{129}I	^{129}I	^{129}I	^{135}Cs
	^{135}Cs	^{94}Nb	^{14}C	^{79}Se
				^{99}Tc
Late times	^{231}Pa (^{235}U)			
	^{226}Ra (^{238}U)	^{231}Pa (^{235}U)	None indicated	^{231}Pa (^{235}U)

Notes:

1) Not stated, but presumably about 10,000 years constrained by glaciation. However, the cases of groundwater flushing (e.g. due to glacial meltwater) and a major rock dislocation are treated in the sensitivity analysis in TVO 92.
2) Related to Canadian regulatory requirements

Timescales for extrapolation/presentation of results are more arbitrary. It is notable that for the AECL 94 site results are only presented to 100,000 years which is insufficient time for uranium isotopes and their progeny to be released and transported to the surface according to the assumed model. Doses calculated in the assessments of spent fuel disposal (SKB 91, TVO 92 and AECL 94) are all dominated by ^{129}I which is effectively absent form the Kristallin-I inventory.

4.4.3 Gross conceptual model choices

All four assessments consider that the primary, indeed the only significant, mechanism for release and transport of radionuclides from the repository to the surface environment is via groundwater. Table 4.6 compares the gross model choices made in each assessment. The main differences can be identified from the table and are commented on below.

The radionuclides are uniformly distributed in the case of the Kristallin-I waste form so that there can be no prompt release component in this case.

The excavation disturbed zone (EDZ) has a significant role in the conceptual models adopted in SKB 91, TVO 92 and Kristallin-I models. In the AECL 94 model, it is implicitly included within the SYVAC3-CC3 geosphere-vault model, although it does not appear as a distinct entity. In the SKB 91, TVO 92 and Kristallin-I cases, the EDZ provides a concentration or flux boundary condition to diffusion through the bentonite and it also provides a pathway for rapid transport along the disposal drifts. In the AECL 94 model, radionuclides must diffuse through the buffer and then, for the repository segments assessed in the Reference Case, also through the backfill, although this is represented by a reduced thickness compared to the actual heights of the disposal caverns.

The transport from the repository and through the geosphere is also treated very differently in each case:

- In the SKB 91 model, groundwater flow is assumed to move through the repository plane and to the surface advectively through a 3-D stochastically generated variable conductivity field. Darcy velocity along each of 88 paths is then used to calculate advective transport velocity in dual-porosity stream tubes.
- In the TVO 92 model, activity passes from the top of a deposition hole to the EDZ and thence to a major fracture zone assumed to intercept the repository. The hydrological properties are conservatively chosen so that this fracture zone is forced to become the transport route. Advective transport velocity in the zone is calculated from Darcy velocity (from groundwater modelling) and assuming a single fracture; this model gives very rapid transport to the surface.
- In the AECL 94 model, the sparsely fractured host rock and the low angle fault, which provides the major pathway for transport to the surface, are both treated as porous media and radionuclides are allowed to be transported by advection and diffusion. However, because of the very low Darcy velocity in the sparsely fractured host rock, transport in this medium is predominantly by diffusion. This provides a very large diffusion barrier compared to any of the other models. The repository is divided into sectors so that different sectors are connected to different potential transport paths to the surface.
- In the Kristallin-I model, fractures and joints in the host rock are represented by a single transmissive element to which alternative geometries and properties can be assigned. Advective transport velocity in the element is calculated from Darcy velocity (from groundwater modelling), accounting for fracture aperture and spacing. The model is potentially applicable to both the low-permeability domain (LPD) host rock and to major water-conducting faults (MWCF) and overlying higher-permeability domain (HPD). However, taking into account their respective properties, the transport resistance of the last two is negligible compared to the first, and

therefore transport in both the MWCF and HPD is conservatively assumed to be instantaneous in the Reference Case.

Differences in the biosphere arise from actual differences in expected discharge zones. All the assessments assume present-day-like climate in their Reference Cases, but the Kristallin-I assessment considers alternative biosphere scenarios representing possible future climate states at the site.

In summary, the differences in gross conceptual model characteristics arise both from actual differences in the disposal system (e.g. the different waste forms and site/repository geometries) and from major differences in assumptions, notably, the treatment of the sparsely fractured host rock as a porous medium in the AECL 94 model. It is unclear whether the parameter sampling practiced in the AECL 94 methodology can sample parameter combinations such that transport pathways are defined that approximate to the transport in fractured rock modelled in the other three cases. However, the AECL 94 median value input case is clearly less conservative than the Reference Cases considered in the other assessments since it implies very long advective groundwater transport time (see section 4.4.5).

Table 4.6: Comparison of gross conceptual model choices and features and processes included in the models

	SKB 91	**TVO 92**	**AECL 94**	**Kristallin-I**
Canister failure	Yes, stochastically chosen	Yes, single canister at 10,000 years	Yes, probabilistic timing over 10,000 years	Yes, all simultaneously at 1,000 years
Radionuclide release	Rapid component plus slower matrix degradation component	Rapid component plus slower matrix degradation component	Rapid component plus slower matrix degradation component	Matrix degradation only
Transport in buffer	Diffusion to host rock and EDZ	Diffusion to EDZ	Diffusion to and through backfill [1]	Diffusion to EDZ
Transport from repository	Spatially distributed source to host rock	Directly along EDZ to major fracture zone	Spatially distributed source to host rock	Along EDZ to transmissive elements in host rock
Transport in sparsely fractured host rock	Advection in dual-porosity stream tubes in variable conductivity field	Neglected	Diffusion or advection in equivalent porous medium [2]	Advection in a fracture or vein
Transport in major fractures	Not significant	Advection in fractures	Advection in porous medium	Rapid
Transport in overlying geounits	None	None	Advection or diffusion in porous media	Rapid
Biosphere	Well, lake and agricultural pathways	Well, lake and agricultural pathways	Well, lake and agricultural pathways	Gravel aquifer, well, river and agricultural pathways

Notes:

1) For the segments assessed in the Reference Case.
2) Diffusion-dominated due to very low Darcy velocity in host rock around the repository.

4.4.4 Detailed model and data choices - the near field

Table 4.7 lists key processes and features that may affect the release of radionuclides from the near field of a single waste canister, and summarises the assumptions and choices made regarding these processes in each assessment. The number of differences is now rather too large to comment on in any detail. Attention here is drawn only to those points that are most striking or are expected to have most impact on performance.

The different canister constructions lead to different failure mechanisms and associated assumptions. The SKB 91 assessment places very great reliance on canister integrity; in the Reference Case, only about 6 of the 5,830 canisters will fail in the timescale considered. Similarly in the TVO 92 assessment, the Reference Case calculates releases from a single failed canister, which (although not stated in the TVO 92 report) can be interpreted as assumed failure due to initial defect with a probability of 1/1,000. However, in the TVO sensitivity analysis, dose results are also calculated pessimistically assuming all canisters fail at 10,000 or 1,000 years.

The reasons for the different assumptions concerning the composition of the gap and grain boundary inventories are unclear and surprising, especially given the similarity between the SKB and TVO fuel types.

The radiolytic oxidation model for degradation of UO_2 fuel matrix employed by TVO and SKB is markedly more conservative than the solubility limited model assumed by AECL. In the case of the AECL model, the median solubility limit for UO_2 is so low, and the transport of uranium away from the waste so restricted, that the waste matrix remains virtually intact even after 100,000 years. This prevents not only release of uranium isotopes but all other nuclides contained in the fuel. The waste matrix dissolution model in the Kristallin-I assessment conservatively assumes the glass is completely dissolved after about 150,000 years in the Reference Case.

Solubility limits are assumed to limit radionuclide concentrations in solution in contact with the wastes in all cases but the data values and their conceptual bases are different, see section 4.4.6. In addition, the AECL 94 model considers a redox front situated in the bentonite which causes precipitation of redox sensitive nuclides, notably technetium.

All models consider diffusion in the bentonite, but the SKB and TVO models used in the Reference Cases ignore the transient phase, leading to much earlier releases following canister failure than seen in the Kristallin-I and AECL models. Although the radial thicknesses of bentonite used in the deposition hole concepts are much less than in the in-tunnel concept, the main diffusive transport route in the SKB and TVO models, and the AECL model for vault segments assessed in the Reference Case, is vertically upwards so that, in all cases, radionuclides must traverse about one metre of bentonite buffer. However, the radial geometry in the Kristallin-I case provides a greater volume of buffer for diffusion, see section 4.3.3. The use of the cavern backfill as an additional sink for diffusing radionuclides in the AECL 94 model has already been mentioned.

The TVO 92 model uses a conservative zero concentration boundary for diffusion; the Kristallin-I assessment considers a zero concentration boundary as a conservative parameter variation. The treatment of the host-rock as a diffusion-dominated porous medium in the AECL case considerably reduces the possible diffusive flux from the near field.

Table 4.7: Key processes and features affecting the release from a single canister, and assumptions or model choices made in the assessments

	SKB 91	TVO 92	AECL 94	Kristallin-I
Resaturation of buffer	Rapid and complete	Rapid and complete	Rapid and complete	Rapid and complete
Canister failure mechanism	Due to initial defect with P=1/1,000, over-pressure & corrosion	Unspecified, but initial defect implied	Several modelled, crevice corrosion dominates	Mechanical following corrosion
Treatment of failed canister	Initial transport resistance due to 5 mm^2 hole	Canister "disappears"	Canister "disappears"	No physical effect, but ensures low Eh
Time of waste contact by water	1,000 y	10,000 y	Probabilistic, over 0-10,000 y	1,000 y
Treatment of gap and grain boundary inventory	100 % C,10 % Cl and I, 5 % Cs released instantly	10 % I, 5 % Cs, 1% C released instantly. 10 % I, Cs, C 100 % Tc, Pd released over 10,000 y	13 % C, 8 % I, Cs and Se, 6 %Tc released instantly	None
Treatment of fuel cladding inventory	Congruent release according to Zircaloy dissolution	Uniform release over 10,000 y	Congruent release according to Zircaloy dissolution. Sol=1.8×10^{-9} M	None
Treament of waste matrix inventory	Congruent release with UO_2 assuming radiolytic oxidation	Congruent release with UO_2 assuming radiolytic oxidation	Congruent release with UO_2 dissolution, Sol=1.6×10^{-10} M	Congruent release with glass corrosion, rate based on measurements
Source term for transport through buffer	Elemental solubility limits calculated for groundwater	Elemental solubility limits conservatively selected	Elemental solubility limits considering oxidising groundwater conditions	Elemental solubility limits calculated for bentonite porewater
Transport through buffer	Radial and axial equilibrium diffusion. Sorption not included for equilibrium case	Axial (1D) transient diffusion with sorption	Axial (1D) transient and equilibrium diffusion with sorption, precipitation at redox front	Radial transient and equilibrium diffusion with sorption
Outer boundary condition	Advective flux in EDZ and host rock	Zero concentration in EDZ	Transfer coefficient preserves mass balance & conc.	Advective flux in EDZ

4.4.5 Detailed model and data choices - repository, geosphere and biosphere

Table 4.8 lists key processes and features that may affect the release of radionuclides from the repository, transport through the geosphere and dose pathways in the biosphere, and summarises the assumptions and choices made regarding these processes in each assessment. Attention here is drawn only to those points that are most striking or are expected to have most impact on performance.

The SKB 91 and AECL 94 models account explicitly for the spatial extent of the repository and variable hydrological conditions over the repository area. In the TVO 92 case, the failed canister is conservatively assumed to be close to a high permeability zone, and in the Kristallin-I case, the EDZ is assumed to provide a fast conduit for radionuclide transport from the bentonite periphery to transmissive elements in the geosphere.

The very different assumptions concerning transport in fractured rock have already been commented on in section 4.4.3. Table 4.9 illustrates calculated groundwater travel times for the Reference Case in each of the assessments, where the large differences are primarily due to the assumptions about water flow in the fractured rock.

The Kristallin-I assessment links geological observations of the detailed structure of potentially transmissive fractures and joints to assessment calculations. In the AECL assessment, a connection was also made between field and laboratory data and larger-scale modelled features although no details are given in GOODWIN et al. (1994). The SKB and TVO assessments rely on geosphere transport parameters derived from more gross hydrogeological characteristics and modelling.

All the biosphere models consider the same basic pathways of drinking water, consumption of cultivated vegetable and animal products, external irradiation and inhalation. However, the AECL 94 model also considers other uses of environmental materials, e.g. burning of wood or peat, and considers wild food products, e.g. water fowl. Only the TVO 92 assessment takes into account the most recent dosimetric advice of ICRP 61 (ICRP 1991), although AECL 94 considers how this recent advice would affect radiation dose and risk compared to the ICRP 30 (ICRP 1979).

Table 4.8: Key processes and features affecting transport from the repository and in the geosphere and biosphere, and model choices made in the assessments

	SKB 91	TVO 92	AECL 94	Kristallin-I
Release from total repository	Repository divided into 88 equal segments each attached to a separate geosphere stream tube	Single failed canister assumed to be located close to a fracture zone	Repository divided into 12 sectors defined on hydraulic conditions and attached to separate geosphere paths	Release from single canister multiplied by total number of canisters and connected to a single geosphere path
Groundwater flow regime in host rock and repository region	Mainly subhorizontal flow beneath major sub-horizontal fracture zone	U-tube flow through repository forced by parameter choice(1)	Slow upward flow to low angle fracture zone or direct to near-surface	Slow flow towards major subvertical faults and up- wards in the cen- tre of LPD blocks
Transport pathway through geosphere	Advection in dual-porosity stream tubes through stochastically generated variable K field	Advection directly up subvertical fracture zone	Diffusion either to low angle fracture zone or direct to near-surface, according to network model	Advection in fractures through LPD and rapid advection in MWCF and HPD
Model for transport through sparsely fractured rock	Advection with Fickian dispersion. Diffusion into rock matrix. LE sorption in matrix	Not encountered	Diffusion (dominant) and advection. LE sorption.	Advection with Fickian dispersion. Diffusion into fracture infill. LE sorption in matrix.
Model for transport through major fractures	Implicit in geosphere models	Advection with dispersion. Diffusion into rock matrix . LE sorption in matrix.	Diffusion and advection with dispersion (dominant). LE sorption.	Instant transport in MWCF and HPD
Biosphere model	1 % release to well, 99 % to lake. Agricultural pathways	2 % release to well, 98 % to lake. Agricultural pathways	Release to well, lake sediment, soil and surface water. Agricultural and "wild" pathways	Release to gravel aquifer. Shallow well, irrigation and agricultural pathways
Dosimetry	ICRP 30	ICRP 60	ICRP 30/60	ICRP 30

Note:

1) The repository is modelled as linking two major fractures, one of which acts as a conduit for water input from the near surface into the repository, the other as a rapid conduit for radionuclide-contaminated water from the repository to the near surface.

Abbreviations: K - hydraulic conductivity; LE - linear equilibrium (sorption); LPD - low permeability domain; HPD - higher-permeability domain; MWCF - major water-conducting fault.

Table 4.9: Calculated advective groundwater travel times in each assessment

Typical water travel times in:	**SKB 91**	**TVO 92**	**AECL 94**	**Kristallin-I**
- low K rock	100 y [1]	-	7,800,000y [3]	20 y [6]
- faults etc.	-	5 y [2]	430 y [4]	~ 0 [7]
- overburden	-	-	200 y [5]	~ 0 [8]

Flow path description:

1 Most probable value from the stochastic calculations for the Reference Case (repository depth 600 m)
2 400 m in a fracture zone with water velocity of 80 m y^{-1}
3 46.5 m sparsely fractured rock with very small hydraulic gradient
4 536 m of extensive fracture zone
5 3.8 m overburden
6 200 m in transmissive element (jointed/cataclastic zone) in fractured host rock
7 Model assumes near instantaneous transport in major water conducting faults
8 Model assumes negligible transit times in HPD and Rhine gravels

4.4.6 Comparison of radionuclide-specific data

Several radionuclide-specific parameters have significant effects on calculated releases and doses. Here, selected data are introduced; the quantitative differences are obvious from inspection of the tables. The effect of some of these differences will be noted in the section 4.5.

Table 4.10 shows near-field solubility limits of selected elements corresponding to the radiologically important radionuclides. For the SKB 91 and AECL 94 assessments, chemical conditioning of the groundwater by reaction with bentonite is neglected, which may be justified due to the smaller masses of bentonite directly surrounding the waste canister in the deposition hole. In these cases, solubility is calculated for various groundwaters as noted below the table. TVO 92 solubilities are conservatively selected for a range of groundwaters and bentonite pore fluids. For Kristallin-I, a range of bentonite porewaters was defined using an empirical model of ground water reaction with sodium bentonite incorporating ion exchange and precipitation of mineral phases. In all assessments, radionuclide solubility in the selected fluids is calculated using equilibrium thermodynamic codes, e.g. MINEQL, PHREEQE, EQ3/6. In the AECL 94 assessment, the calculation used a deterministic equation with input parameters such as ionic strength and equilibrium constants, some of which are defined using pdfs. The randomly sampled calculations yield a distribution of solubility limits, which was then sampled in the radiological release and transport model: for the median value input simulation, the median values of those parameters defined by pdfs were used. A more detailed comparison of solubility limits is presented elsewhere (McKINLEY & SAVAGE 1994).

Table 4.10: Reference near-field solubility limits for selected elements

Solubility limit (M)	SKB 91[1]	TVO 92[2]	AECL 94[3]	Kristallin-I[4]
Carbon	high	high	high	-
Selenium	1×10^{-9}	4×10^{-6}	high	1×10^{-8} (6×10^{-7})
Niobium	1×10^{-5}	high	high	-
Technetium	2×10^{-8}	3×10^{-8}	2.9×10^{-9}	1×10^{-7} (high)
Iodine	high	high	high	-
Caesium	high	high	high	high
Radium	1×10^{-6}	1×10^{-4}	high	1×10^{-10} (2×10^{-5})
Protactinium	1×10^{-6}	1×10^{-5}	high	1×10^{-10} (1×10^{-7})
Uranium	2×10^{-7}	3×10^{-6}	1.6×10^{-10}	1×10^{-7} (7×10^{-5})

Notes:

1) Solubility in reducing fresh Finnsjön water, with chemical effects of bentonite ignored.
2) Highest values selected from solubilities calculated for elements in a range of reducing non-saline and brackish groundwater and bentonite pore fluids.
3) Solubility limits set to 2M (high) for all elements except Tc, Np, Th, U and Pu. Values for Tc and U are median values from probabilistically calculated distributions from sampled ranges of groundwater characteristics.
4) Realistic (and conservative) values based on calculated solubilities in bentonite pore water.

high indicates solubility effectively unlimited.

Tables 4.11 and 4.12 show sorption coefficients in bentonite and in the geosphere, respectively. All assessments use a simple linear equilibrium sorption model, with the exception that non-linear sorption of ^{135}Cs in the geosphere is considered in the Kristallin-I assessment. (Further comparison of sorption data can be found in McKINLEY & SCHOLTIS 1993 and STENHOUSE & PÖTTINGER 1994).

Table 4.11: Reference sorption coefficients in bentonite for selected elements

Sorption coefficient, Kd, (m^3kg^{-1})	SKB 91	TVO 92[1]	AECL 94[2]	Kristallin-I[3]
Carbon	0.	0.	?	-
Selenium	0.003	0.	?	0.005 (0.001)
Niobium	0.2	0.	?	-
Technetium	0.1	0.01	?	0.1 (0.05)
Iodine	0.	0.	?	-
Caesium	0.05	0.2	?	0.01 (0.001)
Radium	?	0.1	?	0.01 (0.001)
Protactinium	?	0.01	?	1.0 (0.1)
Uranium	?	0.5	?	5.0 (0.5)

Notes:

1) Conservatively selected values for non-saline reducing conditions.
2) Data not given in AECL 94 report as SYVAC3-CC3 vault model uses a parameter called the capacity factor which incorporates the Kd.
3) Realistic (and conservative) values selected for calculation of diffusivity

? indicates data not given in available documents.

Table 4.13 shows dose per unit rate of radionuclide input to the biosphere. The doses calculated are the sum of committed weighted dose equivalents from intakes in a single year plus the sum of dose equivalents from external irradiation in the same year, although, in all cases, the latter component is negligible. The TVO 92 dose factors are based on the SKB factors but taking into account the factor of two higher interception of contaminants by a well, plus the radionuclide-specific difference in dose per unit activity ingestion between ICRP 30 and the more recent ICRP 61 recommendations.

It is notable that the biosphere dose factors for Kristallin-I are generally about one order of magnitude lower than for SKB 91 and TVO 92, which is a smaller reduction than would be expected from consideration of initial dilution on entering the biosphere. Inspection of the dose pathways indicates foodstuff pathways are relatively more important in the Kristallin-I model, whereas drinking water is generally more important in the SKB 91 and TVO 92 models. This may indicate a relatively greater build up of radionuclides in the soil compartments of the Kristallin-I biosphere than seen in the SKB 91 and TVO 92 models.

Table 4.12: Reference sorption coefficients in the geosphere for selected elements

Sorption coefficient Kd, (m^3kg^{-1})	**SKB 91[1]**	**TVO 92[2]**	**AECL 94[3]**	**Kristallin-I[4]**
Carbon	0.001	0.0001	?	-
Selenium	0.001	0.0005	?	0.01 (0.001)
Niobium	-	0.00005	?	-
Technetium	1.0 [5]	0.05	?	0.5 (0.05)
Iodine	0.	0.0002	?	-
Caesium	0.15	0.05	?	0.042 *(0.0084)
Radium	0.15	0.05	?	0.5 (0.1)
Protactinium	1.0	0.01	?	1. (0.1)
Uranium	2.0	0.1	?	1. (0.05)

Notes:

1) Selected on the basis of estimated sorption in a range of groundwaters
2) Lowest values selected from values recommended for fresh reducing conditions in two rock types (granite/granodiorite etc. and tonalite/mica-gneiss).
3) Data not given in AECL 94 report as SYVAC3-CC3 uses Kds for sorption on individual minerals.
4) Realistic (and conservative) values; *non-linear sorption considered for Cs, values here derived from realistic and conservative Freundlich isotherm.
5) Technetium assumed to be reduced.

? Indicates value not given in available documents.

Table 4.13: Biosphere dose factors - Dose to a member of the critical group for unit rate of radionuclide input to the biosphere

Biosphere factor, $Sv.y^{-1}$ per $Bq.y^{-1}$	SKB 91[1]	TVO 92[2]	AECL 94[3]	Kristallin-I[4]
^{14}C	1×10^{-14}	2×10^{-14}	?	-
^{79}Se	6×10^{-14}	1×10^{-13}	?	9×10^{-15}
^{94}Nb	-	4×10^{-14}	?	-
^{99}Tc	2×10^{-15}	7×10^{-15}	?	4×10^{-15}
^{129}I	5×10^{-13}	2×10^{-12}	?	-
^{135}Cs	4×10^{-14}	8×10^{-14}	?	2×10^{-15}
^{226}Ra	2×10^{-12}	1×10^{-11}	?	1×10^{-13}
^{231}Pa	1×10^{-10}	4×10^{-11}	?	2×10^{-11}

Notes:

1) 1 % activity to well scenario
2) 2 % activity to well scenario, based on SKB 91 factors but adjusted to include ICRP 61 dose per unit ingestion factors.
3) Data not given in AECL 94 report.
4) R. Klos, pers. comm. 20/10/93.

4.5 Comparison of results

4.5.1 Comparison of near-field performance

Calculated radionuclide releases from the near-field as a function of time for a single canister (SKB 91 and TVO 92), a repository sector (AECL 94) or the total repository (Kristallin-I) are plotted in the assessment reports in a variety of units. For the purposes of comparison, the results from the respective reports have been converted to Bq y^{-1} and normalised to refer to the inventory of *a single canister that has failed*. There are, however, still a number of factors that should be considered when viewing the comparative results.

- Each canister contains wastes from a similar amount of spent fuel expressed in tU, see Table 4.1, but there are marked differences in the radionuclide concentrations per tU, see Table 4.3.
- Releases from the SKB 91 and Kristallin-I canisters both begin at 1,000 years but in the SKB 91 assessment this is regarded as a low probability occurrence, whereas, the failure is assumed to occur in all canisters in the Kristallin-I assessment.
- Release from the TVO 92 canister begins at 10,000 years; this is an assumption made for the purpose of assessment of the multibarrier system.
- The AECL 94 report shows release from the near field of a particular repository sector, which is nearest to the low angle fracture zone, assuming all the canisters fail at time zero; this has been divided by the number of canisters in the sector (~ 2200).

Figures 4.1 to 4.4 show the near field releases of all radionuclides given in Table 4.5 for which results can be extracted from the reports.

Figure 4.1 compares the releases of ^{14}C and ^{129}I from the SKB 91, TVO 92 and AECL 94 near-field models. Although not radionuclides of direct interest in Kristallin-I, this result is included here since ^{129}I is the most important radionuclide for these assessments. Furthermore, ^{14}C and ^{129}I are the only radionuclides released in significant quantities from the AECL model. There is a remarkable agreement in the long-term releases of ^{129}I from the SKB and TVO models; this may be coincidental or related to their similar inventories and diffusion geometries. However, the releases of both ^{129}I and ^{14}C from the AECL model are approximately two orders of magnitude lower than the releases from the SKB and TVO models. The structure in the SKB and TVO results (for example, the change of slope at about 20,000 years in the TVO results) is related to the exhaustion of the gap and grain boundary inventories, see Table 4.7.

Figure 4.2 compares the releases of ^{79}Se and ^{99}Tc from the TVO 92 and Kristallin-I near-field models. Neither radionuclide appears in plotted results in the SKB report, implying releases of less than 1 Bq y^{-1}. Results in the AECL 94 report indicate a maximum release of ^{99}Tc of about 10^{-10} Bq y^{-1} at 100,000 years. Both ^{79}Se and ^{99}Tc are solubility limited in the near field. This gives rise to the constant long-term release in the case of ^{99}Tc, even though ^{99}Tc is decaying significantly in this period (see Table 4.2). However, this is not seen for ^{79}Se (even though it is longer-lived) since stable Se is also present and hence the effective solubility limit for the nuclide declines according to radioactive decay as the fraction of radio-selenium declines. The agreement of results for ^{99}Tc at long times is coincidental; the Kristallin-I solubility limit is greater than the TVO value by a factor of 3 (see Table 4.10) but this seems to be compensated for by the radial geometry of diffusion in Kristallin-I. The Kristallin-I solubility limit for Se is less than the TVO value by a factor of 400, and this together with the geometry factor explains the approximately two orders of magnitude difference seen in releases at longer times.

Figure 4.3 compares the releases of ^{135}Cs from the SKB 91, TVO 92 and Kristallin-I near-field models. ^{135}Cs is long-lived and does not reach a solubility limit. The total inventory per canister in the three cases is very similar, but the fractions associated with gap and grain boundaries (see Table 4.7) give rise to the early structure in the case of SKB 91 and TVO 92. The effect of modelling the transient diffusion phase in the Kristallin-I model is to reduce the early release but, for the case of a long-lived nuclide such as ^{135}Cs this does not greatly affect the peak release rate calculated.

Figure 4.4 compares the releases of ^{226}Ra and ^{231}Pa from the SKB 91, TVO 92 and Kristallin-I near-field models. These are nuclides in the chains of ^{238}U and ^{235}U, respectively. Interpretation of these results is complicated since the time-dependent results are due to the ingrowth of the nuclides at source and during transit and, thus, depend on the solubility and sorption of uranium as well as radium and protactinium themselves. The generally lower calculated near-field releases of both ^{226}Ra and ^{231}Pa for Kristallin-I, may be primarily due to the lower solubility limit of uranium in the waste; while the reversal of relative magnitudes of releases of ^{226}Ra and ^{231}Pa ($^{226}Ra > {}^{231}Pa$ in Kristallin-I but $^{231}Pa > {}^{226}Ra$ in SKB 91 and TVO 92) may be due to the higher sorption coefficient for protactinium assigned in Kristallin-I.

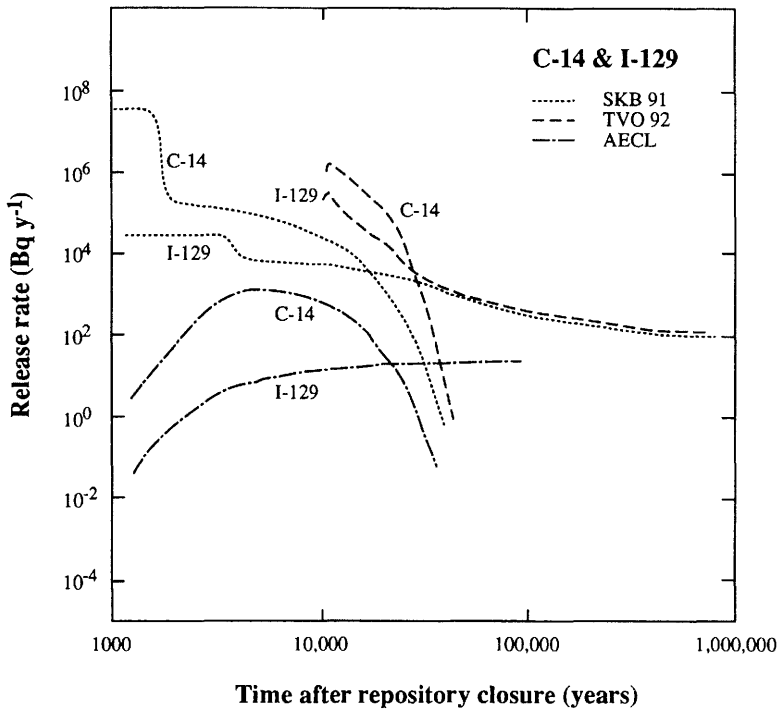

Fig. 4.1: Comparison of radionuclide release rates from the near field for a single failed canister: ^{14}C and ^{129}I

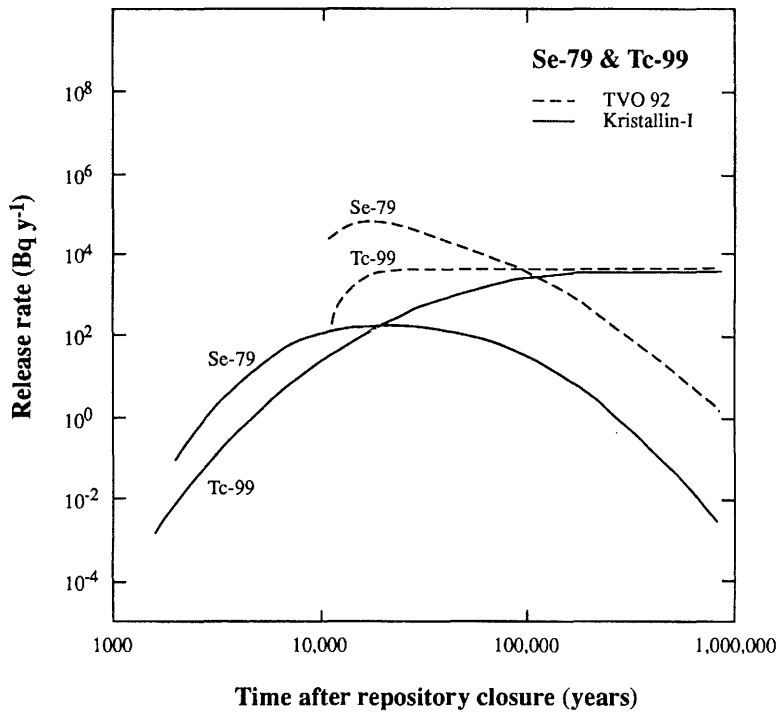

Fig. 4.2: Comparison of radionuclide release rates from the near field for a single failed canister: ^{79}Se and ^{99}Tc

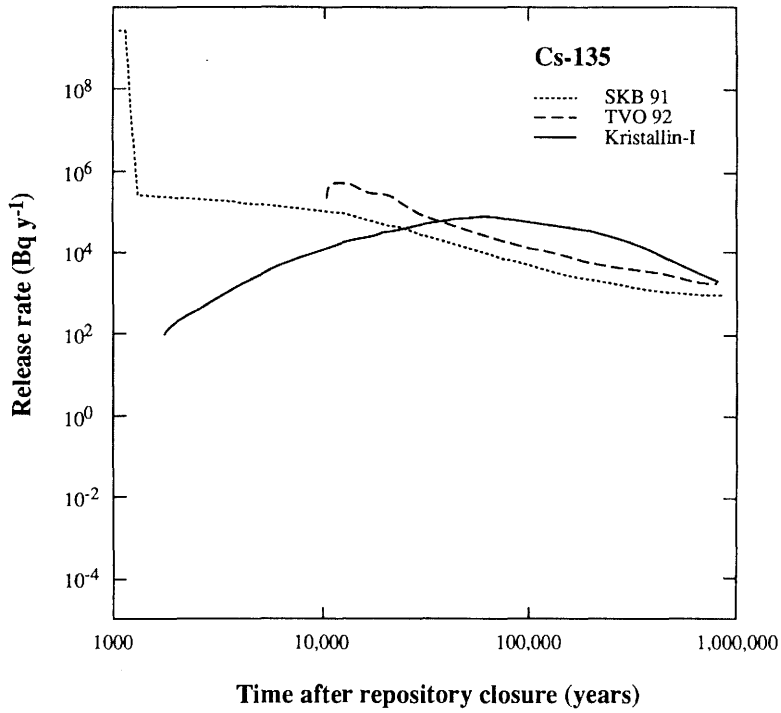

Fig. 4.3: Comparison of radionuclide release rates from the near field for a single failed canister: ^{135}Cs

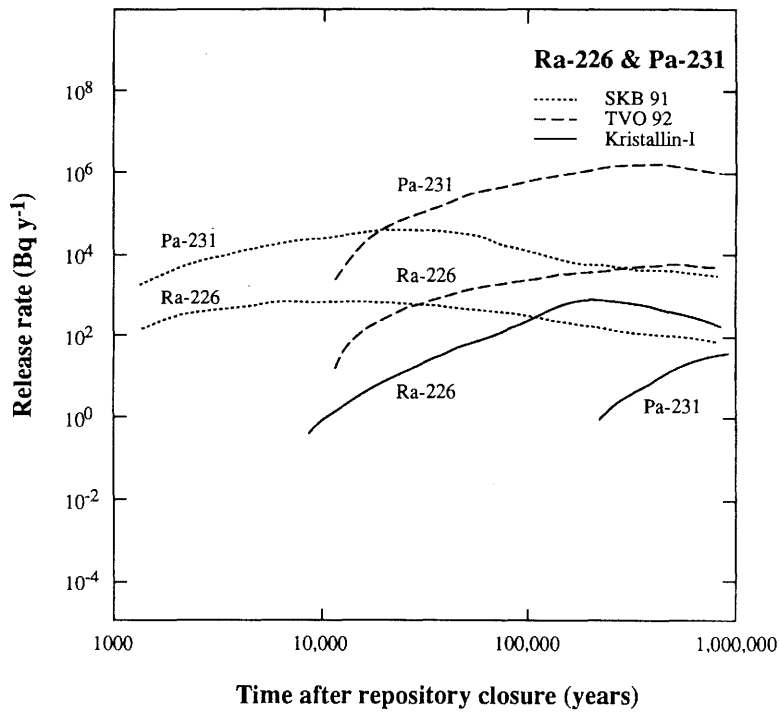

Fig. 4.4: Comparison of radionuclide release rates from the near field for a single failed canister: ^{226}Ra and ^{231}Pa

4.5.2 Comparison of geosphere performance

It is not possible to extract and compare the time-dependent performances of the geosphere models from the assessment reports as the results presented are dependent on very different time-dependent near-field releases as input to the geosphere. To make a comparison, a format used in the TVO 92 report is adopted. This shows maximum release rates from the near field and geosphere, and the respective times of occurrence. Similar information has been extracted to the extent possible from the SKB 91, AECL 94 and Kristallin-I documents. *In each case, the results have been normalised to apply to the release from a single failed canister.*

Table 4.14 shows the calculated near-field and geosphere releases for each assessment. In addition, the geosphere performance is indicated by calculating the ratio of maximum geosphere release to maximum near-field release. The time delay to the maximum is also calculated where possible. A small ratio and a long delay indicate a significant geosphere influence, and a ratio of one and "small" delay indicates no geosphere effect.

The SKB 91 results presented in Table 4.14 refer to a groundwater travel time of 50 years, somewhat less than the median time from stochastic simulation of 110 years, but the longest time for which data can be extracted from the results provided. The delay of radionuclide transport cannot be extracted from the report. Two values of the geosphere/near-field ratio are calculated for ^{135}Cs: one considering the rather short-lived initial peak due to release of the gap and grain boundary from the buffer and one considering the more representative longer-term initial release (see Fig. 4.3) denoted by ^{135}Cs and $^{135}Cs^*$, respectively. For the groundwater travel time given, the results in Table 4.14 indicate that: ^{14}C decays entirely within the geosphere; ^{129}I is moderately reduced; the initial ^{135}Cs peak is very effectively reduced but the longer-term release is less affected. Both ^{129}I and ^{135}Cs are very long-lived so that the mechanism for reduction is diffusion and sorption within the rock matrix which retards and spreads the release. The ratio of greater than one for ^{226}Ra indicates that the geosphere release is dominated by ^{226}Ra that has ingrown from ^{238}U in the geosphere.

For TVO 92, results in Table 4.14 indicate virtually no geosphere effect for ^{14}C, ^{79}Se or ^{94}Nb, and only very moderate effect for ^{129}I. The very long delay for ^{99}Tc indicates very significant sorption and decay in the geosphere. However, because the release of ^{99}Tc from the near field is maintained by the solubility limit at a constant level for up to one million years, and because the sorption process is represented as reversible, a dynamic equilibrium is almost achieved (at one million years) and the geosphere release approaches that of the near field. For ^{135}Cs, a moderate reduction is achieved but this is related to the retardation and spreading of the initial near-field release (see Fig. 4.3): in the longer term, the geosphere release can be expected to approach the near-field release. The times of peak releases of both ^{226}Ra and ^{231}Pa from the near field and from the geosphere closely coincide, indicating that the geosphere output of each is related to input of the nuclide, not to input of uranium. In this case, the ratios and delays are a proper measure of the geosphere performance, and the much better performance for ^{226}Ra is due to its relatively short half-life.

For AECL 94, the results shown in Table 4.14 are for the near-field release from one of the repository zones nearest to the low angle fault, and release to the fault, scaled to refer to the release from a single canister. These indicate very substantial reductions in release due to the geosphere. However, results are only presented in

the AECL report up to 100,000 years, at which time geosphere releases of ^{99}Tc and ^{129}I are still rising. If calculations were continued, then the expected long-term geosphere/near-field ratio for ^{129}I would be to be greater than the 3 % value indicated in the table.

For Kristallin-I, a significant delay and moderate reduction of release is achieved for ^{79}Se; a very substantial delay is achieved for ^{99}Tc allowing radioactive decay to substantially reduce the release; a substantial delay is also achieved for ^{135}Cs but for this much longer-lived nuclide, the effect on maximum release rate is rather small. The coincidence of times of maximum release from the geosphere of uranium isotopes and their daughters, at the very long time of 14 million years, indicates that the daughters are in a secular equilibrium with their parent due to ingrowth in the geosphere.

Comparison of results of all four models confirms the very limited effect of the TVO 92 geosphere and the apparently very large effect of the AECL geosphere, although the limited timescale of assessment must be noted in the latter case. This is directly attributable to the very different gross conceptual models, see Table 4.6, and not an indication of the relative potential performance characteristics of sites in Finland and Canada, see hydraulic data in Table 4.1. Comparing SKB 91 and Kristallin-I, unfortunately there is only one common radionuclide - ^{135}Cs. The valid comparison is of the second $^{135}Cs^*$ geosphere/near-field ratio of 0.25 for SKB with 0.66 for Kristallin-I. The SKB 91 sorption coefficient for caesium is markedly higher than the Kristallin-I value (see Table 4.12), and this accounts for the greater retention in the geosphere in the SKB case, although, it should be noted that the transport models are also different, see Table 4.8.

Table 4.14: Maximum releases from the near field and geosphere normalised to represent releases from a single failed canister: the effect of the geosphere is indicated by the ratio of the maximum releases (GS/NF ratio) and the delay in maximum geosphere release

SKB 91	Max. release from near field		Max. release from geosphere		Geosphere effect	
	Maximum rate	Occurs at	Maximum rate	Occurs at	GS/NF	Delay of max.
Nuclide	$Bq.y^{-1}$	years	$Bq.y^{-1}$	years	ratio	years
^{14}C	$4.0 \times 10^{+7}$	1,000	0.0	?	0.0	?
^{129}I	$5.0 \times 10^{+4}$	1,000	$2.0 \times 10^{+4}$	?	4.0×10^{-1}	?
^{135}Cs	$3.0 \times 10^{+9}$	1,000	$5.0 \times 10^{+4}$	?	1.7×10^{-5}	?
^{135}Cs*	$2.0 \times 10^{+5}$	2,000	$5.0 \times 10^{+4}$	?	2.5×10^{-1}	?
^{226}Ra	$8.0 \times 10^{+2}$	30,000	$1.0 \times 10^{+3}$	?	1.3	?
^{231}Pa	$3.0 \times 10^{+4}$	20,000	$5.0 \times 10^{+1}$	?	1.7×10^{-3}	?
TVO 92	Max. release from near field		Max. release from geosphere		Geosphere effect	
	Maximum rate	Occurs at	Maximum rate	Occurs at	GS/NF	Delay of max.
Nuclide	$Bq.y^{-1}$	years	$Bq.y^{-1}$	years	ratio	years
^{14}C	$2.0 \times 10^{+6}$	11,000	$2.0 \times 10^{+6}$	11,000	1.0	small
^{79}Se	$9.0 \times 10^{+4}$	13,000	$9.0 \times 10^{+4}$	14,000	1.0	1,000
^{94}Nb	$4.0 \times 10^{+6}$	11,000	$4.0 \times 10^{+6}$	11,000	1.0	small
^{99}Tc	$7.0 \times 10^{+3}$	14,000	$5.0 \times 10^{+3}$	1,000,000	7.1×10^{-1}	1,000,000
^{129}I	$5.0 \times 10^{+5}$	10,000	$3.0 \times 10^{+5}$	10,000	6.0×10^{-1}	small
^{135}Cs	$5.0 \times 10^{+5}$	11,000	$9.0 \times 10^{+4}$	53,000	1.8×10^{-1}	40,000
^{226}Ra	$3.0 \times 10^{+6}$	310,000	$1.0 \times 10^{+3}$	330,000	3.3×10^{-4}	20,000
^{231}Pa	$8.0 \times 10^{+3}$	1,000,000	$5.0 \times 10^{+3}$	1,000,000	6.3×10^{-1}	small
AECL 94	Max. release from near field		Max. release from geosphere		Geosphere effect	
	Maximum rate	Occurs at	Maximum rate	Occurs at	GS/NF	Delay of max.
Nuclide	$Bq\ y^{-1}$	years	$Bq\ y^{-1}$	years	ratio	years
^{14}C	$9.0 \times 10^{+2}$	10,000	2.2×10^{-2}	45,000	2.5×10^{-5}	35,000
^{99}Tc	4.5×10^{-10}	>100,000	1.3×10^{-18}	>100,000	3.0×10^{-9}	?
^{129}I	$1.3 \times 10^{+1}$	>100,000	4.5×10^{-1}	>100,000	3.3×10^{-2}	?
K-I	Max. release from near field		Max. release from geosphere		Geosphere effect	
	Maximum rate	Occurs at	Maximum rate	Occurs at	GS/NF	Delay of max.
Nuclide	$Bq.y^{-1}$	years	$Bq.y^{-1}$	years	ratio	years
^{79}Se	$2.1 \times 10^{+2}$	8,000	$9.6 \times 10^{+1}$	65,000	4.6×10^{-1}	60,000
^{99}Tc	$5.7 \times 10^{+3}$	1,300,000	$5.1 \times 10^{+1}$	1,800,000	8.8×10^{-3}	500,000
^{135}Cs	$7.4 \times 10^{+4}$	80,000	$4.9 \times 10^{+4}$	280,000	6.6×10^{-1}	200,000
^{226}Ra	$9.5 \times 10^{+2}$	250,000	5.2×10^{-1}	14,000,000	5.5×10^{-4}	14,000,000
^{238}U	2.8×10^{-1}	10,000,000	2.7×10^{-1}	14,000,000	9.6×10^{-1}	4,000,000
^{231}Pa	6.8×10^{-1}	1,000,000	1.5×10^{-1}	14,000,000	2.2×10^{-1}	13,000,000
^{235}U	1.5×10^{-1}	10,000,000	1.5×10^{-1}	14,000,000	9.5×10^{-1}	4,000,000

4.5.3 Comparison of overall doses

Figure 4.5 shows calculated individual doses for Reference Cases from the SKB 91, TVO 92, AECL 94, H-3 (for comparison) and Kristallin-I assessments. The doses are compared to the annual dose limit of 0.1 mSv which applies in Switzerland, Sweden and Finland, and also to typical levels of natural background radiation in Switzerland (see Chapter 5). The radionuclides which contribute most to dose as a function of time are also indicated; in all cases the radionuclides identified contribute at least 90 % and usually over 99 % of the total doses at times indicated, except at the times of crossover from one radionuclide to another.

Whereas the previous subsections have compared normalised releases, the results in Figure 4.5 refer to total estimated individual doses due to the whole repository. The additional factors now included, over and above the near-field and geosphere performances already discussed, are as follows:

- For SKB 91, stochastic canister failure and the effect of transport in separate geosphere stream tubes is now incorporated. The result presented is the median realisation based on the maximum dose to 10,000 years result from a 500 run simulation. The dose curve represents the sum of releases from probably about 6 failed canisters where the plume from each has made its way separately through the geosphere; this explains the structure seen in the curve.
- For TVO 92, the result does correspond to the results examined in previous subsections and represents the release from a single conservatively placed canister that fails at 10,000 years.
- For AECL 94, the case plotted is a deterministic calculation in which all input parameters are set to their median value. The result represents releases from the total repository containing over 100,000 canisters all of which will have failed before 10,000 years. However, examination of the result shows that the dose is dominated by releases from the three vault sectors nearest to the low angle fault, which together contain about 6,600 canisters. Releases from other sectors do not reach the surface within the assessment calculation period.
- For Kristallin-I, the case plotted is the reference near-field, geosphere and biosphere case. The result represents releases from the total repository containing about 2,700 canisters all of which are conservatively assumed to fail at 1,000 years.
- In all cases, the biosphere response has now been included.

Results for the AECL 94 median value input deterministic calculation allow the closest comparison with Kristallin-I, however, the mean annual dose from a 40000 run probabilistic simulation may be considered to be a more representative result. In this case, at the end of the assessment calculation period, the mean dose is approximately one order of magnitude higher than for the median value input case.

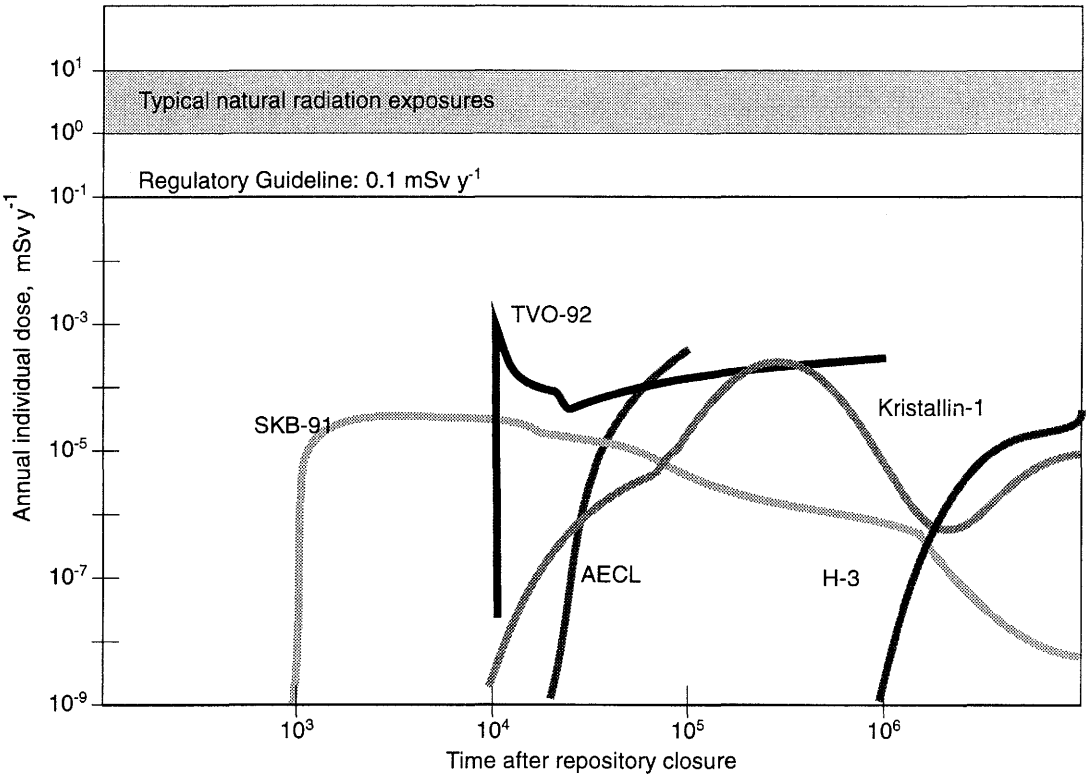

Dominant Radionuclides:

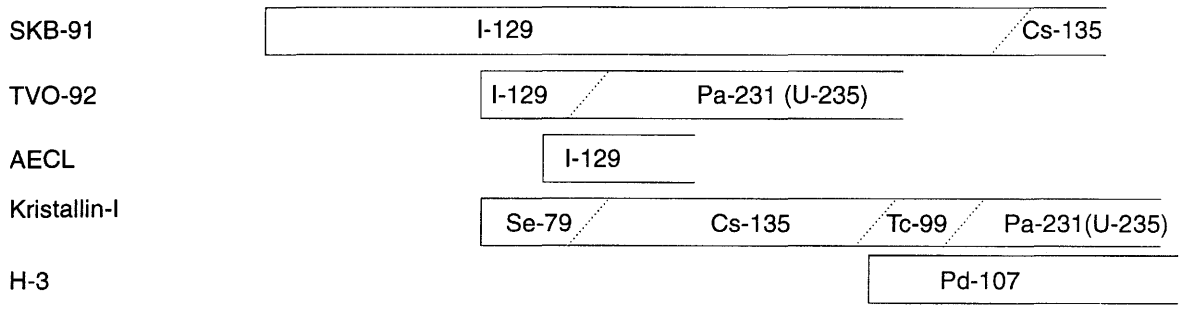

Fig. 4.5: Calculated individual doses for Reference Cases from the SKB 91, TVO 92, AECL 94 and Kristallin-I (H-3 for comparison) assessments and indication of the radionuclides that contribute most to dose in each case

4.6 Identification and discussion of key factors

Considering the individual doses shown in Figure 4.5, it is remarkable that all show a maximum calculated dose between 10^{-3} and 10^{-5} mSv y^{-1}, that is, at least two orders of magnitude less than the regulatory guideline. It should be noted that the aim of safety assessment is not to calculate actual doses arising from disposal but to show that doses would be acceptably low. Given a larger inventory or an intrinsically less favourable site then more realistic, as opposed to conservative, models and data may be required to demonstrate this.

From the discussion and information in previous sections, the following factors can be identified as being most important to the estimated radiological impacts in these four assessments.

1. **Inventory** - Maximum calculated doses in the three spent fuel assessments are all dominated by ^{129}I which is effectively absent in vitrified high-level waste. In addition, the total inventories vary (see Table 4.2): the SKB 91 and AECL 94 assessments offset their larger inventories, to some extent, by modelling the repository as a spatially extensive unit, whereas TVO 92 and Kristallin-I both conservatively neglect this factor. For solubility limited radionuclides, the inventory per canister is a less significant factor.

2. **Canister material and failure** - The assumed integrity of the copper and copper-steel canisters employed by SKB and TVO results in only a very small proportion of canisters failing within timescales of interest, assessed at about 1/1000. This decreases by up to three orders of magnitude the maximum possible dose. Also, for the SKB Reference Case, releases are limited by the small size (5 mm^2) of the hole in the copper canister.

3. **Waste Matrix and nuclide disposition in the wastes** - In the AECL 94 median input value case, the UO_2 waste matrix is assumed to be so insoluble that less than one part in 10^8 of the uranium, and hence other radionuclides assumed to be contained in the fuel matrix, are released to the buffer in the period of the assessment, however, the mean input solubility in the randomly sampled case is three orders of magnitude higher so that significant releases from the UO_2 matrix will occur in this case. The fractions of radionuclides assumed to be available for more rapid release are very important and the reasons for the different assumptions on its inventory by SKB, TVO and AECL are unclear (see Table 4.7).

4. **Solubility limits** - For the actinides, and many activation and fission products, solubility limits are very important in constraining the concentration source to drive diffusion through the bentonite buffer. Indeed the importance of ^{129}I and ^{135}Cs in geosphere releases, and to dose, is related to the fact that they do not reach solubility limits at the waste.

5. **Low-permeability bentonite buffer** - This is a common factor in all four assessments. It is critical to the assumption of no colloid transport through the near field. It is also important in providing mechanical and hydraulic protection to the canister and wastes, and a stable chemical environment. Thus the integrity of the canister is preserved and solubility limits can operate after canister failure.

6. **Excavation damaged zone (EDZ)** - The EDZ is considered as a fast transport pathway in both the TVO 92 and Kristallin-I assessments, and provides a boundary condition for transport in TVO 92, Kristallin-I and SKB 91.

7. **Distance to nearest major water-bearing fracture zone** - The very limited effect of the TVO 92 geosphere is directly related to the conservative placing of the repository so that it is intercepted by a fracture zone. SKB 91, AECL and Kristallin-I all assume a separation between disposal galleries and major fracture zones so that solutes must be transported through sparsely fractured rock.

8. **Conceptual model for transport in fractured rock** - The very good performance of the AECL geosphere is due to the assumption that the fractured rock can be represented as a porous medium so that, given the low Darcy velocity, the transport will be by diffusion. All the other assessments concentrate the water flow into discrete channels with flowing water velocity depending on a single fracture aperture (TVO 92), fracture or vein aperture and frequency (Kristallin-I) or a flowing porosity (SKB 91).

9. **Near-surface dilution and dose factors** - The biosphere dose conversion factors in Kristallin-I are generally lower than in the other three assessments due to the significant dilution expected in the gravel deposits in the Rhine valley. However, this is partly compensated for by higher doses through agricultural pathways, which may be related to greater build-up and retention in local soils in the Kristallin-I biosphere model.

5 REASONABLENESS AND SIGNIFICANCE OF DOSE AND RISK ESTIMATES FROM THE SWISS HLW REPOSITORY

P. Baertschi and T.J. Sumerling

5.1 Introduction

The presentation of the results of performance assessments as profiles of dose as a function of time into the far future is required in order to assess compliance with regulatory protection objectives, but does not present a very clear picture of the hazard involved either to scientists outside the field of radiological protection or to members of the public. This chapter attempts to set the results of post-closure safety assessment, especially the results of the Kristallin-I assessment in context by answering three questions that are often raised when such results are discussed:

1. How reasonable are the results, i.e. is there more direct evidence that indicates a deep geological repository will behave as predicted by the sequence of mathematical models ?
2. How significant are the activities and doses which could arise from a repository in comparison to other sources of radiation in the environment ?
3. What are the risks from such radiation exposures, i.e. what are the hazards (potential ill-effects), how likely are these and how do they compare with other risks?

5.2 How reasonable are the results ? – the evidence of natural analogues

Qualitative evidence that both the individual processes relevant to safe performance of a geological repository will proceed as predicted, and the total system will perform within bounds coinciding with calculated results, is available from various natural analogues. These are situations within the natural environment or in relation to ancient man-made artefacts where the relevant processes have been occurring over long timescales, similar to those of interest in geological disposal safety studies.

5.2.1 Support for estimates of key processes

Amongst the key features and processes that lead to the long-term radiological safety of a deep geological repository for HLW (see NAGRA 1994b) are:

- the long-term stability of the bentonite clay backfill which will surround the HLW canisters;
- the guaranteed lifetime (slow corrosion) of the steel canisters beyond the period of significant heat generation from the wastes;
- the stability and resistance to aqueous corrosion of the vitrified waste matrix;
- the low solubility/immobility of key radionuclides under repository conditions.

In each case, there is evidence from natural analogues that it is reasonable to assume these features and processes will operate as expected.

An essential requirement of the safety concept for the Swiss HLW repository is that a sufficient thickness of the clay backfill surrounding the steel canisters containing the wastes should retain the required properties of swelling capacity, plasticity, low-permeability and cation exchange capacity. In the reference design the clay is MX80, a bentonite with about 75 % montmorillonite content which contains mainly sodium as the exchangeable cation (NAGRA 1994b). Investigations of montmorillonite-rich sediments indicate that there will be no great change in these properties over time periods well in excess of one million years. For example, the clays in the Gulf of Mexico have been studied extensively in connection with oil exploration (MILLER et al. 1994). In sediments over 30 million years old, there are no significant mineral changes that would be precursors to changes of properties, e.g. illitisation, at temperatures below 80 °C. In sediments up to 200 million years old, although some illitisation has occurred, the essential properties are retained.

The function of the steel canister is to ensure complete isolation of the wastes from groundwater for at least 1,000 years after emplacement, that is beyond the period of significant thermal output from the wastes. Evidence from archaeological finds shows that, in the absence of oxygen, steel/iron corrosion proceeds at very slow rates (also found in experimental studies). A well known example (CHAPMAN & McKINLEY 1990) is the case of the disposal in 86AD of 12 tonnes of iron nails by Roman military at Inchtuil in Scotland which was documented at the time. Archaeologists have since recovered more than 875,000 nails from this site. Although nails from the outer few centimetres of the horde are heavily corroded many of those inside are almost intact after nearly 2,000 years. Hence, there is confidence that the 25 cm thick solid steel canister of the reference design will not corrode by more than a few centimetres in 1,000 years.

The radioactive wastes are mixed in a borosilicate glass matrix intended to be sufficiently resistant to aqueous corrosion. Natural basalt glasses have similar SiO_2 content to the vitrified waste glass although they contain practically no boron or lithium which are important elements in HLW waste glass. The SiO_2 content is one of the most important parameters determining the stability of the glass. Hence, the longevity and low corrosion rates of these natural glasses, which can be established from field investigations (PETIT 1991; MILLER et al. 1994), gives confidence in similar slow degradation of the waste glass matrix in a deep repository. In particular, the behaviour of natural glasses indicate that recrystallisation (devitrification) will be insignificant on the relevant timescales, the natural corrosion mechanisms are basically those observed in the laboratory and, in low flow conditions such as will exist within the bentonite buffer, hydration layers form which can be expected to protect the glass from further attack by water for a long time (CHAPMAN & McKINLEY 1987).

A key limitation on calculated doses for the most radionuclides in the wastes is that, following dissolution from the wastes, the maximum aqueous concentration will be constrained by solubility limits, i.e. excess concentrations will be precipitated to solid or gel (immobile) phases. The overwhelming evidence from natural analogue studies (e.g. NAGRA 1993; MILLER et al. 1994) is that in reducing conditions such as will pertain in the Swiss HLW repository, both uranium and thorium (which can be partly analogous to plutonium) isotopes and many of their daughters remain essentially insoluble and immobile. The low solubility of uranium and thorium, as well as information on chemical species that control solubility, can be inferred from measurements

of rock minerals and adjacent groundwaters. Although there are difficulties with sampling, data can be obtained which provides important checks on the thermodynamic models used to calculate speciation and solubility in performance assessment (SCHWEINGRUBER 1983).

5.2.2 Support for estimates of total system performance

In the last ten years, numerous natural analogue investigations have been carried out. Particular mention should be made of the natural reactors at Oklo, Gabon, Africa (BERZERO & d'ALESSANDRO 1990; BROOKINS 1990), the Cigar Lake uranium ore deposit in Canada (CRAMER & SMELLIE 1994), the uranium and thorium/rare earth ore deposits in Poços de Caldas, Brazil (CHAPMAN et al. 1993; NAGRA 1993) and the uranium ore deposit at Alligator Rivers in Australia (DUERDEN 1994). Recent overviews of natural analogue studies and their application are provided by MILLER et al. (1994) and BRANDBERG et al. (1993).

The Oklo natural nuclear reactors, set in Precambrian argillaceous sandstones and shales, provide an excellent analogue for assessing the behaviour of fission products, actinides and actinide daughters in rocks. At Oklo, the fracture systems have provided convenient sites for entrapment of uranium-bearing solutions leached from local low-grade ore deposits, and, as more reducing conditions were encountered, the uranium was again reduced and precipitated out of solution as pitchblende. This type of deposit at Oklo is unusually rich in grade, with several tens of percent of uranium oxide not uncommon. In several places along these fractures, conditions were favourable for nuclear reactions to take place. The reactor zone UO_2 is an analogue for spent nuclear fuel. It is surrounded by ferromagnesian clay minerals (chlorite and illite) that may, in part, be taken as analogous to clay buffer/backfill materials.

The Oklo reactors were operative about 1,800 million years ago, for periods between 0.1 and 0.8 million years. The reactor core temperatures were in the order of several hundred degrees, thus simulating somewhat higher temperatures than those reached in man-made radioactive waste repositories. The data from Oklo support the view that very little of the radionuclide inventory migrated away from the sites of reaction during

Table 5.1: Summary of elemental behaviour at the Oklo natural nuclear reactors (summarised from BROOKINS 1990)

	Retained in UO_2 matrix	Retained in nearby mineralisation	Lost from mine site
Noble gases, e.g. Kr, Xe	none	uncertain	probably
Alkali elements, e.g. Cs, Rb	very little	largely	possibly
Alkaline earth elements, e.g. Sr, Ba	partly	most probably	uncertain
Zr, Nb, Y	largely	uncertain	none
Mo, Tc, Ru	partly	partly	uncertain
Rh, Pd, Te	largely	uncertain	–
Ag, Sn	largely	partly	–
Halides, e.g. I	little	uncertain	probable
Rare earth elements, e.g. La, Ce	mainly	possibly	none
Actinides, e.g. Th, U, Np, Pu	almost entirely	little	none

the 800,000 years or so of reactor operation, this despite a significant hydrothermal circulation (BROOKINS 1990). This is related to the low oxygen content of circulating fluids emphasising the importance of maintaining reducing conditions in a waste repository. Even for the measurable elements that have migrated (detectable by their stable decay products), the small distance of movement indicates high sorption factors. After 1,800 million years most of the radionuclides and their decay products have either not migrated at all, or moved only a few metres maximum, see Table 5.1. Exceptions are the noble gases, halides (e.g. iodine) and alkali elements (e.g. caesium), which have largely been lost from the UO_2 but may be retained to some extent in neighbouring mineralisation. This is in agreement with performance assessment modelling which also predicts that these elements will be largely lost from the repository following degradation of the waste matrix.

The large uranium ore deposit at Cigar Lake, Canada, with approximately 1.5×10^5 tonnes uranium, is 1,300 million years old and is particularly interesting because it is unusually rich (up to 55 % uranium) and, despite its relatively shallow depth of 430 m, there is no detectable anomaly at the surface (CRAMER & SMELLIE 1994). This deposit lies at the junction of crystalline basement and overlying sandstones, and the uranium ore is surrounded by 5 to 30 metres of clay which has isolated the ore in a similar way to which the thick clay backfill of the Swiss HLW repository is expected to isolate the nuclear fuel wastes. Figure 5.1 compares features of the Cigar Lake deposit with those of a HLW repository in crystalline basement of Northern Switzerland and identifies the main differences and similarities. A number of beneficial features of the HLW repository not shared by the natural uranium deposit, especially the positioning of the repository away from major water-conducting faults and profoundly reducing conditions, give confidence that the HLW repository will retain the sparingly soluble elements present in the wastes, e.g. U, Th, Pu and most daughters, at least as well as the natural uranium deposit for which there is little evidence of loss by migration in over 1000 million years.

A geographically nearer case to Northern Switzerland is that of the Krunkelbach uranium ore deposit in the Black Forest region, Germany. This is a small deposit of around 1,000 tU and is located at a depth of 100 to 300 m. Again, no enhanced uranium concentrations have been found in surface waters and near-surface groundwaters in the vicinity of the deposit (HOFMANN 1989). In both the Cigar Lake and Krunkelbach cases, the several hundred metre thick rock layer above the ore deposit together with the hydrological situation has formed an effective barrier, even though the ore bodies come into contact with oxidising groundwaters.

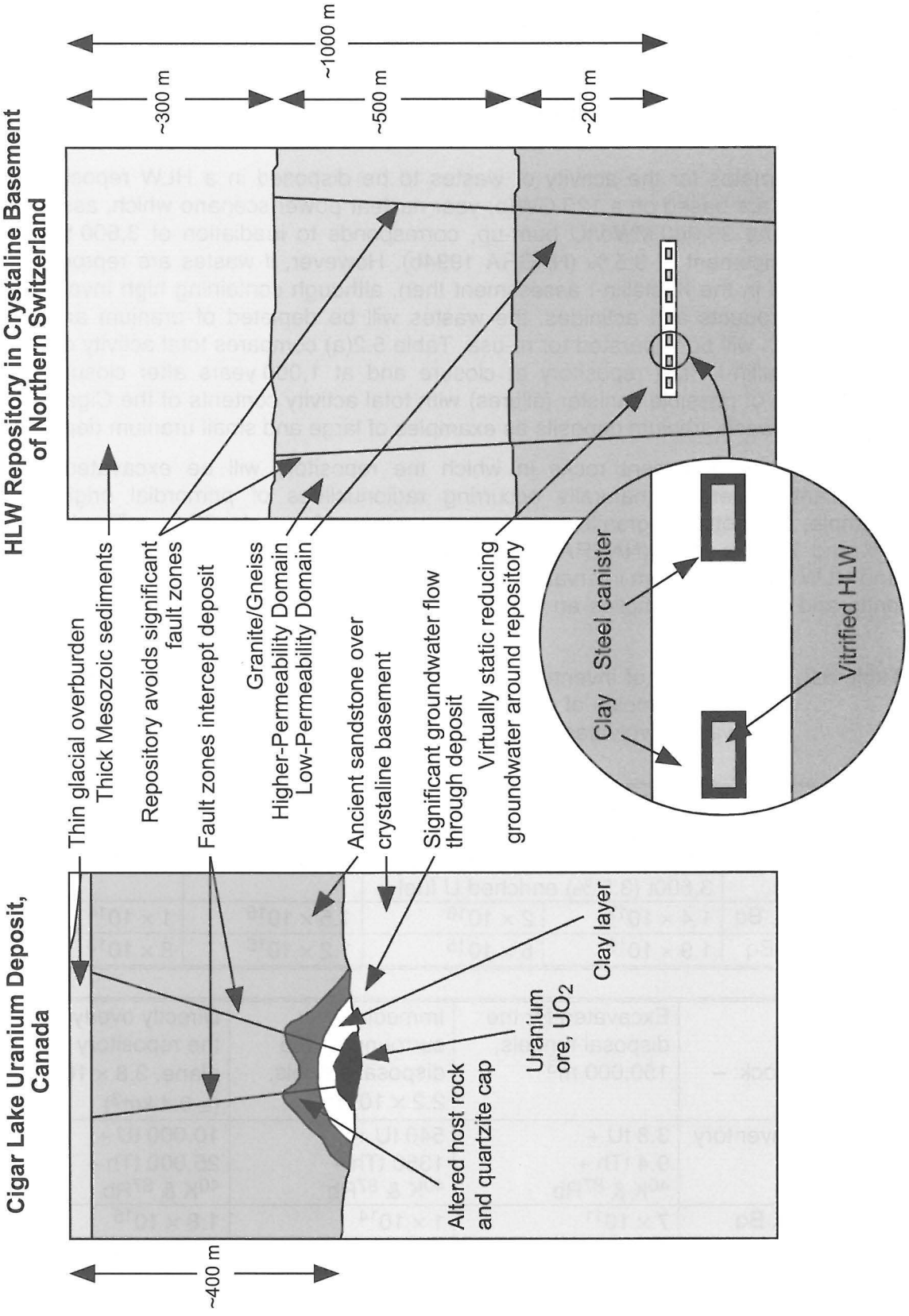

Fig. 5.1: A comparison between the Cigar Lake natural uranium deposit and a HLW repository in crystalline basement of Northern Switzerland

5.3 How significant are the activities and calculated doses ? – comparison to natural occurrences

5.3.1 Total activities in perspective

Current estimates for the activity of wastes to be disposed in a HLW repository in Switzerland are based on a 120 GW(e) year nuclear power scenario which, assuming PWR fuel and 33,000 MWd/tU burn-up, corresponds to irradiation of 3,600 tU with average enrichment of 3.5 % (NAGRA 1994b). However, if wastes are reprocessed as assumed in the Kristallin-I assessment then, although containing high inventories of fission products and actinides, the wastes will be depleted of uranium and plutonium which will be separated for re-use. Table 5.2(a) compares total activity content of the Kristallin-I HLW repository at closure and at 1,000 years after closure (the earliest time of possible canister failures) with total activity contents of the Cigar Lake and Krunkelbach uranium deposits as examples of large and small uranium deposits.

The crystalline basement rocks in which the repository will be excavated have significant content of naturally occurring radionuclides of primordial origin. For example, the Böttstein granite contains on average 10 ppm U, 25 ppm Th, 4.7 ppm ^{40}K and 73 ppm ^{87}Rb (NAGRA 1985b). Assuming 3.7 m diameter disposal tunnels and HLW canisters at 5m intervals (NAGRA 1994b) then, even neglecting connecting drifts and shafts, this implies an excavated volume of 150,000 m^3, or almost half a

Table 5.2: Comparison of inventories and total activity of the Swiss HLW repository with (a) examples of a large and a small natural uranium deposit and (b) with various volumes of crystalline rock

(a)	Swiss HLW repository		Cigar Lake U deposit	Krunkelbach U deposit
	at closure	at 1000 y		
Assumed inventory	wastes from reprocessing of 3,600t (3.5 %) enriched U fuel		150,000 tU	1,000 tU
Total alpha, Bq	1.4×10^{17}	2×10^{16}	1.5×10^{16}	1×10^{14}
Total beta, Bq	1.9×10^{19}	6×10^{15}	1.2×10^{16}	8×10^{13}

(b) Volumes of crystalline rock: –	Excavated for the disposal tunnels, 150,000 m^3	Immediately surrounding the disposal tunnels, 2.2×10^7 m^3	Directly overlying the repository plane, 3.8×10^8 m^3 ($\cong 0.4$ km^3)
Assumed inventory	3.8 tU + 9.4 tTh + ^{40}K & ^{87}Rb	540 tU + 1350 tTh + ^{40}K & ^{87}Rb	10,000 tU + 25,000 tTh + ^{40}K & ^{87}Rb
Total alpha, Bq	7×10^{11}	1×10^{14}	1.8×10^{15}
Total beta, Bq	9×10^{11}	1.3×10^{14}	2.4×10^{15}

Notes:

1 mg of natural uranium comprises 12.4 Bq ^{238}U plus 0.57 Bq ^{235}U; 1 mg of natural thorium comprises 4.04 Bq ^{232}Th. Total alpha and total beta activities are calculated assuming all daughters of the ^{238}U, ^{235}U and ^{232}Th decay series are present in equilibrium.

million tonnes of rock, containing approximately 3.8 tonnes of uranium and 9.4 tonnes of thorium plus other radionuclides as above. In the Kristallin-I reference design, disposal tunnels are excavated at 40.m separation on a single level leading to a plan area of 540,000 m^2. Multiplying this by 40 m representing rock immediately above and below the repository plane leads to an estimate of 2.2×10^7 m^3 of rock immediately surrounding the HLW disposal area, or, multiplying by 700 m which is the approximate thickness of crystalline rock encountered in drilling to a depth of 1,000 m in the Kaisten-Leuggern-Böttstein area (THURY et al. 1994) leads to an estimate of 3.8×10^8 m^3 (0.4 km^3) of crystalline rock overlying the repository. The estimated uranium and thorium content and total activities of these volumes of rock are given in Table 5.2(b).

Table 5.2 indicates the total activity content of the HLW repository at 1,000 years is similar to the total activity content of the Cigar Lake uranium deposit, and is about an order of magnitude greater than the total activity of 0.4 km^3 of crystalline rock overlying the repository. However, these simple comparisons disguise some significant differences due to the different radionuclide contents. Table 5.3 compares

Table 5.3: Comparison of activities of key safety-relevant nuclides in the Swiss HLW repository with naturally occurring radionuclides in crystalline rock overlying the repository

Key safety-relevant radionuclides in the Swiss HLW repository at 1,000 years and 10,000 years				Key radionuclides in (0.4 km^3) crystalline rock directly overlying the repository plane		
Radio-nuclide	Half-life, years	1,000 year Inventory, Bq	10,000 year Inventory, Bq	Radio-nuclide	Half-life, years	Inventory
Beta emitters				Beta emitters		
^{79}Se	65,000	5.9×10^{13}	5×10^{13}	^{40}K	1.28×10^9	1.2×10^{15}
^{99}Tc	210,000	1.8×10^{15}	1.7×10^{15}	^{87}Rb	4.8×10^{10}	2.3×10^{14}
^{135}Cs	2.3×10^6	5.1×10^{13}	5.1×10^{13}			
Alpha emitters (see note)				Alpha emitters (see note)		
^{241}Am	432	1.7×10^{16}	7.5×10	–		
^{237}Np	2.1×10^6	5.8×10^{13}	6.1×10^{13}	–		
^{242}Pu	380,000	1.6×10^{12}	1.6×10^{12}	–		
^{238}U	4.5×10^9	6.5×10^{10}	6.7×10^{10}	^{238}U	4.5×10^9	1.2×10^{14}
^{234}U	245,000	1.6×10^{12}	1.6×10^{12}	^{234}U	245,000	1.2×10^{14}
^{239}Pu	24,000	3.7×10^{14}	5.4×10^{14}	–		
^{235}U	7.0×10^7	4.7×10^9	8.8×10^9	^{235}U	7.0×10^7	5.7×10^{12}
^{240}Pu	6,500	9.2×10^{14}	3.6×10^{14}	–		
^{232}Th	1.4×10^{10}	1.2×10^4	9.2×10^4	^{232}Th	1.4×10^{10}	1.0×10^{14}
Total alpha	–	2×10^{16}	1.8×10^{15}	Total alpha*	–	1.6×10^{15}
Total beta	–	6×10^{15}	3.4×10^{15}	Total beta*	–	2.6×10^{15}

Notes: Alpha emitting radionuclides are arranged by decay series:
4n+1 (neptunium) chain includes ^{241}Am and ^{237}Np;
4n+2 (uranium) chain includes ^{242}Pu, ^{238}U and ^{234}U;
4n+3 (plutonium) chain includes ^{239}Pu and ^{235}U;
4n (thorium) chain includes ^{240}Pu and ^{232}Th.
* including all decay chain nuclides (equilibrium)

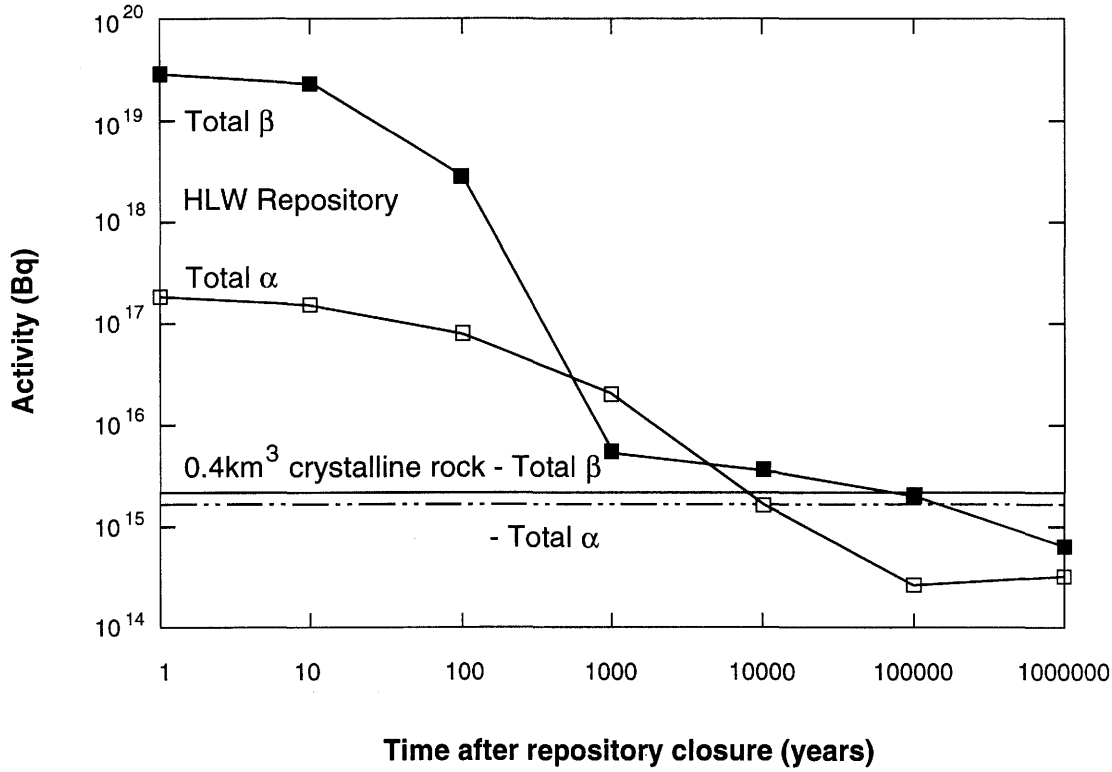

Notes: Repository contains vitrified HLW from 120 GW(e) year nuclear power programme.
Crystalline rock (Böttstein Granite) is assumed to contain 10 ppm U, 25 ppm Th, 4.7 ppm ^{40}K, 73 ppm ^{87}Rb and U and Th daughters in equilibrium.

Fig. 5.2: Total alpha and beta content of the Swiss HLW repository as a function of time compared to total alpha and beta content of 0.4 km^3 of crystalline rock overlying the repository

inventories of key safety-relevant radionuclides in the HLW repository with the estimated inventory of radionuclides in 0.4 km^3 of crystalline rock. Although at early times the HLW contains much greater inventories of both alpha and beta emitters, it contains lower inventories of very long-lived nuclides so that after about 10,000 to 30,000 years the residual activity is less than that of the rock overlying the repository. This is illustrated in Figure 5.2.

5.3.2 Local gamma-radiation doses

At the reference time of disposal, 40 years after discharge of fuel from the reactor, the external-gamma dose rate at the surface of a flask of vitrified HLW is estimated at 4×10^6 Gy y^{-1} which is over one thousand million times greater than typical natural gamma-radiation dose rates (see Table 5.8). However, the thick steel canister in which the waste will be placed for disposal will provide shielding so that the dose rate at the surface of the canister will be about 4 Gy y^{-1}. The thick annulus of compacted bentonite surrounding the canister will further attenuate the gamma radiation so that the dose rate at the bentonite-host rock interface due to the wastes after emplacement will be only 2×10^{-8} Gy y^{-1}, which is 6 orders of magnitude less than typical dose rates in crystalline rock (~ 10^{-2} Gy y^{-1}). That is, the excess external radiation level due to the wastes will be reduced to insignificant (undetectable above background) levels within the engineered barriers.

5.3.3 Radionuclide concentrations in groundwaters of the crystalline basement

The expected pathway by which radionuclides will be released from a HLW repository is via diffusion and advection in groundwater. Table 5.4 shows maximum concentrations of radionuclides in groundwater at the bentonite-host rock interface, i.e. leaving

Table 5.4: Maximum concentrations of radionuclides in groundwater at the bentonite-host rock interface as calculated in the Kristallin-I assessment (NAGRA 1994b)

Radionuclide	Maximum concentration at bentonite-host rock interface, Bq m^{-3}	Approximate time of maximum, years after closure
Fission products (beta emitters)		
^{79}Se	1.9×10^5	8,000
^{99}Tc	5.2×10^6	100,000
^{126}Sn	5.9×10^5	200,000
^{135}Cs	6.6×10^7	90,000
Actinide decay chains		
^{237}Np	3.4×10^2	> 10,000,000 *
^{233}U	1.1×10^4	2,000,000
^{229}Th	7.7×10^3	2,000,000
^{242}Pu	1.8×10^3	500,000
^{238}U	2.4×10^2	> 10,000,000 *
^{234}U	2.3×10^2	600,000
^{226}Ra	8.5×10^5	300,000
^{239}Pu	9.8×10^2	200,000
^{235}U	1.4×10^2	> 10,000,000 *
^{231}Pa	6.2×10^2	> 10,000,000 *

Notes: Alpha emitting radionuclides are arranged by decay series:
Concentrations of 4n (thorium) chain are negligible.
* Concentrations only plotted to 10,000,000 years in NAGRA 1994b.

the engineered barriers, as calculated in the Kristallin-I assessment (NAGRA 1994b).

Neglecting short-lived nuclides of the actinide decay series, the total beta activity concentration, ~ 7×10^7 Bq m^{-3}, is dominated by ^{135}Cs and the total alpha activity concentration, ~ 9×10^5 Bq m^{-3}, is dominated by ^{226}Ra, although the times of maximum concentrations are widely separated.

As a result of leaching processes, all groundwaters (and surface waters) contain natural uranium, radium and other nuclides of the three natural decay series, in addition to ^{40}K and ^{87}Rb. Table 5.5 shows, for example, determinations of radionuclides in groundwaters from the crystalline basement of Northern Switzerland. The high concentrations of the noble gas radon, ^{222}Rn, are supported by ^{226}Ra in the adjacent rock. High concentrations of ^{222}Rn would also be expected near to the bentonite-host rock boundary of the HLW repository, supported by ^{226}Ra migrating from the repository, but have not been calculated in Kristallin-I due to their limited radiological significance.

Neglecting ^{222}Rn, the total alpha and beta concentrations due to the HLW repository, as indicated in Table 5.4, will reach maxima approximately 10,000 and 100,000 times greater than the typical concentrations of naturally occurring radionuclides in the crystalline groundwater, although, these maxima occur far in the future. These high concentrations are due to the very limited groundwater flow (3 m^3 y^{-1} through the projected area of the repository tunnels, see NAGRA 1994b for a precise definition) in the low-permeability domain crystalline basement in which the repository is sited. A radiologically more apposite comparison is to consider the flux of radionuclides diluted in the typical volume of a deep groundwater well sunk into the crystalline basement. To be viable, such a well must abstract water from a region of higher permeability in which case greater dilution will be available. In the Kristallin-I assessment, a well in the crystalline basement with an abstraction rate of 3×10^5 m^3 y^{-1} is considered. In this case, even neglecting any attenuation or decay of radionuclide concentrations between the bentonite-host rock interface and the well, the concentrations in water at abstraction would be a factor of 100,000 less than those given in Table 5.4, i.e. would be similar or less than typical concentrations of naturally occurring radionuclides in waters from the crystalline basement given in Table 5.5.

Table 5.5: Naturally occurring radionuclides in groundwaters from the crystalline basement of Northern Switzerland measured in Nagra hydrochemistry programme (NAGRA 1992)

Borehole (depth of sample)	Concentrations of radionuclides in groundwater, Bq m^{-3}					
	U total *	^{226}Ra	^{222}Rn	^{228}Th	^{40}K	^{87}Rb
Böttstein (312 m)	20	26	26,000	155	524	123
Böttstein (621 m)	22	26	49,000	41	33	85
Kaisten (1,272 m)	113	28	252,000	74	347	61
Zurzach (415 m)	11	26	20,000	16	224	45
Säckingen, Germany (ca. 140 m)	347	22	184,000	17	2533	754
Range	10 - 350	20 - 30	20,000 - 250,000	15 - 160	30 -2500	40- 750

Note: * U total = $^{238}U + ^{234}U + ^{235}U$

5.3.4 Radiation doses due to drinking groundwater

In Switzerland, the natural uranium concentrations in drinking-water are generally between 0.2 and 2 $\mu g\ l^{-1}$, but can be significantly higher. There are numerous locations in the Alps, particularly in the Rhône and Rhine catchment area, where the uranium concentrations in the water are in excess of 10 $\mu g\ l^{-1}$ (BAERTSCHI & KEIL 1992; BOSSHARD et al. 1992). Fracture- and spring-waters from uranium-rich granites of the Alps and the Southern Black Forest frequently have uranium concentrations in the order of 100-1000 $\mu g\ l^{-1}$ (BAERTSCHI & KEIL 1992; DOMINIK et al. 1991), and it has to be assumed that such waters will also enter drinking-water systems, albeit with some dilution. The highest uranium concentrations in the world (up to 20 $mg\ l^{-1}$) were encountered in crystalline waters in drinking-water supply boreholes in southern Finland (LAHERMO & JUNTUNEN 1991). ANDERSON (1992) provides a world-wide overview of uranium concentrations in groundwaters, together with their relationship with other water parameters and with lithology.

Table 5.6: Maximum concentrations of radionuclides from a HLW repository in water from a well abstracting water from the crystalline basement and doses due to drinking well water calculated in Kristallin-I assessment (NAGRA 1994b)

Key radionuclides						
Fission products			Actinide chains *			
			4n + 1	4n + 2	4n + 3	4n
^{79}Se	^{99}Tc	^{135}Cs	^{237}Np	^{226}Ra	^{235}U	^{236}U
Concentrations of radionuclides in well water (Bq m^{-3})						
1	0.5	490	1.1×10^{-3}	5.4×10^{-3}	1.5×10^{-3}	1.0×10^{-2}
Doses due to drinking 0.73 m^3y^{-1} of water (mSv y^{-1})						
2×10^{-6}	1×10^{-7}	6×10^{-4}	2×10^{-6}	9×10^{-6}	8×10^{-6}	5×10^{-7}
Time of maximum concentration and dose (years after closure)						
65,000	1.8×10^6	280,000	$> 10^7$	$> 10^7$	$> 10^7$	$> 10^7$

Notes:

* In the case of the actinide chains, the radionuclide controlling total dose through the chain is identified and the concentration of this nuclide given; other radionuclides in the chain may also contribute to dose but are in approximate equilibrium with the nuclide given.

Table 5.6 shows maximum concentrations of radionuclides, due to a HLW repository, in water from a well assumed to be abstracting water from the crystalline basement and consequent doses due to drinking water calculated in Kristallin-I assessment (NAGRA 1994b). An appropriate comparison in this case is the concentration and doses due to drinking mineral water, which are often abstracted from deep groundwater sources. Table 5.7 gives mean values and ranges of activities measured for seven of the most widely consumed Swiss mineral waters (BAG 1992b). The analytical data for the individual sources were weighted according to their estimated market component. The seven brands cover around 80 % of the Swiss mineral water consumption. The typical per capita consumption of mineral water in Switzerland is 75 litres per year, however, to make the estimates compatible, in both cases, doses due to drinking water are calculated assuming a total annual intake of 730 litres (2 $l\ d^{-1}$)

which is the total fluid intake for ICRP reference man (ICRP 1975), and the water consumption rate assumed in Kristallin-I. Comparison of Tables 5.6 and 5.7 shows that the peak dose due to the Kristallin-I well scenario (from ^{135}Cs) is a factor of 50 less than the dose that would be received from drinking an equal quantity of mineral water.

Table 5.7: Ranges and weighted mean of key radionuclide activities measured for seven of the most widely consumed Swiss mineral waters* (BAG 1992b) and calculated doses assuming consumption of 2 l d^{-1}.

Key radionuclides					
$^{234}U + ^{238}U$	^{226}Ra	^{210}Pb	^{210}Po	^{228}Th	^{40}K
Range and weighted mean concentrations in mineral water (Bq m^{-3})					
14 - 560	6 - 45	9 - 18	1 - 3	0.1 - 3.0	37 - 280
150	28	13	2.6	1.0	95
Dose due to drinking 0.73 m^3 y^{-1} of water with mean concentrations as above (mSv y^{-1})					
8×10^{-3}	6×10^{-3}	1.3×10^{-2}	8×10^{-4}	1.4×10^{-4}	– **
Total dose due to above nuclides = 3×10^{-2} mSv y^{-1}					

Notes:

* Brands analysed are Aproz, Eptinger, Henniez, Lostorf, Passugger, Rhäzünser, Valser.

** Potassium is homeostatically controlled and the ratio $^{40}K/^{stable}K$ is constant so that additional intake of potassium cannot give rise to additional dose.

5.3.5 Total natural background radiation in Switzerland

The sources, mean value and range of natural radiation doses to individuals in Switzerland are presented in Table 5.8. In addition to doses from natural sources, individuals receive variable doses from anthropogenic sources with an average of around 1.2 mSv y^{-1}, of which 1 mSv y^{-1} can be attributed to medical diagnostics and 0.2 mSv y^{-1} to other sources (fallout from nuclear weapons testing and the Chernobyl accident, and discharges from nuclear facilities, hospitals and industry). The mean total annual radiation dose in Switzerland is thus around 4.6 mSv y^{-1} (BAG 1992a).

Table 5.8: The sources, mean value and range of annual effective dose equivalents from natural radiation sources to individuals in Switzerland (BAG 1992a)

Origin of radiation	Mean value mSv y^{-1}	Range mSv y^{-1}
Radon + decay products (inhalation)	2.2	0.3-150
Terrestrial radiation (external irradiation)	0.45	0.2-1.5
Cosmic radiation (external irradiation)	0.34	0.25-0.9
Internal radiation (ingestion)	0.38	0.25-0.5
Total (natural)	3.37	1-153

Considering each of the contributions identified in Table 5.8:

- The dose due to inhalation of the short-lived decay products of radon occurs mainly in houses and other buildings where, depending on the radium concen- tration and the gas permeability of the soil, and the ventilation conditions in the building, very different radon daughter concentrations can build up. Taken together with the living patterns of the inhabitants, this leads to a very large range for doses to individual persons of 0.3 to 150 mSv y^{-1} (BAG 1992c). This represents the largest component of the natural radiation dose and, by extrapolation of dose-risk estimates (see section 5.4.2), might be responsible for 10 to 15 % of all lung cancer cases in Switzerland (BAG 1992c). The dose can be reduced significantly by means of suitable construction and ventilation measures.
- Terrestrial radiation is due mainly to the activities of potassium-40, uranium daughters and thorium daughters in the uppermost soil layer and in building materials; each contributes around one third to the total. The resulting mean dose shows considerable local variations; for example, in Locarno, the terrestrial radiation dose of 0.85 mSv y^{-1} is double that of many locations in Central and Northern Switzerland (BAG 1992b).
- The contribution of cosmic radiation, due mainly to secondary radiation from interactions of high-energy cosmic radiation in the upper atmosphere, increases with altitude. For example, at the top of the Jungfraujoch (3475 m.a.s.l.) the value is 1.3 mSv y^{-1}, while in Central Switzerland (about 400 m.a.s.l.) the value is 0.38 mSv y^{-1}.
- Of particular significance for the purpose of comparison with performance assessment results is the internal radiation dose of around 0.38 mSv y^{-1} caused by ingestion of radionuclides. This is the principle route for exposure in the case of radionuclides released from a deep repository which subsequently enter the water sources utilised by man and in agricultural systems. Table 5.9 gives the mean contributions of the individual radionuclides to the total internal dose from natural sources. These are values taken from UNSCEAR (1988), but they are also applicable in principle to the Swiss situation.

Potassium (which naturally contains 0.0117 % of the primordial radioactive isotope ^{40}K) is essential to human life and the potassium content of the human body is regulated homeostatically at about 2 g per kg of soft tissue so that the concentration of ^{40}K in tissue and hence the radiation dose is relatively constant and practically independent of supply rate. Carbon and hydrogen (mainly as water) are also controlled metabolically but, in this case, the concentration ratios of $^{14}C/^{stable}C$ and $^{3}H/^{stable}H$ in ingested foodstuffs and water vary slightly so that doses also vary to some degree.

The other radionuclides in Table 5.9 are not essential to human life and their inventory and radiation effects in the body are determined largely by supply, absorption in the stomach-intestinal tract and the metabolism of accumulation and secretion. The contributions of primordial ^{87}Rb (associated with potassium) and cosmogenic ^{7}Be are relatively constant. On the other hand, the contribution of the three natural decay series of ^{238}U, ^{235}U and ^{232}Th to the ingested dose, of which they make up around half, can vary widely as the concentrations of these radionuclides in waters and foodstuffs vary.

Table 5.9: Internal radiation doses due to ingestion of natural radionuclides (UNSCEAR1988; except *)

Nuclide and decay sub-series	Type of radiation	Typical ingestion mBq d^{-1}	Average concentration in man mBq kg^{-1}	Effective dose equivalent $\mu Sv\ y^{-1}$
^{14}C	β,	8×10^4	4.8×10^4	12
^{3}H	β	6×10^3	1.7×10^3	0.01
^{7}Be	γ			3
^{40}K	β, γ	10^5	6.0×10^4	180
^{87}Rb	β	2×10^3	8.5×10^3	6
^{238}U, ^{234}U	α, γ	27	4	5
		50*	~ 7*	10*
^{230}Th	α, γ	5.5	2.5	7
^{226}Ra	α, γ	50	14	7
^{210}Pb	β, γ	110	280	12
^{210}Po	α, γ	110	210	120
^{232}Th	α, γ	5.5	1.2	3
^{228}Ra–^{228}Th–^{224}Ra	α, β, γ	80	7	13
^{235}U whole series	α, β, γ	1.2	0.2	3

Notes:

* Increased ingestion (compared to UNSCEAR 1988) of approximately 2 μg d^{-1} (~50 mBq d^{-1}) estimated for Switzerland (BOSSHARD et al. 1992) and corresponding increase in effective dose equivalent of around 10 μSv y^{-1}

In Figure 5.3, radiation doses calculated for the Reference Case in the Kristallin-I assessment (NAGRA 1994b) are compared with various doses due to natural sources discussed in this and the previous section. It is clear that the doses calculated as due to a HLW repository are orders of magnitude smaller than those which are known to occur, or are calculated, due to natural sources. This is despite a large measure of conservatism in assumptions and data for the calculation of doses due to the HLW repository, so that the results should be regarded as upper bounds for expected doses (NAGRA 1994b). The peak dose calculated to be due to the HLW repository in the Reference Case, 2×10^{-4} mSv y^{-1} from ingestion of ^{135}Cs, is approximately 0.05 % of dose due to ingestion of naturally occurring radionuclides and, moreover, occurs at a very long time in the future, ~ 300,000 years after repository closure. This peak dose is also roughly equal to the dose that would be received from drinking just 5 litres of mineral water per year, i.e. only 1/15th of typical Swiss annual mineral water consumption of 75 l y^{-1}.

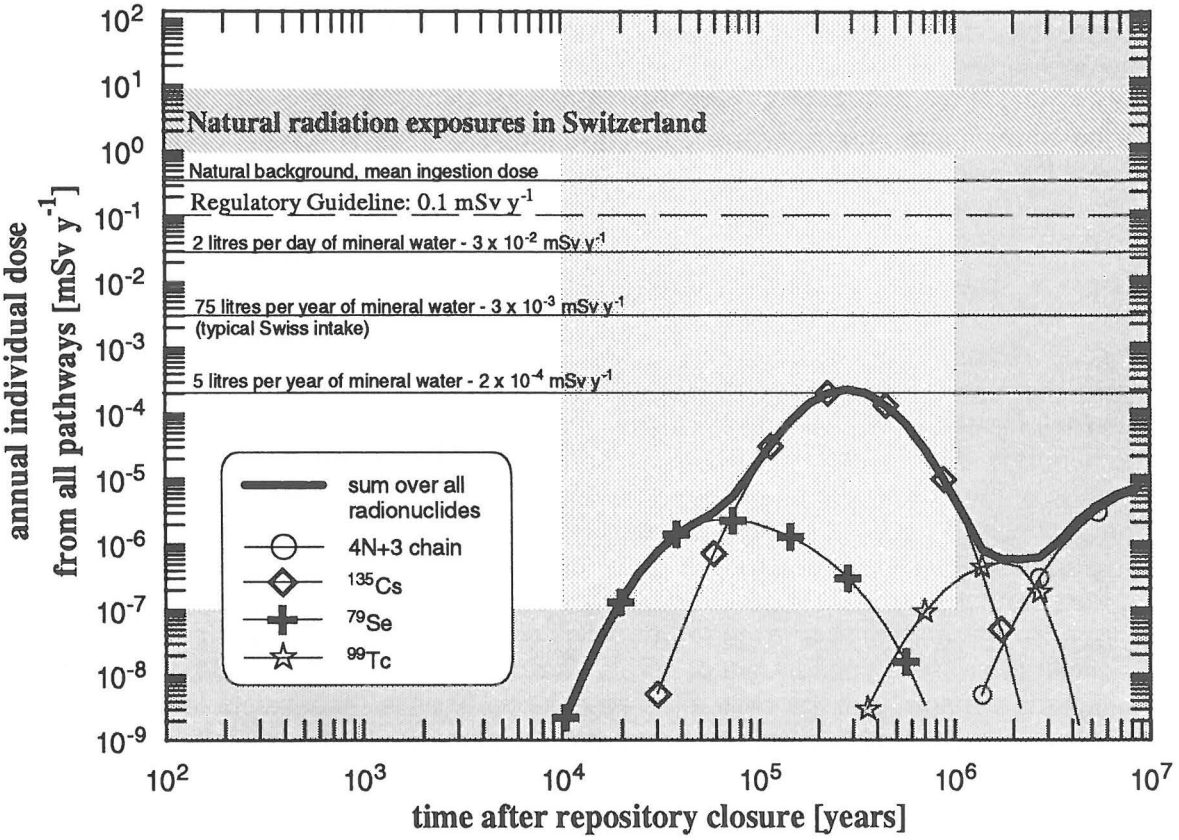

Fig. 5.3: Comparison of doses as a function of time from a HLW repository calculated in the Kristallin-I assessment (NAGRA 1994b) with various doses due to natural radiation sources discussed in the text

5.4 What are the risks from radiation exposures ? – evaluation and comparison of risks

5.4.1 General comment on risk

Before discussing risks quantitatively it is important to understand the scientific concept of "risk", which has a more exact meaning than in common usage. As used here, risk is the product of two components: a defined effect (usually undesirable) and the probability of the effect. Thus:

Risk = Effect x Probability of Effect

For example, there is a potential hazard or effect to be avoided when driving a motor vehicle, the hazard of being involved in a motor accident which might, *in extremis,*

lead to the effect of death. Fortunately, the probability of being involved in a serious accident is low so that the risk per journey of fatality or serious injury is correspondingly low. The fact that a potential effect of death is very serious does not, necessarily, make the risk unacceptable; indeed, millions of persons voluntarily accept the risk every day.

5.4.2 Potential effects of radiation at low dose rates

Ionising radiation has the potential to cause damage at the cellular level through micro-chemical disruption due to the energy of ionisation. In most cases, the damage is transitory or insignificant and there is no effect since the cell will be repaired or replaced by the normal biological processes. However, if there is damage to the nucleus of the cell, then there is the potential for more serious effects. The most likely effect will be to cause the cell to be non-viable, i.e. not able to reproduce. Provided the proportion of cells affected is small, which is the case at low dose rates, this is not serious because non-viable cells will be replaced by division of other cells. However, it is theorised that if some change to the cell is caused and this has the potential to be transmitted or affect subsequent generations of cells then there is some probability of malignant disease, or if the cells affected are ova or cells responsible for sperm production, some probability of genetic defects in offspring. Some models require multiple damage to generations of cells to induce malignant changes or suppression of the body's normal defence mechanisms for dealing aberrant cellular changes. Man and all animals have evolved in a naturally radioactive environment and hence have evolved relatively efficient means of repairing or rejecting cellular damage due to radiation (and other abuses).

As indicated above, the fundamental mechanisms by which malignant disease and genetic defects are caused and develop are not well understood. However, it is accepted that low radiation dose levels are associated with stochastic radiation damage based on cell degeneration, the effects of which only become apparent a relatively long time after the dose has been received. The principal effects are malignant disease (cancer) and hereditary (genetic) defects, see Table 5.10. However, the evidence that is available refers entirely to exposures at higher dose rates than occur naturally and, in the case of genetic defects, relies on extrapolation from animal experiments, mainly on mice.

Table 5.10: Harmful effects of radiation at low dose rates typical of natural background (after NRPB 1989)

Effect	Presumed condition for occurrence and manifestation	Information
Malignant disease (cancer, e.g. leukaemia, solid tumours)	Any dose or dose rate. Probability of effect depends on dose. Manifested several years (leukaemia) or tens of years (solid tumours) later.	Risk data for humans by linear extrapolation from popula tions exposed at high doses and dose rates (e.g. Hiroshi ma and Nagasaki survivors)
Hereditary (genetic) defects	Any dose or dose rate. Probability of effect depends on dose rate. Manifested in descendants.	Risk data for humans by inference from mouse data.

5.4.3 Risks of radiation at low dose rates

When estimating risks, i.e. probability of defined cancers and/or genetic defects, due to low levels of radiation, the conservative assumption is made that there is no dose threshold, i.e. there is no dose that is so small that there is no attendant risk. Rather dose-effect factors estimated from the statistical excess of deleterious effects observed in populations that have been exposed at much higher dose rates are extrapolated down to the low dose region. A linear extrapolation is generally used, but corrections are made to take account of the decrease in risk at low dose and dose rate levels. For radiological protection purposes, the International Commission on Radiological Protection (ICRP 1991) recommends risk coefficients as a mean for all age groups and for low dose and dose rate levels as follows:

Fatal cancer in exposed individual	0.05	Sv^{-1}
Serious hereditary defect in all generations of offspring	0.01	Sv^{-1}
Allowance for loss of life expectancy and non-fatal cancer	0.01	Sv^{-1}

Leukaemia contributes around 10 % to the value for fatal cancer. Based on this model, if 1,000,000 people were irradiated with 1 mSv, around 50 would die of radiation-induced cancers (around 5 of these would die of leukaemia within 20 years and 45 would die of other cancers after sometimes significantly longer periods of 10 to 40 years), about 10 cases of serious hereditary defect might occur in all future generations of offspring (about 5 in the first two generations plus 5 in all subsequent generations) and about 25 would develop some non-fatal malignant disease.

Comparison of risks of genetic defects are difficult because of the uncertainty in risk estimates and because the effects occur over different generations and entail different degrees of disability. Comparison of risks of non-fatal cancer are also fraught with difficulty because of the subjectivity of equating different cancers with different implied loss of quality of life or life shortening. Therefore the following concentrates on risks of fatal cancer because death is a well-defined effect and fatal cancer is, as indicated above, the predominant risk due to radiation exposure at low dose levels.

For the case of continuous irradiation at low dose levels, for example due to environmental radioactivity, the simplifying assumption is made that the lifelong total risk of dying of a radiation-induced cancer is also an average 0.05 Sv^{-1} where the dose is integrated over the whole lifetime. Table 5.11 provides an overview of calculated risks and the expected mortality rates for the different sources of radiation, some of which have been discussed in previous sections.

All the risks of fatality given in Table 5.11 lie well below the level that can be shown statistically. Even the effect of the total natural radiation, which according to this model would contribute around 1.2 % to all fatalities and 4 to 5 % to all cancer deaths, lies on the limit of what can be demonstrated statistically because radiation-induced cancers cannot be distinguished from those caused by other factors. Of the numerous investigations carried out in areas of high natural radioactivity, e.g. India, Brazil, USA (CULLEN & PENNA FRANCA 1977), China, Japan, USA, France etc. (GALLE & LATARJET 1993), there was no indication of a significant increase in cancer and leukaemia fatalities, even though the natural radiation dose can be a factor of 5 to 10 higher than the normal level of 3 to 4 mSv y^{-1}. Some studies even indicate an inverse correlation, with lower rates of fatal cancer in regions of higher natural background (WACHSMANN 1989). Even allowing for the problems associated with such epide-

miological studies, the findings underline the conservative nature of the linear dose-effect extrapolation and indicate that the estimated lifelong risk of cancer death of 1.2 % from normal natural radiation is most likely over- rather than under-estimated.

In view of all the above considerations, the calculated annual and lifetime risks of fatal cancer of 10^{-8} and 7×10^{-7} for individuals of a population living in the vicinity of a HLW repository at 300,000 years in the future are completely trivial risks. A further estimate that can be made is the total number of fatal cancers in a given period assuming that there is a population dwelling in the vicinity. Taking the maximum size of population that could be following the highly conservative habits defined in the assessment calculations as 100 persons, and noting that the dose will remain within an order of magnitude of the peak value over the period from about 100,000 to 800,000 years after closure (see Fig. 5.4), i.e. a total of 700,000 years, this indicates the expectation value for fatal cancers due to the repository is 0.7. That is, it is most likely that only one additional death might occur over the next one million years as a result of the repository, this in a population of over one million persons presumed to receive lifelong exposures at the peak dose rate due to the repository in that time.

Table 5.11: Risks of radiation-induced fatal cancer for various sources of exposure

Radiation source		Radiation dose		Radiation induced risk of fatal cancer (1)		Deaths per million persons and year (2)
		Annual mSv y^{-1}	Lifetime mSv	Annual y^{-1}	Lifetime -	
Natural radiation sources						
Total		3.4	240	1.7×10^{-4}	1.2×10^{-2}	170
Internal radiation	Total	2.6	182	1.3×10^{-4}	9.1×10^{-3}	130
Inhalation:	Rn	2.2	154	1.1×10^{-4}	7.7×10^{-3}	110
Ingestion:	Total	0.38	27	1.9×10^{-5}	1.4×10^{-3}	19
	^{40}K	0.18	12.6	9.0×10^{-6}	6.3×10^{-4}	9
	^{14}C	0.012	0.8	6.0×10^{-7}	4.2×10^{-5}	0.6
	^{87}Rb	0.006	0.4	3.0×10^{-7}	2.1×10^{-5}	0.3
U+Th-series		0.163	11.4	8.2×10^{-6}	5.7×10^{-4}	8
Radionuclides in mineral water (3)						
730 l y^{-1} (2 l d^{-1})		3×10^{-2}	2	1.5×10^{-6}	1.0×10^{-4}	1.5
75 l y^{-1}		3×10^{-3}	0.2	1.5×10^{-7}	1.0×10^{-5}	0.15
5 l y^{-1}		2×10^{-4}	1.4×10^{-2}	1.0×10^{-8}	7×10^{-7}	0.01
Man-made or artificially enhanced sources						
Integrated dose due to Chernobyl fallout in Switzerland		-	~ 0.7	5×10^{-7}	3.5×10^{-5}	0.5
Diagnostic medical applications (typical)		1	70	5×10^{-5}	3.5×10^{-3}	50
10 hr flight at altitude of 10 km (due to enhanced cosmic radiation)			0.05	3.6×10^{-8}	2.5×10^{-6}	0.04
HLW repository calculated maximum at 300,000 y after closure		2×10^{-4}	1.4×10^{-2}	1×10^{-8}	7×10^{-7}	0.01

Notes:

(1) Risks of fatal cancer (annual and lifetime) are products of radiation dose (mSv y^{-1} and mSv per 70 years, respectively) and risk factor (5×10^{-5} mSv^{-1}).
(2) For information, the present population of Switzerland is 6.7 million.
(3) Consumption of extreme, typical and small quantities of mineral water.

Table 5.12: Estimated frequency of factors which can be considered as causing cancer deaths (USA population according to DOLL & PETO (1981))

Factor	Estimated % of total cancers due to given factors	
	Mean, %	Range, %
Food	35	10 - 70
Smoking	30	25 - 40
Reproduction, sexual behaviour	7	1 - 13
Occupation	4	2 - 8
Alcohol	3	2 - 4
Environmental radiation		2 - 4
Ultraviolet (sunlight)	~ 1.5 (2)*	(1 - 3)*
Ionising radiation	~ 1.5 (4)*	(2 - 6)*
Environmental pollution	2	1 - 5
Medical treatment	1	0.5 - 3
Other factors	15 (12)*	
Infections (viruses, parasites), hereditary factors, etc.		

* Estimated values for Switzerland in parentheses: ultraviolet according to statistics 1985/89 (melanoma); ionising radiation calculated with a risk factor of 0.05 Sv^{-1} and a mean lifetime dose from natural radiation of 0.24 Sv

5.4.4 Risks of radiation in perspective

There are numerous other causes of cancer besides ionising radiation; DOLL & PETO (1981) have estimated the various relative frequencies of causes presented in Table 5.12.

Factors such as smoking, alcohol consumption and eating habits are very dependent on lifestyle. The cancer-inducing effect comes both directly from carcinogenic substan ces in smoke and in certain foodstuffs and, also, indirectly from over- or undernutrition and from synergisms (e.g. smoking and alcohol) which can trigger the multistage process of inducing cancer.

More than 2,000 carcinogenic substances are known today, around 40 of which have been identified by the International Agency for Research on Cancer (IARC) as clearly causing cancer in human beings (RODRICKS 1992). The majority of cancers are chemically induced and, compared to these, radiation-induced cancers are of secondary importance (HENSCHLER 1990). However, it has not yet been possible to quantify the cancer risk associated with individual carcinogenic substances; experiments with animals are insufficiently representative and statistical surveys of cancers in humans are generally inconclusive due to poor definition of dose, insufficient numbers of cases and difficulty of selecting control populations. Thus, despite the numerous uncertainties involved, the radiation-induced cancer risk is easier to determine than the much greater risk of cancer following intake of, or contact with, carcinogenic chemical substances.

Table 5.13: Classification of annual risks of death according to FRITZSCHE (1992) with examples

Classification	Risk range death rate year^{-1}	Examples	Risk death rate year^{-1}
extremely high	$> 10^{-2}$	Circulatory illnesses	
		M> 55 y	1.7×10^{-2}
		W> 65 y	2.4×10^{-2}
very high	10^{-3} - 10^{-2}	Cancer, all types + ages (M+W)	2.5×10^{-3}
		Lung + bronchial cancer M> 45a	2.2×10^{-3}
high	3×10^{-4} - 10^{-3}	Diabetes M+W > 55 y	6×10^{-4}
		Cancer of the colon M+W > 55 y	8×10^{-4}
medium	10^{-4} - 3×10^{-4}	Leukaemia M+W > 35 y	1.3×10^{-4}
		Influenza M > 55 y	1.5×10^{-4}
low	3×10^{-5} - 10^{-4}	Multiple sclerosis M+W > 45 y	3.7×10^{-5}
		Infectious disease (without AIDS)	8×10^{-5}
very low	3×10^{-6} - 3×10^{-5}	Leukaemia M+W 1-25 y	1.5×10^{-5}
		Bone cancer M+W, all	5×10^{-6}
negligible	$< 3 \times 10^{-6}$	Lightning strike	5×10^{-7}

Notes: M = Male population; W = Female population

In order to give an idea of the risks of fatality from cancer, it is useful to draw a comparison with other risks. FRITZSCHE (1992) has classified the risks to which we are typically exposed during the course of our lives and this information is presented in Table 5.13. According to this classification, the annual risks of various radiation-induced cancers shown in Table 5.11 (column 4) lie in the range of medium to negligible risks. Assuming that the linear dose-effect model is valid, then the cancer deaths as a result of total natural radiation would reach the total frequency of leukaemia fatalities (from age 35) and the incidence of death from internal ^{14}C activity would correspond more or less to the risk of being killed by lightning. The internal radiation from ^{40}K or the U+Th series would produce more or less the same number of deaths as bone marrow cancer, and risks from radon inhalation would correspond to the risk of death from all infectious diseases (not including AIDS related illnesses). The calculated peak lifetime risk from a HLW repository would be similar to the annual risk of being struck by lightning.

To provide a better understanding of the significance of a lifetime risk of one in a million, 10^{-6}, which is often considered to be tolerable, WILSON (1979) has identified various activities that are estimated to give risks of this size. These have been adapted to take account of recent statistics, as well as the situation in Switzerland and Germany (FRITZSCHE 1992; ZIMMERLI et al. 1992), and are presented in Table 5.14. These data should be taken only as rough estimates; this is particularly true of risks associated with radiation and carcinogenic materials. In both these cases, the linear extrapolation to very low doses is questionable and the risk associated with the different activities could, in reality, be much smaller than 10^{-6}. Nevertheless, the compilation in Table 5.14 does give a feeling for the estimation and significance of various, very small risks.

Table 5.14: Activities which are estimated to carry a risk of fatality of one in a million

Activity	Potential Hazard(s) +
Smoking 2 cigarettes	Cancer and circulatory diseases
Living with a cigarette smoker for 2 months	Cancer and circulatory diseases
Driving 300 km	Accident
Cycling 50 km	Accident
Flying 4,000 km (commercial airline)	Accident
4 hour flight at an altitude of 10 km	Cancer from cosmic radiation
1 chest X-ray with modern equipment	Cancer from X-rays
3-week holiday in Southern Switzerland (Tessin)	Cancer from enhanced natural environmental radiation
Annual consumption of:	
- 7 l mineral water	Cancer from radionuclides
- 200 g fresh mushrooms	Cancer from hydrazine derivatives
- 2 kg meat from charcoal grill	Cancer from pyrolitic products
- 4 g peanuts *	Liver cancer from aflatoxin B
100 years living at the zone of highest surface activities due to a HLW repository, during the period of peak radiation dose	Cancer from radionuclides released from the repository

Notes:

* Assuming 1 μg aflatoxin B1 kg^{-1} (concentration is generally very much lower)

\+ Potential hazard leading to a risk of one in a million; some of the activities also entail other hazards.

5.5 Summary

The aim of this chapter is to put the results of post-closure assessment, particularly the Kristallin-I assessment of a HLW repository in crystalline basement of Northern Switzerland, into perspective by answering three questions.

How reasonable are the results ?

Natural analogues provide qualitative evidence and confidence that key individual processes will proceed as predicted and that the total disposal system will perform within bounds coinciding with the results calculated by mathematical models. In the case of the Swiss HLW repository concept such properties as

- the long-term stability of the clay backfill,
- slow corrosion of the steel canisters,
- resistance to aqueous corrosion of the vitrified waste matrix, and
- low solubility/immobility of key radionuclides

can be inferred from study of natural analogues or ancient man-made artefacts. Support for estimates of total system performance can be found from the apparent stability and lack of radionuclide migration from natural geochemical anomalies such

as the Oklo nuclear reactors, Cigar Lake uranium deposit and Poços de Caldas uranium and thorium/rare earth deposits.

How significant are the activities and calculated doses ?

Comparison of total activities, geo-environmental concentrations and doses due to radionuclides originating from a HLW repository with natural activities, concentration and doses, show that although the initial total activity and near-field concentration are above those usually found in nature, concentrations in regions of accessible environment and calculated doses are comparable or smaller than those occurring naturally. For example, the total activity of the Swiss HLW repository at 1,000 years after closure is similar to that of the Cigar Lake uranium deposit and only an order of magnitude greater than the estimated total activity of crystalline rock overlying the repository. Concentrations of radionuclides eventually diffusing from the engineered barriers will far exceed natural concentrations of radionuclides in groundwater but will be sufficiently diluted in passage to any possible human water source, e.g. a deep well in the crystalline basement, to be brought to total concentrations similar to those found naturally in the crystalline rock. The peak annual dose conservatively calculated as due to a HLW repository in the Kristallin-I Reference Case is equivalent to the dose that would be received from drinking just 5 l y^{-1} of mineral water and is approximately 0.05 % of the total average internal radiation dose due to ingestion of naturally occurring radionuclides in Switzerland.

What is the risk from radiation exposures ?

Risk, as used here, is the product of two components: a defined effect and the probability of the effect. The potential detrimental effects of radiation at low dose rates are damage to cells which carry small probabilities of later development of cancer in the exposed person and even smaller probabilities of genetic defects in offspring. At radiation doses typical of natural background, ~ 1 mSv y^{-1}, the annual risks are of the order of 50 in a million for radiation-induced fatal cancer and 10 in a million for genetic defects in future generations. By the conservative calculations of Kristallin-I, the annual risk of fatal cancer to an individual living at the time and place of peak environmental concentrations of HLW radionuclides (~ 300,000 years in the future) is only 10^{-8}, one chance in 100 million. Assuming a population exists in the future following the very conservative habits defined in the assessment, then it is calculated that only one person might contract fatal cancer as a result of the repository in the next one million years. Many human activities and exposure to non-radioactive substances lead to putative risks of similar kind. To put an annual risk of death of 10^{-8} into context, this is approximately the average risk associated with living with a cigarette smoker for 12 hours per year, driving 3 km y^{-1}, drinking 7 l y^{-1} of mineral water or eating 4 g y^{-1} of peanuts. All these risks are completely trivial.

6 SUMMARY AND CONCLUSIONS

F.B. Neall and I.G. McKinley

In this final chapter, the results of the previous three chapters are first summarised and then integrated in order to draw conclusions about how reasonable the Kristallin-I analytical approach and results are when viewed in a wider context.

6.1 Comparison of Project Gewähr, H-3 and Kristallin-I

The similarity of disposal concept and models used allows a relatively detailed quantitative comparison between Kristallin-I, its predecessor, Project Gewähr, and H-3. Quantitative analysis shows that differences in maximum near-field radionuclide releases and in maximum geosphere releases between the three assessments can be attributed to:

- unlimited matrix diffusion and sorption in the H-3 geosphere model. The importance of this difference between H-3 and Kristallin-I/Project Gewähr varies for the different radionuclides but is responsible for most of the difference (several orders of magnitude for ^{135}Cs and ^{79}Se) in performance between the geosphere models;
- the zero concentration outer bentonite boundary condition used in H-3 for the near-field diffusion model results a factor of around two orders of magnitude greater radionuclide release than would be the case with a finite water flow equivalent to that used in Kristallin-I;
- sharing of elemental solubility limits between isotopes, including stable isotopes, reduces the maximum release rates of some less abundant isotopes (e.g. ^{233}U, ^{234}U and ^{107}Pd, due to stable Pd) in Kristallin-I and Project Gewähr (not including stable isotopes) by up to about three orders of magnitude compared to release rates if isotopes have elemental (unshared) solubility limits as in H-3;
- differences in solubility constants and Kds for some elements.

From such a comparison, it is also clear that there is a difference of emphasis between the assessments; Kristallin-I and Project Gewähr aim for a relatively realistic near-field model but handle the geosphere in a more conservative manner, whereas H-3 has a somewhat simpler and idealised, in a non-conservative manner, geosphere but a relatively more conservative near field. Hence, the geosphere provides a more significant barrier in H-3 than Kristallin-I although, in both cases, the near-field provides the largest part of the retardation for most radionuclides.

The conservative Kristallin-I geosphere results from the deliberate choice of the most unfavourable water-conducting feature geometry, based on the results of parameter variation which indicated the high sensitivity of the results to this element of the model. Thus, in the absence of sufficient geological data to better constrain the necessary parameters, the values giving the worst performance are used. The model of the water-conducting features is constrained by geological data in both Kristallin-I and Project Gewähr. In H-3, in contrast, no host-rock or site-specific data are available, which could be used to improve the simple parallel-plate fracture model and

make it more geologically realistic. As a consequence, this generalised model is rather non-conservative, as it allows unlimited diffusion and sorption into the whole volume of host rock. In a similar way, the conservative assumption of zero concentration at the outer boundary of the bentonite in the H-3 near-field diffusion model, arises from a lack of local hydrological information which could constrain the local groundwater flow rate.

So, although the differences in models can be used to explain the different results for the near- and far-field releases in H-3 and Kristallin-I, these model differences, themselves, arise from a difference in emphasis between the assessments: Kristallin-I (and Project Gewähr) seeking to incorporate actual host-rock-specific data whereas H-3 is a more generic assessment which has yet to incorporate detailed geological data. This reflects the currently greater maturity of the Swiss geological investigation programme compared to that of Japan.

6.2 Comparison of Kristallin-I with other performance assessments

Despite the different waste type and disposal concepts employed in the TVO 92, SKB 91 and AECL 94 assessments, the comparison with Kristallin-I yields benefits in terms of identifying the critical factors influencing the eventual dose arising from HLW disposal.

Due to the variety of concepts and methods involved in these four assessments, it has not been possible to make the same sort of quantitative comparison that was possible for H-3 and Kristallin-I. Hence the factors which influence the results of the assessments have been identified but no effort was made to quantify their relative influence in the different assessments.

The observation that the maximum calculated doses for the 3 spent fuel assessments are all dominated by ^{129}I, compared to ^{135}Cs in Kristallin-I, indicates the effect of the different waste form. Prompt release of a significant proportion of the inventory of some fission products immediately after canister failure is a feature of spent fuel disposal which does not exist in the case of vitrified waste. Gap inventory ^{129}I, in particular, is assigned very high solubility and low sorption and hence can result in a high release concentration peak. Assumptions about the fraction of iodine in the prompt release inventory and, to some extent, the distribution of canister failures are a key contribution to differences between the spent fuel assessments. The slow congruent dissolution of nuclides from vitrified waste, constrained by solubility limits, means that releases are much less sensitive to assumptions about waste glass properties or canister failure times/distributions.

In addition, the waste form has another important repercussion in terms of the modelling of the near field. This is in the different models for the waste form dissolution: dissolution of glass being relatively simply and conservatively modelled by a constant rate which is dependent on the glass surface area. For the spent fuel, release of the radionuclides (except for the gap and grain boundary inventory) is dependent on the dissolution of UO_2 which is redox sensitive. Thus, the model for the near-field redox conditions, a notoriously difficult area which is further complicated by relatively high radiolysis rates (when compared to vitrified waste), and the uranium dioxide solubility limit assume a greater importance for these assessments than for Kristallin-I. The solubility limits and sorption Kds for all the key radionuclides are

clearly important parameters, both in the near- and far-fields, and there appears to be a rather wide range of values used for some elements over the various assessments. The importance of ^{129}I and ^{135}Cs is clearly a function of their assumed lack of solubility limits, long half-lives and relatively poor sorption properties.

There is an emerging consensus that massively engineered barriers allow more confident modelling of the near-field, because the system is more easily defined and analysed, and thus its behaviour predicted, than is the case for the geosphere. There is a tendency for the models to predict a very highly performing near-field, culminating in the TVO 92 assessment with its extremely long-lived waste canisters, and a much more conservative geosphere. An exception to this would perhaps be the AECL study which assumes diffusion-dominated transport in the host rock. However, the near-field performance predicted in this assessment was also very good although it relies heavily on low U solubility.

6.3 Risk comparison with environmental radioactivity and other hazards

A persuasive case is made for confidence in the results of the Kristallin-I assessment by showing how natural analogues can be used to confirm, at least qualitatively, that key processes will proceed as predicted. The importance of natural analogues is that they can provide support for results without the necessity to understand the complexities of the mathematical models involved in the assessment, hence providing the sort of examples which could be widely used outside the radiological/waste disposal community for public relations purposes.

Comparison of the predicted doses and associated risks arising from a HLW repository with those from naturally-occurring sources is particularly instructive, serving to emphasise how negligible are the risks involved. Predicted doses are generally at a level comparable to or below those derived from "everyday" practices, which through experience are not considered to be radiologically hazardous, such as intercontinental jet flights and drinking mineral water. For example, the peak annual dose calculated for the Kristallin-I Reference Case is equivalent to that obtained from drinking 5 litres of mineral water per year; this is also approximately 0.05 % of the average internal dose due to ingestion of naturally-occurring radionuclides in Switzerland. The analogy with natural mineral water is apt as results from Kristallin-I suggest that levels of radioactivity due to high natural concentrations of α-emitting ^{222}Rn in crystalline groundwaters may only be exceeded by a few of the β-emitting fission products at their time of maximum release from the repository and by the peak of ^{226}Ra occurring several hundred thousand years after repository closure (Tables 5.4 and 5.5).

Conservative calculations suggest that the annual risk of fatal cancer to an individual living at the time of maximum release from the repository is only one in 100 million. Such risks are completely trivial, being approximately equivalent to the average risk associated with driving 3 km per year or eating 4 g of peanuts per year.

6.4 Kristallin-I in perspective

Viewed in the light of other recent assessments, Kristallin-I clearly represents the current state-of-the-art in terms of both methodology and calculational tools/databases. Such a comparison gave no indications of errors or deficiencies in the performance assessment and the results obtained, in terms of long term consequences, are similar to those reported elsewhere. As noted above, the relative weighting given to the various components of the multiple barrier system varies between analyses but this is related to the individual concept adopted and the amount of site-specific geological data available. Given the requirement to achieve certain regulatory performance goals, it is apparent that (implicitly or explicitly) credit is taken for well-characterised, favourable processes until a sufficient margin of safety is built up to cover uncertainties in potentially negative processes. The features, events and processes chosen to build this 'Robust' safety case and those held in reserve vary from case to case.

If unconstrained by availability of finance and manpower, it seems likely that a much more consistent performance assessment methodology could be adopted which would take full credit for all the engineered and natural barriers. This would allow more direct comparison of the various concepts involved but, very probably, the comparison would involve consequences which, in all cases, are completely insignificant relative to those from the natural radiation environment. Indeed, present assessments indicate that all the concepts examined should achieve levels of safety far beyond those associated with any normal industrial process. Further developments in models and databases are thus not required unless they cover identified open questions for specific concepts, are focused on confirmation of a specific process or increase the transparency of the analysis for public relations purposes.

7 ACKNOWLEDGEMENTS

I would like to thank external reviewer J. Haderman (PSI) for his comments on this report and also B. Goodwin, C. Davison, L. Johnson, A. Wikjord (AECL), T. Eng (SKB) and T. Vieno (VTT) for taking the time to review the minutae of Chapter 4 for accuracy in representing their respective performance assessments.

Thanks also to the many people who assisted in the production of this report, especially B. Kunz, S. McCombie, R. Oezkan, A. Playfair, S. Spescha and my co-authors.

Finally, thanks to I. McKinley for offering me the opportunity to undertake this project in the first place.

8 REFERENCES

ALDER, J.C. & McGINNES, D. (1994): Model radioactive waste inventory for Swiss waste disposal projects. Nagra Technical Report, NTB 93-21. Nagra, Wettingen, Switzerland.

ANDERSON M.T. E.T.R.A. (1992): Aqueous uranium concentrations in the natural environment. AECB Project 5.138.1, Research report INFO-0411 Environmental and Technological Research Associates Limited, prepared for Atomic Energy Control Board, Ottawa, Canada.

ANDERSSON, J (Editor) (1989): The Joint SKI/SKB Scenario Development Project. SKI Technical Report 89:14.

BAERTSCHI, P. & KEIL, R. 1992: U-Gehalte von Oberflächen-, Quell- und Grundwässern der Schweiz. Nagra Technical Report NTB 91-26. Nagra, Wettingen, Switzerland.

BAG (1992a): Radioaktivität der Umwelt in der Schweiz; Bericht für die Jahre 1989 und 1990. Bundesamt für Gesundheitswesen, Abteilung Strahlenschutz, Bern, Switzerland.

BAG (1992b): Radioaktivität der Umwelt in der Schweiz; Bericht für das Jahr 1991. Bundesamt für Gesundheitswesen, Abteilung Strahlenschutz, Bern,Switzerland.

BAG (1992c): Radonprogramm Schweiz "RAPROS"; Bericht über die Ergebnisse der Jahre 1987-1991. Bundesamt für Gesundheitswesen, Abteilung Strahlenschutz, Bern,Switzerland.

BERZERO, A. & D'ALESSANDRO (1990): The Oklo phenomenon as an analogue of radioactive waste disposal, a review. CEC Nuclear Science and Technology EUR 12941 EN.

BOSSHARD, A., ZIMMERLI, B. & SCHLATTER, CH. (1992): Uranium in the diet - Risk assessment of its nephro- and radiotoxicity. Chromosphere **24** (3), 309-321.

BRANDBERG, F., GRUNDFELT, B., HÖGLUND, L.O., KARLSSON F., SKAGIUS, K. & SMELLIE, J. (1993): Studies of natural analogues and geological systems. Their importance to performance assessment. TVO Report YJT-93-07. TVO, Helsinki, Finland.

BROOKINS, D.G. (1990): Radionuclide behaviour at the Oklo nuclear reactor, Gabon. Waste Management, **10**, 285-296.

CHAPMAN, N.A. & McKINLEY, I. (1987): The Geological Disposal of Nuclear Waste, Wiley Sons.

CHAPMAN, N.A. & McKINLEY, I. (1990): Radioactive waste: back to the future? In New Scientist, 5 May 1990 and Atom, November/December 1990.

CHAPMAN, N.A., McKINLEY, I., SHEA, M.J. & SMELLIE, J.A.T. (eds) (1993): The Poços de Caldas Project: Natural analogues of processes in a radioactive waste repository. Elsevier, Amsterdam 603p. Reprinted from the Journal of Geochemical Exploration **45**, Nos 1-3 (1992).

CRAMER, J. J. & SMELLIE, J. A. T. (1994): The AECL/SKB Cigar Lake Analog Study: Some implications for performance assessment. In Proc. of and International Workshop, Toledo, Spain, October 1992. CEC Report EUR 15176 EN, 137-155.

CULLEN, TH.L. & PENNA FRANCA, E. (1977): Review of Brazilian investigations in areas of high natural radioactivity, Part I and II. Internat. Symp. on Areas of high natural radioactivity, Poços de Caldas, Brazil, 16-20 June 1985, 29-64. Academia Brasiliera de Ciências, Rio de Janeiro, R.J., Brazil.

DOLL, R. & PETO, R.V. (1981): Avoidable risks of cancer in the USA. J. Natl. Cancer Inst., **66**, 1193.

DOMINIK, J., CUCCODORO, S., GOURCY, L. & SANTIAGO, S. (1991): A high natural uranium level in the surface and groundwaters of the Alpine Rhône watershed (Switzerland). In Proc. Internat. Conf. on heavy metals in the environ- ment, Edinburgh, September 1991, **1**, 342-346 (J.G. Farmer ed.) CEP Consul- tants Ltd., Edinburgh, UK.

DUERDEN, P. (1994): Alligator Rivers Natural Analogue Project, Final Workshop, An Introduction, Proc. International Workshop, Toledo, Spain, October 1992. CEC Report EUR 15176 EN, 27-29.

FRITZSCHE, A.F. (1992): Wie gefährlich leben wir? Der Risikokatalog, Verlag TÜV Rheinland GmbH, Köln, Germany.

GALLE, P., & LATARJET, R. (1993): Effets sanitaires potentiels du stockage des déchets nucléaires: Comparaisons quantitives avec ceux de la radiation naturelle et ceux des déchets chimiques génotoxiques. Actes de la conférence internationale "Safewaste 93", Avignon, 13-18 June 1993, 114-131.

GOODWIN, B.W., McCONNELL, D.B., ANDRES, T.H., HAJAS, W.C., LENEVEU, D.M., MELNYK, T.W., SHERMAN, G.R., STEPHENS, M.E., SZEKELY, J.G., WUSCHKE, D.M., BERA, P.C., COSGROVE, C.M., DOUGAN, K.D., KEELING, S.B., KITSON, C.I., KUMMEN, B.C., OLIVER, S.E., WITZKE, K.H., WOJCIECHOWSKI, L.C. & WIKJORD, A.G. (1994): Postclosure Assessment of a Reference System for Disposal of Canada's Nuclear Fuel Waste. AECL Report AECL-10717, COG-93-7. AECL, Pinawa, Manitoba, Canada.

HENSCHLER, D. (1990): Stochastische Risiken von Stoffen - Risikoerkennung, Risikosituation, Grenzwerte. 1. Weltkongress für Sicherheitswissenschaft, Tagungsbericht, pp 427-437, Verlag TÜV Rheinland GmbH, Köln, Germany.

HOFMANN, B. (1989): Genese, Alteration und rezentes Fliess-System der Uranlagerstätte Krunkelbach (Menzenschwand, Südschwarzwald). Nagra Technical Report NTB 88-30. Nagra, Wettingen, Switzerland.

ICRP (1991): 1990 Recommendations of the International Commission on Radiological Protection. ICRP Publication 60, Annals of the ICRP Vol. 21, No. 1-3. Pergamon Press, Oxford.

ICRP (1979-1982): Limits for intakes of radionuclides by workers. ICRP Publication 30, parts 1, 2 and 3. Pergamon Press, Oxford.

ICRP (1975): Report of the Task Group on Reference Man. ICRP Publication 23, Pergamon Press, Oxford.

KBS (1977): Handling of spent nuclear fuel and final storage of vitrified high-level reprocessing waste. SKBF/KBS Report (5 Vols), Stockholm.

KBS (1978): Handling and final storage of unreprocessed spent nuclear fuel. SKBF/KBS Report (2 Vols), Stockholm.

KBS (1983): Final Storage of Spent Fuel - KBS-3. SKBF/KBS Report, Stockholm, ISSN 0349-6015.

LAHERMO, P. & JUNTUNEN, R. (1991): Radiogenic elements in Finnish soils and groundwaters. Appl. Geochemistry, **6**, pp 169-183.

McCOMBIE C., McKINLEY, I.G. & ZUIDEMA, P. (1991): Sufficient validation: the value of robustness in performance assessment and system design. GEOVAL-1990. Symposium on validation of Geosphere flow and transport models, p. 598-610. OECD/NEA, Paris, France.

McKINLEY, I.G. & SAVAGE, D. (1994): Comparison of solubility databases used for HLW performance assessment. J. Contam. Hydrol., in press.

McKINLEY, I.G. & SCHOLTIS, A. (1993): A comparison of radionuclide sorption databases used in recent performance assessments. J. Contam. Hydrol., **13**, pp 347-363.

MILLER, W.M., ALEXANDER, W.R., CHAPMAN, N.A., McKINLEY, I.G. & SMELLIE, J.A.T. (1994): Natural analogue studies on the disposal of radioactive waste. Nagra Technical Report NTB 93-03. Nagra, Wettingen, Switzerland and Elsevier, Amsterdam.

NAGRA (1985a): Project Gewähr 1985 - Nuclear waste management in Switzerland - Feasibility studies and safety analyses. Nagra Project Gewähr Report series, NGB 85-09, Nagra, Baden, Switzerland

NAGRA (1985b): Sondierbohrung Böttstein - Untersuchungsbericht. Nagra Technical Report NTB 85-01. Nagra, Wettingen, Switzerland.

NAGRA (1992): Hydrochemische Synthese Nordschweiz - Buntsandstein-, Perm-und Kristallin-Aquifere. Nagra Technical Report NTB 91-30. Nagra, Wettingen, Switzerland.

NAGRA (1993): Nagra Bulletin 1/1993.

NAGRA (1994a): Kristallin-I - Conclusions from the regional investigation programme for siting a HLW repository in the crystalline basement of Northern Switzerland. Nagra Technical Report NTB 93-09E, Nagra, Wettingen, Switzerland.

NAGRA (1994b): Kristallin-I Safety Assessment Report. Nagra Technical Report NTB 93-22E, Nagra, Wettingen, Switzerland.

NRPB (1989): Living With Radiation, 4th Edition. National Radiological Protection Board.

PETIT, J.-C. (1991): The use of natural analogues in the design and performance assessment of solid radioactive wasteforms. Proc. 4th NAWG Mtg. Pitlochry, Scotland. CEC Report EUR 13014 EN, pp 31-72.

PNC (1992): Research and development on geological disposal of high level radioactive waste. First progress report. PNC TN 1410 93-059, Japan, September 1992.

RODRICKS, J.V. (1992): Calculated risks. Cambridge University Press.

SCHWEINGRUBER, M. (1983): Actinide solubility in deep groundwater: estimates for upper limits based on chemical equilibrium calculations. EIR-Bericht 507. Paul Scherrer Institute, Würenlingen, Switzerland.

SKB (1992): SKB 91 Final Disposal of Spent Nuclear Fuel: Importance of the Bedrock for Safety. SKB Technical Report 92-20, Stockholm, May 1992.

SKI (1991): SKI Project 90. SKI Technical Report 91:23 (Summary and 2 volumes).

SMITH, P.A. (1993): Quantifying the performance of the geosphere as a barrier to the migration of radionuclides. Nagra Internal Report, Nagra, Wettingen, Switzerland.

STENHOUSE, M.J. & PÖTTINGER, J. (1994): Comparison of sorption databases used in recent performance assessments involving crystalline host rock. J. Contam. Hydrol. in press.

SUMERLING, T.J., SMITH, P., ZUIDEMA, P. GROGAN, H.A. & VAN DORP, F. (1993): "Scenario Development for Safety Demonstration for Deep Gelogical Disposal in Switzerland", Proc. of the 4th Annual International Conference on High Level Radioactive Waste Management, Las Vegas, USA, 26-30 April 1993, Proc. 1085-1092.

SUMERLING, T.J. & GROGAN, H.A. (1994): Scenario development for Kristallin-I. Nagra Technical Report NTB 93-13, Nagra, Wettingen, Switzerland.

THURY, M., GAUTSCHI, A., MAZUREK, M., MÜLLER, W.M., NAEF, H., PEARSON, F.J., VOMVORIS, S. & WILSON, W. (1994): Geology and Hydrogeology of the Crystalline Basement of Northern Switzerland. Nagra Technical Report NTB 93-01E, Nagra, Wettingen, Switzerland.

UNSCEAR (1988): Sources, effects and risks of ionizing radiation. UN, New York.

VIENO, T. HAUTOJÄRVI, A., KOSKINEN L. & NORDMAN H. (1992): TVO-92 Safety Analysis of Spent Fuel Disposal. YJT Technical Report YJT-92-33 E, English edition, Helsinki, August 1993.

WACHSMANN, F. (1989): Die Strahlengefahr - realistisch gesehen, Naturwissenschaften 76, p. 45-51.

WILSON, R. (1979): Analyzing the risks of daily life. Technology Review **81** (4), pp 41-46.

ZIMMERLI, B., BOSSHARD, E. & ZELLER, W. (1992): Gesetzliche Regelung von chemischen Kanzerogenen und Radionukliden in Lebensmitteln. Mitt. Gebiete Lebensm. Hyg. **83**, pp 509-548.